

DEVELOPMENT AND CHARACTERIZATION OF AFFINITY AND PSEUDO-AFFINITY BASED METHODS FOR CELL CULTURE-DERIVED INFLUENZA VIRUS CAPTURING

Dissertation

zur Erlangung des akademischen Grades

Doktoringenieur

(Dr.-Ing.)

von: Dipl.-Ing. Lars Opitz

geb. am: 10.01.1978

in: Elsterwerda

genehmigt durch die Fakultät für Verfahrens- und Systemtechnik
der Otto-von-Guericke-Universität Magdeburg

Gutachter: Prof. Dr.-Ing. Udo Reichl
Dr. Paula Marques Alves

eingereicht am: 02.03.2010

Promotionskolloquium am: 29.07.2010

Forschungsberichte aus dem Max-Planck-Institut
für Dynamik komplexer technischer Systeme

Band 28

Lars Opitz

**Development and characterization of affinity-
and pseudo-affinity-based methods for
cell culture-derived influenza virus capturing**

Shaker Verlag
Aachen 2010

Bibliographic information published by the Deutsche Nationalbibliothek

The Deutsche Nationalbibliothek lists this publication in the Deutsche Nationalbibliografie; detailed bibliographic data are available in the Internet at <http://dnb.d-nb.de>.

Zugl.: Magdeburg, Univ., Diss., 2010

Copyright Shaker Verlag 2010

All rights reserved. No part of this publication may be reproduced, stored in a retrieval system, or transmitted, in any form or by any means, electronic, mechanical, photocopying, recording or otherwise, without the prior permission of the publishers.

Printed in Germany.

ISBN 978-3-8322-9482-3

ISSN 1439-4804

Shaker Verlag GmbH • P.O. BOX 101818 • D-52018 Aachen

Phone: 0049/2407/9596-0 • Telefax: 0049/2407/9596-9

Internet: www.shaker.de • e-mail: info@shaker.de

Acknowledgement

This work was carried out in the Bioprocess Engineering group from the Max Planck Institute for Dynamics of Complex Technical Systems in Magdeburg.

First, I would like to thank my PhD advisor Prof. Dr.-Ing. Udo Reichl for allowing me to work in his group on this interesting and exciting topic, and for his fruitful advice and discussions. Additionally, I would like to thank Dr. Paula M. Alves from the ITQB/IBET in Portugal for being the second reviewer of this dissertation.

I am deeply grateful to all my colleagues at the Max Planck Institute and also to the master students Jatuporn Salaklang and Jonas Hohlweg, who supported this work with discussions, advice and laboratory assistance. I would like to emphasize my sincere thanks to Dr. Michael W. Wolff for his excellent supervision throughout all of the stages of the project. Thanks to the upstream processing and downstream processing team for their laboratory assistance and to Dr. Erdmann Rapp for protein identification by mass spectrometry analysis.

I also would like to thank Dr. Volkmar Thom and Dr. Rene Faber from Sartorius Stedim Biotech GmbH, Göttingen, Germany for supplying epoxy-activated wide-porous membranes as well as unmodified reinforced cellulose membrane sheets. Additional, thanks go to Dr. Peter Landgraf and Dr. Karl-Heinz Smalla from the Leibniz-Institute for Neurobiology in Magdeburg, Germany for allowing me to use their Biacore 2000 equipment.

Special thanks go to my family for their advice and support throughout the whole of my studies, and to my girlfriend Ines for her mental support and patience.

February 2010

Lars Opitz

Index of content

Acknowledgement	III
Index of content	V
Abbreviations	IX
Symbols	XI
Abstract	XIII
Zusammenfassung	XV
1 Introduction and task	1
2 Theory and background	4
2.1 Influenza disease and influenza virus	4
2.2 Influenza surveillance and vaccine production processes	7
2.2.1 Traditional egg-based influenza vaccine production processes	8
2.2.2 Establishment of cell culture-based vaccine productions	10
2.2.3 Alternative influenza vaccine manufacturing technologies	12
2.3 Chromatography	12
2.3.1 Affinity chromatography	14
2.3.2 Pseudo-affinity chromatography	19
2.3.3 Column versus membrane-based chromatography	23
2.4 Regulations and purity requirements for influenza vaccines	24
2.5 Binding studies by surface plasmon resonance technology	25
3 Material and Methods	29
3.1 Influenza virus production, harvest, clarification, inactivation and concentration	29
3.1.1 Influenza virus A/Puerto Rico/8/34 production for LAC method development	31
3.1.2 Influenza virus A/Puerto Rico/8/34 production for LAC matrix selection	32
3.1.3 Influenza virus production for LAC transferability studies	33
3.1.4 Influenza virus production for pseudo-affinity chromatography studies .	34
3.2 Material and methods for the LAC development	34
3.2.1 Ligand screening for LAC	34
3.2.2 Characterization of LAC-FPLC using the model strain A/Puerto Rico/8/34 and the lectins ECL and EEL	36
3.3 Material and methods for the LAC matrix selection	38

3.3.1	Chromatographic materials.....	38
3.3.2	Matrix screen for LAC with influenza virus strain A/Puerto Rico/8/34	40
3.3.3	Comparison of EEL-membrane and EEL-polymer beads	41
3.4	Material and methods for LAC transferability studies.....	42
3.4.1	Lectin binding to influenza virus strains used for vaccine production from 2006/07 and 2007/08 epidemic seasons	42
3.4.2	Purification of A/Wisconsin/67/2005 and B/Malaysia/2506/2004 by EEL-AC	44
3.5	Material and methods for the pseudo-affinity chromatography	45
3.5.1	Preparation of SCM	45
3.5.2	Experiments for comparison of influenza virus purification by SCM and Cellufine® sulphate.....	46
3.6	Analysis	48
3.6.1	Hemagglutination activity.....	49
3.6.2	DNA concentration.....	49
3.6.3	Total protein concentration	50
3.6.4	Hemagglutinin content – single radial immunodiffusion assay.....	50
3.6.5	SDS-PAGE	51
3.6.6	Size distribution analysis.....	52
3.6.7	Quantification of sulphate content from membrane adsorbers.....	52
4	Lectin affinity chromatography	53
4.1	Development of an LAC step for DSP of MDCK cell culture-derived human influenza virus A/Puerto Rico/8/34	53
4.1.1	Results.....	53
4.1.2	Discussion	58
4.2	Impact of adsorbent selection on capture efficiency using LAC.....	62
4.2.1	Results.....	62
4.2.2	Discussion	68
4.3	Transferability of LAC: Different influenza virus strains and host cells.....	74
4.3.1	Results.....	74
4.3.2	Discussion	80
5	Pseudo-affinity chromatography using sulphated cellulose membrane adsorbers	86
5.1	Results.....	86

5.1.1	Cellulose membrane sulphatation.....	86
5.1.2	Separation of influenza virus particles by sulphated cellulose membranes 86	
5.1.3	Separation of influenza virus particles by column-based CSR.....	88
5.1.4	Influenza virus capturing by cation-exchange membrane adsorbers	88
5.1.5	Enhanced process productivity of SCM compared to CSR.....	88
5.2	Discussion	91
6	Summary.....	99
7	Outlook.....	102
8	References.....	103
9	Index	115
9.1	Index of figures	115
9.2	Index of tables	118

Abbreviations

AB1, AB2, AB3	adsorption buffer 1, 2 and 3
AC	affinity chromatography
AEX	anion-exchange chromatography
AIL	<i>Artocarpus integrifolia</i> lectin, Jacalin
CEX	cation-exchange chromatography
CSR	Cellufine [®] sulphate resin
DNA	deoxyribonucleic acid
dsDNA	double stranded deoxyribonucleic acid
EB1, EB2	elution buffer 1 and 2
EEL	<i>Euonymus europaeus</i> lectin
ECL	<i>Erythrina christagalli</i> lectin
FCS	fetal calf serum
FPLC	fast protein liquid chromatography
GMEM	Glasgow minimum essential medium
HA	hemagglutinin
HIC	hydrophobic interaction chromatography
IEX	ion-exchange chromatography
IMAC	immobilized metal affinity chromatography
IP	isoelectric point
LAC	lectin affinity chromatography
M1	matrix protein 1
M2	matrix protein 2 (ion channel)
MAL I	<i>Maackia amurensis</i> lectin I
MDBK	Madin Darby bovine kidney
MDCK	Madin Darby canine kidney
MF	microfiltration
NA	neuraminidase
NA-activity	neuraminidase activity
PA	component of influenza RNA-polymerase
PA-I	<i>Pseudomonas aeruginosa</i> lectin
PAC	pseudo-affinity chromatography
PB1	component of influenza RNA-polymerase

X

PB2	component of influenza RNA-polymerase
PBS	phosphate buffered saline
PNA	<i>Arachis hypogaea</i> agglutinin
PVDF	polyvinylidene difluoride
RCA	<i>Ricinus communis</i> agglutinin
RNA	ribonucleic acid
cRNA	complementary RNA
mRNA	messenger RNA
vRNA	viral RNA
RNP	ribonucleoprotein
SCM	sulphated cellulose membranes
SEC	size-exclusion chromatography
SNA	<i>Sambucus nigra</i> bark lectin
SOP	standard operating procedure
SPR	surface plasmon resonance
SRID	single radial immunodiffusion assay
UF	ultrafiltration
WHO	World Health Organization

Symbols

A	Absorption [-]
C	concentration of free target P [M]
c_{DNA}	DNA concentration [ng/ml] or [$\mu\text{g/ml}$]
c_{HA}	hemagglutinin concentration [$\mu\text{g/ml}$]
c_{L}	ligand concentration in solution [mol l^{-1}]
c_{prot}	protein concentration [$\mu\text{g/ml}$]
d	dilution factor HA-activity assay [-]
HA-activity	hemagglutination activity [HAU/ml] or [kHAU/ml]
i_{prot}	protein impurity [$\mu\text{g}/\mu\text{g HA}$] or [$\mu\text{g/kHAU}$]
i_{DNA}	DNA impurity [ng/ $\mu\text{g HA}$] or [$\mu\text{g/kHAU}$]
K_{a}	association constant [M^{-1}]
K_{d}	dissociation constant [M]
k_{a}	association rate constant [$\text{M}^{-1}\text{s}^{-1}$]
k_{d}	dissociation rate constant [s^{-1}]
R	response signal [RU]
R_{max}	maximum response signal [RU]
t	time [s]
ε	molar absorption coefficient [$\text{l mol}^{-1}\text{m}^{-1}$]

Abstract

Influenza is one of the most worldwide-spread diseases, which infects several million people every year. Besides antiviral medical treatments, prophylactic vaccinations are crucial for controlling seasonal influenza epidemics. Hence, every year large amounts of vaccine doses have to be produced. Conventionally, embryonated chicken eggs are used for human influenza vaccine production. However, this production process has only a limited scalability. In addition, these vaccines contain egg-derived proteins, which may cause allergic reactions. Hence, cell culture-based vaccine production processes have been developed, which require an adapted downstream processing strategy for virus purification.

The scope of this dissertation was the development of affinity- as well as pseudo-affinity-based chromatographic unit operations for the downstream processing of cell culture-derived influenza virus particles. Therefore, two major approaches were investigated: lectin-based affinity chromatography and sulphated cellulose matrices-based pseudo-affinity chromatography. In both fields membrane- and bead-based techniques were considered and compared.

Lectin affinity chromatography was developed first for the Madin Darby canine kidney (MDCK) cell culture-derived human influenza virus A/Puerto Rico/8/34 (H1N1). This dissertation showed that the α 1,3-galactose-specific *Euonymus europaeus* lectin (EEL), immobilized on polymer beads, is a suitable ligand for affinity purification of glycosylated viral envelope proteins such as the hemagglutinin. The dissociation of the virus-ligand complex was done by competitive elution with lactose. More than 90% of the influenza virus hemagglutination activity was recovered in the product fraction, while the majority of host cell proteins and nucleic acids were depleted.

For chromatography, matrix selection plays an important role regarding purification efficiency. Therefore, different matrices for EEL as ligand were screened. These supports included stabilized reinforced cellulose membranes, polymer and porous glass particles, cellulose and agarose beads. Strong virus binding was achieved by EEL-modified cellulose membranes and polymer beads. Furthermore, reinforced cellulose membranes had a far better binding capacity than other tested adsorbents. To determine the general applicability of EEL-affinity chromatography, studies were extended for two other MDCK cell-derived influenza virus strains

(A/Wisconsin/67/2005 (H3N2), B/Malaysia/2506/2004). Both virus strains were captured efficiently by the ligand EEL. These results emphasized the EEL-affinity chromatography as a valuable technique for capturing MDCK cell-derived influenza virus particles. Additionally, the impact of host cells on lectin affinity chromatography has been evaluated. In contrast to findings with viruses propagated in MDCK cells, Vero cell-derived influenza virus A/Puerto Rico/8/34 bound to β 1,4-galactose-specific *Erythrina christagalli* lectin (ECL) but only very limited to the α 1,3-galactose-specific EEL.

The second major project part of this dissertation describes a capturing method for influenza viruses (A/Wisconsin/67/2005 (H3N2), A/Puerto Rico/8/34 (H1N1), B/Malaysia/2506/2004) using sulphated reinforced cellulose membranes. Purification efficiency with regards to viral yield as well as total protein and host cell dsDNA depletion was directly compared to commercially available cation-exchange adsorbers and to column-based Cellufine[®] sulphate resin. With the sulphated membranes, high product recoveries and contaminant reductions were possible. Due to a fast binding kinetic and a low back pressure, these membrane adsorbers enabled the capturing process to be operated at an increased flow rate leading to significantly enhanced productivity. Hence, sulphated membrane adsorbers are a valuable choice for industrial influenza vaccine purification processes.

Zusammenfassung

Influenza ist eine weltweit verbreitete Infektionskrankheit, an der jährlich mehrere Millionen Menschen erkranken. Um saisonale Epidemien zu kontrollieren, spielen vorbeugende Impfungen neben antiviraler medikamentöser Behandlung eine sehr wichtige Rolle. Aus diesem Grund werden jährlich große Mengen an Influenzaimpfstoffen produziert. Die traditionelle Herstellung humaner Influenza-Impfstoffe erfolgt in Hühnereiern. Diese Methode besitzt nur eine begrenzte Skalierbarkeit. Außerdem können solche Impfstoffe allergische Reaktionen auf Hühnereiweiße hervorrufen. Alternativ dazu wurde in den letzten Jahren die Virusproduktion in Säugetierzellkulturen etabliert. Darauf aufbauend sind neue und innovative Aufreinigungsstrategien für Influenzaviren notwendig.

Das Ziel dieser Dissertation war die Entwicklung von affinitäts- und pseudo-affinitätschromatografischen Aufreinigungsmethoden für Influenzaviren aus Zellkulturüberständen. Dafür wurden zwei Methoden näher untersucht: die Lektin-Affinitätschromatographie und die auf sulfatierten Zellulosematrizen basierende Pseudo-Affinitätschromatographie. In beiden Fällen verglich man Membran-Adsorption und gelbasierende Säulenchromatographie miteinander.

Zunächst wurde die Lektin-Affinitätschromatographie für den in Hundenierenzellen (Madin Darby canine kidney, MDCK) produzierten Influenzavirusstamm A/Puerto Rico/8/34 (H1N1) etabliert. Es wurde gezeigt, dass das α 1,3-Galaktose spezifische *Euonymus europaeus* Lektin (EEL), immobilisiert auf Polymerpartikel, ein geeigneter Ligand für glykosylierte Influenzavirushüllproteine (z.B. Hämagglutinin) ist. Die Viren wurden desorbiert durch kompetitive Verdrängung mit Laktose. Dabei betrug die Wiederfindung der Influenzavirus-Hämagglutinationsaktivität in der Produktfraktion mehr als 90% während Großteile der Wirtszellproteine und -nukleinsäuren abgetrennt worden.

Da die Chromatographiematrix ein wichtiger Parameter ist, wurde die Verwendbarkeit des Liganden EEL an verschiedenen Matrizen, wie z.B. stabilisierte Zellulosemembranen sowie poröse Polymer-, Glas-, Zellulose- und Agarosegelpartikel, untersucht. Hohe Virusadsorptionen erreichte man durch EEL-modifizierte Zellulosemembranen und Polymerpartikel, wobei die Membranadsorber

höhere Bindungskapazitäten bezogen auf die immobilisierte Ligandenmenge besaßen.

Die Übertragbarkeit der Methode wurde an zwei weiteren in MDCK-Zellen produzierten Influenzavirusstämmen (A/Wisconsin/67/2005 (H3N2), B/Malaysia/2506/2004) gezeigt. Die Ergebnisse zeichnen die EEL-Affinitätschromatographie als eine effiziente Methode aus, um Influenzaviren aus MDCK-Zellkulturbrühen abzutrennen. Zusätzlich wurden die Auswirkungen unterschiedlicher Wirtszellen während der Virusproduktion auf die Lektin-Affinitätschromatographie untersucht. Influenzaviruspartikel A/Puerto Rico/8/34 aus Vero-Zellkulturen adsorbierten besser an das β 1,4-Galaktose spezifische *Erythrina christagalli* Lektin (ECL) als an das α 1,3-Galaktose spezifische EEL.

Als eine alternative Methode wurde die Aufreinigung von Influenzaviren (A/Wisconsin/67/2005 (H3N2), A/Puerto Rico/8/34 (H1N1), B/Malaysia/2506/2004), welche auf sulfatierten stabilisierten Zellulosemembranen beruht, beschrieben. Dabei wurden sowohl die Virusausbeute als auch die Abreicherung der Wirtszellproteine und -nukleinsäuren mit Ergebnissen von kommerziell erhältlichen Kationenaustauschermembranen und sulfatierten Zellulosepartikeln (Cellufine® sulfate) verglichen. Mit den sulfatierten Membranadsorbern waren hohe Virusausbeuten und gute Kontaminantenabreicherungen möglich. Aufgrund schneller Bindungskinetik und niedrigem Rückdruck sind diese sulfatierten Membranadsorber bei höherer Fließgeschwindigkeit anwendbar und stellen daher eine attraktive Methode für die industrielle Aufreinigung von Influenzaviren zur Impfstoffproduktion dar.

1 Introduction and task

Influenza infection is a worldwide-spread contagious disease of the respiratory tract, which affects several million humans (up to 10% of the world population (Gerdil 2003)) and animals every year. Additionally, influenza has the potential to cause pandemics. Hence, this disease remains a major public health concern. Strategies to control influenza outbreaks are mainly focused on prophylactic vaccinations in conjunction with antiviral medications.

Over the past 10 years the number of human vaccine doses produced annually has increased steadily, reaching an overall number of 565 million doses in 2007 (WHO 2007). Commonly used human influenza vaccines are a blend of 3 different virus strains. For example, vaccines for the northern hemisphere from the seasons 2006/07 and 2007/08 contained the two influenza A virus strains A/Solomon Islands/3/2006 (H1N1) and A/Wisconsin/67/2005 (H3N2), and the influenza virus B/Malaysia/2506/2004. Due to frequent genetic drifts of the influenza virus, the viral surface glycoproteins are subject to constant changes. Thus, annual adaptation of human influenza vaccines to newly evolved virus strains is required. Hence, crucial requirements for influenza vaccine production processes are its strain independency and robustness. In addition, these processes need to be fast to ensure the vaccine distribution within sufficient time. Especially in a pandemic outbreak there is a need for rapid vaccine preparations.

Human influenza vaccines are conventionally produced in the allantoic fluid of embryonated chicken eggs. Afterwards, virus particles are purified using a combination of several downstream processing unit operations including ultrafiltration and centrifugation steps, in particular continuous sucrose gradient ultracentrifugation (Gerdil 2003; Ikizler and Wright 2002; Matthews 2006; Reimer et al. 1967; Valeri et al. 1977; Wolff and Reichl 2008). This labour-intensive production method requires a large quantity of eggs, approximately 1 to 3 eggs per trivalent dose, which can lead to a supply shortage, especially in cases of a pandemic outbreak (Chalumeau 1994; Hervé 1994; Oxford et al. 2005). Additional disadvantages are the limited production process scalability and that egg-produced vaccines can cause allergic reactions induced by egg proteins.

Such concerns have led to significant efforts by several pharmaceutical companies to establish cell culture-based vaccine manufacturing processes over the last few years (Barrett et al. 2009; Brands et al. 1999; Doroshenko and Halperin 2009; Gröner and Vorlop 1997; Howard et al. 2008; Kistner et al. 1999; Kistner et al. 1998; Lohr et al. 2009; Pau et al. 2001; Rappuoli 2006; Youil et al. 2004). Cell culture-derived influenza virus particles are either purified by traditional methods applying sucrose density gradient ultracentrifugation (Barrett et al. 2009; Howard et al. 2008) or by recently developed technologies based on filtration and size-exclusion as well as ion-exchange chromatography (Kalbfuß et al. 2007a; Kalbfuß et al. 2007c). These techniques rely on either size or charge of the virus particles. In addition, sulphated cellulose beads are used industrially for cell culture-derived influenza virus pseudo-affinity purification (Palache et al. 1997). This application demonstrates the high potential of specific virus adsorption chromatography. However, there are currently no affinity-based purification methods characterized for influenza vaccine manufacturing purposes.

Purification of biological products is generally divided into three parts: capture or concentration, separation or fractionation, and polishing. Concerning the overall process economics, the capture step is the most important unit operation. Both, product selectivity and the concentration factor of the capture step define the efforts required for all further purification steps. The introduction of an affinity capture step into the downstream process for virus purification may increase the virus yield and productivity of vaccine manufacturing. Additionally, this would lead to a decreased number of process steps. Therefore, the choice of the specific ligand for the affinity capture step defines purification efficiency. Affinity ligands need to be specific enough to ensure high purities, but on the other hand they should guarantee the robustness of the process regarding the application of different influenza virus strains. If the specificity is too high, frequent ligand substitutions would be necessary, leading to increased costs and production delays. For example, immunochromatography is not suitable for vaccine manufacturing processes, because viral antigens underlie frequent evolutions. In addition, interaction of antibodies and antigens are mostly very strong, requiring harsh desorption conditions. This would lead to antigen degradation.

The selection of the chromatographic matrix also plays an important role. For example, it has an impact on ligand-binding capacities (Kang et al. 1992) and its structure influences virus accessibility to ligands and consequently the purification

efficiency. Furthermore, the pore or channel sizes of the matrix have a big impact on the generated back pressure and, therefore, on the maximum flow rates and residence times. In addition, the mechanical stability of the matrix affects the maximum pressure limit. Hence, the selection of the optimal ligand and matrix is necessary for a successful industrial downstream process with an affinity-based capture step.

Creating an efficient purification process for cell culture-derived influenza viruses, the vaccine production capacities could be increased. Existing production capacities and processes are normally designed to provide vaccines for annual influenza epidemics. However, during the past few seasons (e.g., 2004/2005) the demand exceeded the vaccine supply (Schoch-Spana et al. 2005). Therefore, an optimization of the purification process for influenza viruses could not only have a beneficial impact on the short-term delivery of vaccines during a pandemic, it could potentially also help to overcome the shortage of influenza vaccines on the global market.

The aim of this dissertation was to investigate the feasibility of whether influenza virus particles can be purified by specific adsorption chromatographic methods. Therefore, capture steps for the purification of cell culture-derived human influenza virus particles using affinity as well as pseudo-affinity chromatography were developed and characterized.

The initial approach was the establishment of a lectin-based affinity capture step. This subproject was divided into three parts. First, the lectin affinity chromatography (LAC) was developed for a widely used Madin Darby canine kidney (MDCK) cell culture-derived human influenza virus strain (A/Puerto Rico/8/34, H1N1). Second, the influence of different ligand supports on the virus adsorption efficiency and economics was evaluated and an appropriate matrix was selected for the LAC application. Third, the LAC method was tested for robustness regarding the transferability to different influenza virus strains. This subdivided structure of the LAC approach will be found throughout the dissertation.

The second approach was the establishment of a pseudo-affinity chromatography capture step for influenza virus particles, based on sulphated cellulose membranes (SCM). Therefore, purification efficiency and economics was evaluated and compared to sulphated cellulose bead-based column chromatography using three influenza virus strains.

2 Theory and background

This chapter describes aspects of influenza disease and the influenza virus, as well as established methods and recent developments in influenza vaccine production processes. In particular, separation methods based on affinity and pseudo-affinity chromatography are addressed in more detail. Furthermore, the advantages of membrane-based virus purification compared to bead-based column chromatography are emphasized. Additionally, binding studies using surface plasmon resonance technology are explained.

2.1 Influenza disease and influenza virus

Influenza is a contagious respiratory-tract disease. Without medical treatment the disease has a high mortality rate especially under high-risk groups such as the elderly or infants. Alone in the US there are about 36000 influenza-associated deaths annually (Thompson et al. 2003). In addition, such epidemics are leading to an enormous economic burden, which was estimated for the US to be \$87.1 billion (2003, C.I. \$47.2, \$149.5), and for Germany 5 billion DM (1996, corresponding to approximately 2.5 billion €) (Molinari et al. 2007; Szucs et al. 2001).

Influenza viruses are enveloped viruses from the Orthomyxoviridae family, which have either a spherical (diameter about 80-120 nm) or filamentous (length about 300 nm) shape (Bouvier and Palese 2008; Webster et al. 1992). They are divided into three types: A, B and C, whereby type C is clinically not as important as types A and B. The negative-stranded and segmented RNA genome of the influenza type A encodes the nucleoprotein (NP), which forms with the RNA and the corresponding RNA polymerases (PB1, PB2, PA) the Ribonucleoprotein (RNP). Furthermore, there are the matrix proteins (M1), ion channels (M2), non-structural proteins (NS1, NS2) and the two major viral-envelope glycoproteins hemagglutinin (HA) and neuraminidase (NA) (Figure 1). An overview covering more details about the 8 RNA segments and their encoded proteins of influenza virus type A is given, for example, by Cheung and Poon (Cheung and Poon 2007) and Hay (Hay 1998).

The protein composition of influenza virus type B differs marginally to type A regarding structure of the integral ion channel (NB) and the additional membrane protein BM2 (Bouvier and Palese 2008).

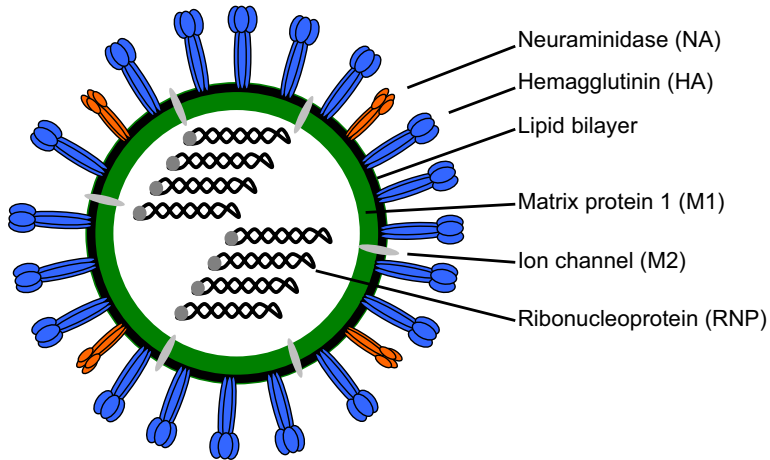


Figure 1: Schema of influenza virus type A

Influenza virus type A is further divided into various subtypes based on the structure and conformation of its two major envelope glycoproteins: HA and NA. Currently, there are 16 HA and 9 NA subtypes classified (Bouvier and Palese 2008; Fouchier et al. 2005). The HA, the most abundant influenza virus surface antigen, which is responsible for the attachment of the virus to the host cell receptors, forms trimeric structures. Each monomer contains 3 to 9 *N*-linked glycosylation sites and consists of two subunits HA1 and HA2 (Cross et al. 2001; Schulze 1997; Webster et al. 1992). No *O*-glycosidic bonds have been identified (Keil et al. 1985). The glycosylation, a post-translational protein modification of eukaryotic cells, takes place in the endoplasmic reticulum of the host cells (Jones et al. 2005). The type of glycosylation and the glycan structure depend, among other things, on the virus subtype, culture conditions and, in cases of cell culture-derived virus, on the glycan processing capabilities of the host cell (Deom and Schulze 1985; Webster et al. 1992). The carbohydrates cover about 20% of the HA surface of influenza A/Hong Kong/1968 (Wilson et al. 1981). Mir-Shekari et al. described the major glycan structures observed on the HA monomer from Influenza A/WSN/33 (H1N1) viruses propagated in Madin Darby bovine kidney (MDBK) cells (Mir-Shekari et al. 1997). These studies identified a high degree of terminal α -galactose. In addition, they identified fucosylated side chains and some minor β -galactose and mannose residues. Other groups observed for different

influenza A virus strains propagated in diverse mammalian host cells mainly the carbohydrates N-acetylglucosamine, mannose, galactose, and fucose in their glycan structure (Basak et al. 1981; Deom and Schulze 1985; Keil et al. 1985).

N-glycosylation analysis of cell culture-derived influenza virus HA from different cell lines was studied recently. There, isolated viral proteins were deglycosylated and *N*-glycan fingerprints were obtained from HA *N*-glycan pools using capillary gel electrophoresis – laser-induced fluorescence (Schwarzer et al. 2009; Schwarzer et al. 2008).

Gambaryan et al. have shown that the glycosylation of the HA can have an impact on the receptor-binding characteristics of influenza viruses (Gambaryan et al. 2005). However, for the specific recognition between influenza viruses and host cells the glycosylation of the host cell surface proteins seems to play the major role.

The predominant terminal carbohydrate of complex *N*-glycosylated structures is sialic acid, which is bound to galactose in either α 2,3- or α 2,6-linkage (Debray et al. 2002). Influenza virus HA is either specific for α 2,3- or α 2,6-linked sialic acid and mediates the attachment between virus particle and host cell. The question of which organisms can be infected, depends on the type of sialic acid linkages found on the cell surfaces of the respiratory tract: in humans mainly α 2,6- and in birds α 2,3-linkages (Gambaryan et al. 2005). However, recent studies have shown that also human epithelial cells contain terminal α 2,3-linked sialic acid, which makes humans susceptible to infections with avian-specific influenza viruses (Matrosovich et al. 2004; Shinya et al. 2006; van Riel et al. 2006).

The influenza virus replication cycle was described before (Bouvier and Palese 2008; Hay 1998). Briefly, after attachment of the HA receptor-binding pocket to sialic acid of the host cell surface the virus enters the cell by endocytosis. The inner low pH of the endosome triggers the release of the viral RNPs into the cytoplasm from which they are imported into the host cell nucleus for replication. Within the nucleus the negative-stranded viral RNA (vRNA) is used to synthesize positive-stranded messenger RNA (mRNA) and complementary RNA (cRNA). Viral mRNA is then exported from the nucleus into the cytoplasm and translated like the host mRNA. From the cRNA the viral RNA-polymerase transcribes the negative-stranded genomic vRNA, which is then brought together with the NP and exported from the nucleus by M1 and NS2. Afterwards, viruses are assembled from expressed viral proteins and are released by

budding from the cell membrane. For successful virus release from the host cell surface, the viral NA has to cleave the sialic acid residues from the host cells.

There are two different types of influenza outbreaks: epidemics and pandemics. Seasonal epidemics are based on the high mutation rate during influenza virus propagation, leading to constant changes of their envelope glycoprotein structures (antigenic drift). Therefore, new vaccine compositions have to be produced frequently (described below) to counteract the spread of such new influenza virus particles.

Due to the presence of both HA receptors (α 2,3- or α 2,6-linked sialic acid) on swine epithelial cells, this host could get infected by more than one influenza virus strain at the same time, leading most likely to the assembly of completely new virus particles (reassortment, antigenic shift). Such newly evolved viruses may cause pandemic outbreaks as observed, e.g., in 2009 (Dawood et al. 2009)

2.2 Influenza surveillance and vaccine production processes

Influenza epidemics are counteracted mainly by prophylactic vaccination. There are two types of influenza vaccines: inactivated and live attenuated vaccines. Inactivated vaccines represent the major part (>90%, Matthews 2006) of the worldwide-produced influenza virus vaccines and are subdivided into different types: whole virus, split and subunit vaccines (Bardiya and Bae 2005; Matthews 2006; WHO 2006). While whole virus vaccines consist of complete virus particles, the split or subunit vaccines contain only disrupted virus particles or viral surface antigens, respectively. In addition, virosomal vaccines with reconstituted virus-like particles, containing the viral surface antigens but lacking the viral genetic material, are licensed (de Bruijn et al. 2005; de Bruijn et al. 2006; Mischler and Metcalfe 2002; Wilschut 2009).

Human influenza vaccines are trivalent blends, consisting currently of two influenza A subtypes and one influenza type B strain. Due to frequent mutations of influenza virus envelope glycoproteins (antigenic drift), the vaccine composition has to be updated regularly. Therefore, the World Health Organization (WHO) constantly coordinates the worldwide surveillance of influenza virus strains and predicts for the northern and southern hemisphere virus strains, which will most likely occur in the upcoming epidemical season, and recommends three strains for the corresponding vaccine composition. However, often a mismatch between vaccine and circulating strains leads to diminished vaccine effectiveness as reported for recent epidemical seasons in

North America (Belongia et al. 2009; Jackson 2009; Skowronski et al. 2009). From the moment of the WHO's decision to the point of time when vaccines have to be delivered to medical distributors, the manufacturers have about 6 months for the production. Influenza vaccine production processes differ depending on the vaccine type as well as manufacturer (Bardiya and Bae 2005; Brady and Furminger 1976; Furminger 1998; Gerdil 2003; Matthews 2006; Palese 2006; WHO 2006). Such production processes are addressed briefly below.

2.2.1 Traditional egg-based influenza vaccine production processes

Traditionally, the influenza virus particles are propagated in embryonated chicken eggs. Compared to the influenza virus type B, for each of the both influenza A subtypes high-growth seed strains are produced in chicken eggs through reassortment with a high-yield laboratory H1N1 subtype (A/Puerto Rico/8/34). Afterwards, it has to be confirmed that the obtained seed strains contain no A/Puerto Rico/8/34 envelope glycoproteins. Influenza B isolates are used directly as seed strains for vaccine productions. Once the seed strains have been prepared, egg-based bulk vaccine production starts with propagation of each virus strain in the allantoic cavity of embryonated chicken eggs. From there, virus particles are harvested and preclarified by centrifugation or filtration. Additionally, virus particles may be concentrated by ultrafiltration. The subsequent ultracentrifugation on a sucrose gradient (Reimer et al. 1967) represents the main purification step, which is a well-established and still most preferred method by the manufacturers. Chemical inactivation of viral particles by treatment with β -propiolactone or formaldehyde takes place either before the ultracentrifugation or in a later process stage. For whole virus vaccines the concentrations of purified virus particles are adjusted and blended to trivalent doses. In contrast, split and subunit vaccines are further processed. Therefore, viral particles are disrupted by treating them with detergent (e.g., Tween 80, Triton X100 or CTAB) and solvent (e.g., tri(*n*-butyl) phosphate). After removal of splitting reagent, for example, by phase separation, dialysis or another ultracentrifugation step, the split vaccines are blended into trivalent doses. The production of subunit vaccines, also called surface antigen vaccines, includes the separation of both viral surface antigens, HA and NA, from the remaining viral proteins and lipids. This can be done by an additional sucrose density gradient ultracentrifugation containing a detergent (e.g., Triton N101) (Brady and Furminger 1976). After detergent removal, the antigen

concentrations are adjusted and antigens are blended into trivalent subunit vaccines. Furthermore, the immunogenicity of vaccines can be enhanced by blending them with immunopotentiators (e.g., aluminium). This is also an effective possibility to increase the vaccine supply for a pandemic virus strain (Banzhoff et al. 2008; Clark et al. 2009; Hehme et al. 2002). A production scheme for inactivated egg-derived influenza vaccines is given exemplarily in

Figure 2. The number and sequence of the single unit operations vary among vaccine manufacturers.

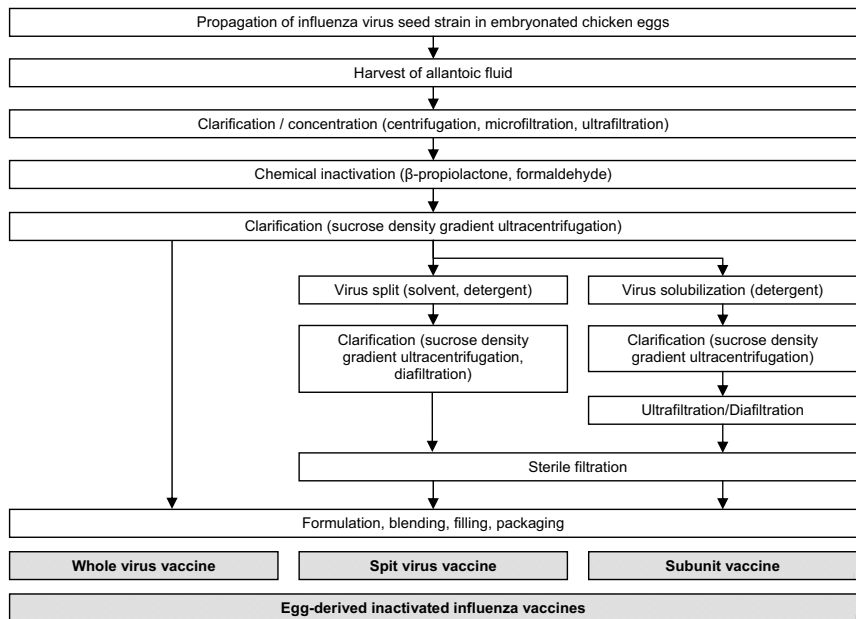


Figure 2: Example for the production procedure of egg-derived influenza virus vaccines

There are several disadvantages of egg-derived influenza virus vaccines, such as possible allergic reactions to egg proteins, limited production scalability, and possible shortages of egg supply during pandemics.

To overcome these disadvantages mammalian cell culture-derived influenza vaccine production processes are currently being established.

2.2.2 Establishment of cell culture-based vaccine productions

Several disadvantages of egg-derived vaccines or vaccine production processes, mentioned above, led to the development of cell culture-based production technologies. In 1995 the WHO recommended the investigation of different cell lines for vaccine production purposes (WHO 1995). Several cell lines, e.g., Madin Darby canine kidney (MDCK), African green monkey kidney (Vero), PER.C6 cells and St. Jude porcine lung cells, have been used to propagate influenza viruses (Alyмова et al. 1998; Doroshenko and Halperin 2009; Genzel et al. 2004; Genzel et al. 2006; Govorkova et al. 1996; Gröner and Vorlop 1997; Kistner et al. 1999; Kistner et al. 1998; Pau et al. 2001; Seo et al. 2001; Tree et al. 2001; Youil et al. 2004). There are, for example, vaccine products introduced by Novartis Behring (Optaflu[®]) (Doroshenko and Halperin 2009) or Baxter International Inc. (Celvapan). Additionally, production of H5N1 and H1N1 pandemic vaccines in Vero and MDCK cells has been performed and studied (Clark et al. 2009; Howard et al. 2008; Hu et al. 2008; Kistner et al. 2007).

In cell culture-based vaccine production processes mammalian cells are first cultivated in bioreactor systems. These cells are growing either adherently on surfaces or are adapted to suspension growth. The surface, which is available for adherent cell growth, can be increased artificially by using microcarriers. After a sufficient cell density is reached, cells are infected with the seed influenza virus strain. Three to 5 days post infection the virus-containing cell culture broth can be harvested.

Purification of cell culture-derived virus particles can be accomplished using methods established for egg-derived viruses (Barrett et al. 2009; Howard et al. 2008). However, for an optimized purification from large-scale bioreactor cultures these upstream modifications require the development of appropriate downstream procedures. Therefore, generic purification schemes were established for separation of cell culture-derived influenza virus particles using e.g., ultracentrifugation, cross-flow filtration, size-exclusion and anion-exchange chromatography (Brands et al. 1999; Kalbfuß et al. 2007a; Kalbfuß et al. 2007c; Nayak et al. 2005; Wickramasinghe et al. 2005). Sakudo et al. developed an anionic magnetic bead-based capturing method for both egg- and cell culture-derived human influenza virus particles (Sakudo et al. 2009). These purification methods rely on separation principles based on size or charge of the virus particles. In contrast to that, options for the use of more specific affinity capture unit operations to purify influenza viruses have been investigated. There are several possibilities to capture influenza viruses or viral proteins by affinity or pseudo-affinity

chromatography. These include, for example, the use of Cellufine[®] sulphate (Oka et al. 1985; Palache et al. 1997; Peterka et al. 2007; Van Scharrenburg and Brands 1998), which already has industrial relevance; heparinized media (Anonym 2006); immobilized zinc ions (Opitz et al. 2009); antibodies (Gerantes et al. 1996) or lectins (Kristiansen et al. 1983). These promising studies and applications justify the thorough investigation into whether affinity-based methods are applicable for vaccine manufacturing. Hence, the main focus of this dissertation was to study the feasibility of affinity chromatography for cell culture-derived influenza virus separation. Therefore, novel affinity- as well as pseudo-affinity chromatography methods for the purification of influenza virus particles were developed and characterized.

An example for a production scheme of inactivated cell culture-derived influenza vaccines based on available technologies mentioned above is given exemplarily below. To eliminate DNA impurities from host cells an intermediate nuclease treatment can be placed before the separation steps.

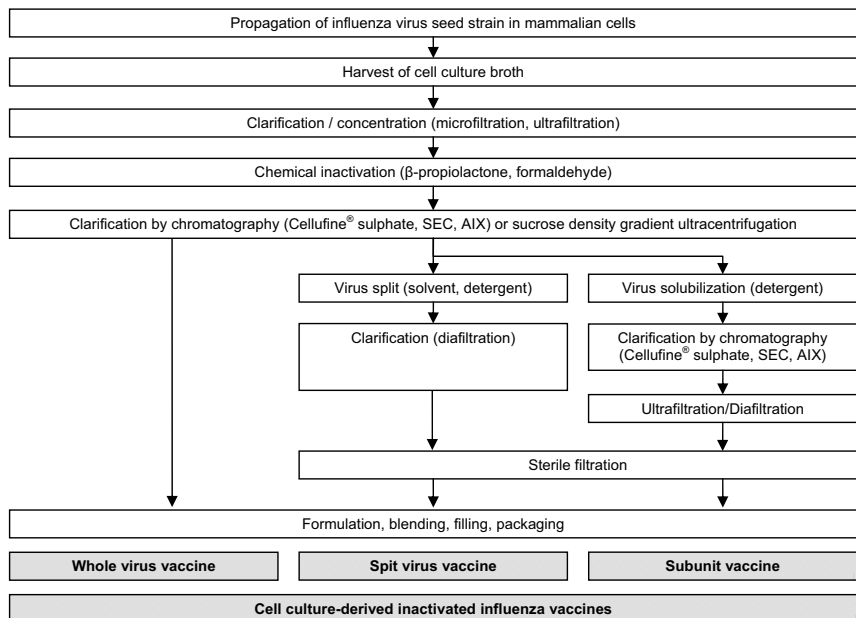


Figure 3: Example for the production procedure of cell culture-derived influenza virus vaccines

2.2.3 Alternative influenza vaccine manufacturing technologies

In addition to above described processes, an approach for recombinant HA expression in a continuous insect cell line (*expresSF+*[®]) for trivalent recombinant HA vaccine production was established (FluBlok[®], Protein Sciences Cooperation (Cox and Hollister 2009)).

Some further vaccine technologies were developed during recent decades, including DNA vaccines. Furthermore, vaccines with immune-stimulating complexes (ISCOMS) were generated (Bardiya and Bae 2005; Kemble and Greenberg 2003). However, both approaches were only studied or licensed, respectively, for veterinary application. DNA vaccines are consisting of engineered plasmids encoding viral antigens that, expressed in the host cells, are eliciting immune responses. So far, there are only animal (e.g., mice, chickens, primates) studies for DNA vaccines (Chen et al. 2008; Laddy et al. 2009; Rao et al. 2008; Zheng et al. 2009). ISCOMS are cage-like structures (about 40 nm in diameter) consisting of viral antigens and components like cholesterol, phospholipids and glycosides of the adjuvant Quil A (Brügmann et al. 1997; Morein et al. 1984; Rimmelzwaan and Osterhaus 1995; Rimmelzwaan and Osterhaus 2001). The efficiency of ISCOMS was compared to conventionally produced influenza vaccines in macaques (Rimmelzwaan et al. 1997) showing high immunogenicity. Successful application of this technology is shown by a registered equine influenza vaccine (Iscovac Flu vet[®], Equip F, Schering-Plough, Rimmelzwaan and Osterhaus 2001).

2.3 Chromatography

Conventional purification of influenza virus particles by sucrose density gradient centrifugation is based on virus and contaminants size and is well established and optimized for egg-derived influenza viruses (Matthews 2006; Reimer et al. 1967). However, cell culture-based virus production permits new purification techniques including chromatographic separations, which are more suitable for large volumes of cell culture broths than gradient centrifugations.

Chromatography is an important and widely used technique for downstream processing of biological and pharmaceutical products (Curling and Gottschalk 2007). The chromatographic separation depends on the distribution of the target components between two phases: the stationary and the mobile phase. For bioseparations the

stationary phases are mostly porous solids such as beads, monolithic polymers or membrane layers. The mobile phase containing the biological components, which have to be separated, moves through or along the stationary phase. Chromatographic techniques addressed below are classified according to their separation mechanisms that rely on size, charge, hydrophobicity or specific binding characteristics of the target components.

The stationary phase of the size-exclusion chromatography (SEC) matrix is characterized by a certain range of pore sizes. That leads to a separation based on the accessibility of components from the mobile phase to the pores, as well as their velocity through the porous volume of the beads. Other types of chromatography, such as ion-exchange (IEX), hydrophobic interaction (HIC), affinity (AC) or pseudo-affinity chromatography (PAC), rely on adsorption to the stationary phase based on electrostatic and hydrophobic attraction or biospecific interaction, respectively. AC and PAC, playing the major role in this dissertation, are described in detail below.

IEX, which is often used in biotechnology for protein separation processes, is based on ionic attraction of the chromatographic matrix possessing charged functional groups. The choice of whether cation- (CEX, negatively charged) or anion-exchanger (AEX, positively charged) are applied, depends on the net charge of the target components at the pH value from the mobile phase. A pH greater than the isoelectric point (IP) of the target results in a negative net charge of this component. If the pH is below the IP, the net charge will be positive. The IP of egg-derived influenza virus A/PR/8 and A2/Singapore/57 was estimated to pH=5.3 (Miller et al. 1944) and 5.0 (Zhilinsk.In et al. 1972), respectively. However, viral particles have positively and negatively charged regions allowing the adsorption to both AEX and CEX adsorber for a certain level. Many types of matrices exist within both these groups, differing in chemistry, density and strength of matrix modification. For example, cation-exchange adsorbers, which are relevant for this dissertation, are modified with sulfonic acid (strong CEX) or carboxylic acid (weak CEX). Desorption can be accomplished by increasing of the ionic strength shielding the charge from the stationary phase or by adjusting the pH value of the mobile phase.

Both, SEC (Heyward et al. 1977; Kalbfuß et al. 2007c; Nayak et al. 2005) and IEX (Kalbfuß et al. 2007b; Kalbfuß et al. 2007c; Matheka and Armbruster 1958; Neurath et al. 1967) have been applied for the purification of influenza virus particles derived either from embryonated chicken eggs or mammalian cell cultures.

Furthermore, calcium (Lapidus 1969; Pepper 1967) and aluminium (Miller and Schlesinger 1955) phosphate adsorption chromatography was used for influenza virus preparations.

So far, HIC has not been considered for influenza virus purification. This type of chromatography uses hydrophobic groups located on target molecules for adsorption onto the hydrophobic stationary phase. Therefore, ionic interactions between stationary phase and targets are suppressed due to high ionic strength of the mobile phase. Hence, HIC could be very useful, especially after IEX. Release of target components is accomplished by decreasing the salt concentration of the mobile phase.

Due to the increased relevance of AC and PAC for the present dissertation both techniques are described in detail below.

2.3.1 Affinity chromatography

The chromatographic technique, exploiting the specific recognition between a ligand covalently bound to the stationary phase and a target molecule from a complex mixture, is called affinity chromatography (AC).

There are several different groups of ligand-target pairs, which are used for AC, such as, e.g., antibodies and antigens, enzymes and substrates, cofactors or inhibitors as well as lectins and carbohydrate structures. Before ligands can be immobilized, the stationary phase needs to be activated. Several types of activated matrices are commercially available including epoxide- or aldehyde-modified matrices, which were applied in the present dissertation. Both, epoxide and aldehyde groups can bind to protein amine residues forming stable secondary amine linkages. In addition, thiol, hydroxyl or carboxyl groups from potential ligands can form bonds with epoxide residues under certain condition (Rangan Mallik 2006; Turkova 2002). Spacer molecules, introduced between matrix and ligand, may enhance the accessibility to the ligand by overcoming steric hindrance of the target. Exemplarily, the covalent ligand immobilization to epoxy-activated matrices via amine or hydroxyl ligand residues, respectively, is illustrated below.

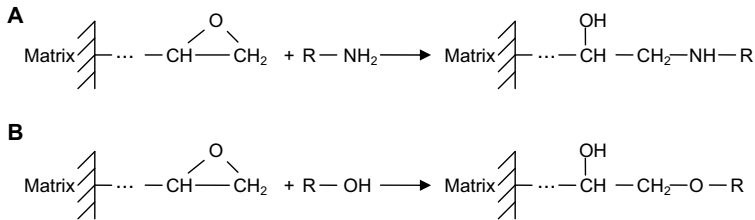


Figure 4: Schematic illustration of covalent ligand immobilization to epoxy-activated matrices via amine (A) and hydroxyl (B) ligand residues (Rangan Mallik 2006; Scopes 1994)

A simple monovalent and reversible binding of a target P to a ligand L forms a ligand-target complex PL as written in (1) (Patel et al. 1999):



The relevant kinetic constants are the association rate constant k_a [$M^{-1}s^{-1}$] and the dissociation rate constant k_d [s^{-1}]. The dissociation constant K_d [M], which measures the binding strength of P and L, can be calculated from both rate constants as shown in (2).

$$K_d = \frac{k_d}{k_a} \quad (2)$$

The association constant K_a [M^{-1}], also called affinity constant, corresponds to the reciprocal value of K_d . The affinity of the ligand to the target should be high enough to form a stable complex, and low enough to enable desorption at conditions that are not damaging to both binding partners. Compared to other chromatographic techniques, such as IEX or HIC, dissociation constants K_d of affinity-based adsorption have a wide range from 10^{-4} to 10^{-10} M (Patel et al. 1999).

The binding of virus particles to affinity ligands used in chromatography are multivalent interactions. Hence, monovalent binding models cannot be applied for determination of the association constant. However, based on Lauffenburger and Lindermann (1993) it can be used for estimation of the avidity of a multivalent binding event, which describes the overall tendency of the multivalent interaction. That means that the avidity of a complex consisting of one virus particle and multiple ligands may be higher compared to the affinity constant of one ligand bound to a single virus.

An affinity capture step is divided into different phases (Figure 5). First, the mixture is applied and transported through the porous volume of the stationary phase by the mobile phase (adsorption buffer) leading to biospecific adsorption of target components to the ligands. Second, the stationary phase is washed to remove all unbound material and, finally, the retained material is desorbed. The desorption can be done by varying the chromatographic conditions, for example, by changing the ionic strength, pH value or temperature of the mobile phase or by competitive displacement using molecules with higher concentration or increased affinity to the ligand than the adsorbed target.

Next to conventional bead-based fixed-bed chromatography, affinity interactions were utilized in expanded bed (Howard Allaker 1998) and membrane (Boi et al. 2006a; Mellado et al. 2007; Sorci et al. 2006) adsorption processes as well as affinity cross-flow filtration (Mattiasson and Ling 1986) and precipitation techniques (Gupta et al. 1996; Hilbrig and Freitag 2003; Irwin and Tipton 1995). Relevant methods for this dissertation were membrane adsorption and bead-based column chromatography, which are important techniques for industrial purification of biologicals (Curling and Gottschalk 2007). In the following, the principle of a typical bead-based affinity chromatography is exemplarily illustrated (Figure 5).

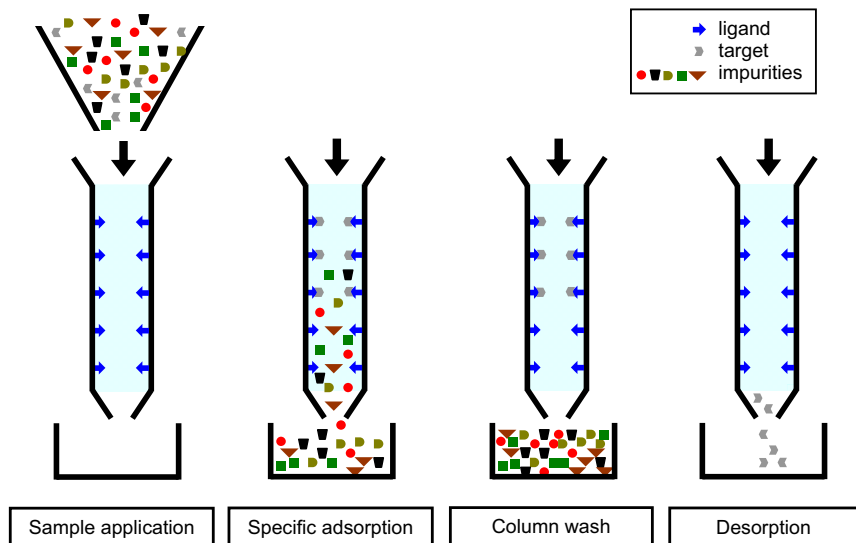


Figure 5: Principle of bead-based affinity chromatography

A major advantage of an AC process is the high selectivity, which enables good separation and concentration of the target component. Hence, affinity separations should be preferred over generic chromatography, such as IEX or SEC, whenever a safe and cost-effective ligand is available. However, AC implicates some disadvantages. For example, stability of the immobilized ligand is one of the main problems, especially during regeneration and sanitation cycles. The majority of biospecific affinity ligands, such as antibodies, lectins or enzymes, will degrade in the presence of harsh acidic or alkaline reagents. In addition, ligand leakage from the chromatographic matrix may occur. This is especially critical for leakage of toxic ligands into purified product fractions. Furthermore, naturally occurring ligands need to be produced initially, which might be cost-intensive for large-scale purposes. Certainly, that could be overcome by using small synthetic affinity ligands.

In the following paragraphs, different affinity chromatography types are described exemplarily.

Lectin affinity chromatography

Lectins are proteins, which specifically bind reversibly to a carbohydrate or a group of carbohydrates without any catalytic activity. They are ubiquitous in nature; are responsible, e.g., for cellular recognition; and usually have at least two carbohydrate-binding sites enabling them to cross-link cells possessing the corresponding carbohydrate structures (Lis and Sharon 1998). For example, *Euonymus Europaeus* lectin binds specifically to $\alpha(1,3)$ linked galactose.

Immobilized lectins have already been used for purification of glycoproteins, glycopeptides, glycolipids and virus particles (Cartellieri et al. 2002; Kristiansen et al. 1983; Merkle and Cummings 1987; Pyle et al. 1991; Smith and Torres 1989). After disintegration of the virus particles by detergents, Hayman et al. adsorbed influenza virus envelope proteins to *Lens-culinaris* phytohemagglutinin-modified sepharose (Hayman et al. 1973). A similar approach was pursued by Kristiansen et al., who used the galactose-specific *Crotalaria juncea* lectin for purification of both antigens HA and NA from detergent-treated allantoic fluids (Kristiansen et al. 1983). There, the adsorbed proteins were detached by the addition of lactose, which exhibits an increased affinity to the lectin compared to galactose.

Immunochromatography

Immunochromatography represents a further affinity-based purification method, which could be used to capture influenza virus particles with very high selectivity. However, the interactions between antibodies and antigens are mostly very strong. That requires harsh desorption conditions, which could lead to antigen degradations (Wilchek et al. 1984). Due to the constant evolution of influenza virus envelope proteins, a screen for antibodies with favourable elution conditions would have to be conducted for every single strain. Hence, the development of an antibody-based capture step was not intended in the present dissertation. Gerantes et al. purified HA and NA antigens from two egg-derived influenza virus A reassortant strains (A/Beijing/32/92 (H3N2) and A/Johannesburg/33/94 (H3N2), virus particles were pre-purified by sucrose gradient centrifugation) by virus solubilization and subsequent immunochromatography using anti-NA and anti-HA monoclonal antibodies (Gerantes et al. 1996). In that case, anti-HA-derived HA kept its antigenic properties, whereas anti-NA-derived NA was degraded partly by using an acidic desorption buffer. Sweet et al. captured heterologous egg-derived whole influenza virus particles by disulphide-linked antibodies (Sweet et al. 1974a; Sweet et al. 1974b).

Receptor-ligand interaction chromatography

Sheffield et al. established an affinity purification strategy based on the HA receptor-binding properties to human erythrocytes (Sheffield et al. 1954). In that study, 4 cycles of influenza virus adsorption and subsequent elution led to final recoveries between 13 to 29% of pure virus. A similar approach was described by Becht et al., who conjugated HA receptors from human erythrocytes to agarose beads for separation of avian influenza HA (Becht and Rott 1972). Furthermore, Holmquist et al. recovered 40% of non-inactivated egg-derived influenza virus particles from a column of α -N-acetylneuraminic acid-sepharose (Holmquist and Nilsson 1979). However, due to low viral recoveries compared to conventional purification techniques, these laboratory methods are not applicable for industrial purposes.

Cuatrecasas and Illiano described an affinity chromatography step for viral neuraminidases utilizing a neuraminidase inhibitor (*N*-(*p*-aminophenyl) oxamic acid) bound to agarose beads (Cuatrecasas.P and Illiano 1971). That method was further developed, including immunogenic characterization of influenza virus neuraminidase

vaccines in mice and rabbits (Bucher 1977; Hocart et al. 1995; Kharitononkov et al. 1982).

Aptamer affinity chromatography

Another affinity-based purification approach is the application of nucleic acid aptamers, which are small synthetic oligonucleotides binding specifically to certain proteins. They have been successfully used as ligands in protein purification processes (Hutanu and Remcho 2007; Romig et al. 1999). This technique may also be useful for influenza virus capturing (Gopinath et al. 2006; Misono and Kumar 2005). However, precautions, such as nucleotide backbone modifications, are necessary to protect the aptamers against digestion by nucleases from cell culture supernatant. Therefore, aptamer-based large-scale purification might be very cost intensive.

Recombinant tagged protein purification

Due to the construction of fusion proteins containing affinity tags, recombinant proteins can be purified easily and efficiently by AC. Therefore, several affinity tags are available, which were reviewed recently (Terpe 2003). As an example, HA from influenza virus A/FPV/Rostock/34 was modified with six histidine residues, produced in insect and mammalian cells and subsequently purified by immobilized nickel chromatography (Daublebsky von Eichhain 1997). However, due to genetic drift of the viral envelope proteins new recombinant HA has to be produced constantly if this technique is to be intended for vaccine manufacturing. This would be an additional time-consuming step, which could delay the vaccine production process.

2.3.2 Pseudo-affinity chromatography

Affinity separation methods exhibit important advantages, such as high target selectivity, which leads to high purity at a reduced number of purification steps. However, biospecific ligands are often expensive, difficult to produce and have a narrow range of conditions where ligand stability is guaranteed. Pseudo-affinity chromatography (PAC), which applies robust and reasonable-priced substitutes for the biological ligands, may overcome such drawbacks (Vijayalakshmi 1989). These ligands may be specific enough to allow single-step purification protocols with similar

purity results compared to biospecific ligands. As examples, Vijayalakshmi reviewed immobilized metal, dye-ligand and histidine-ligand PAC (Vijayalakshmi 1989). In this dissertation, the definition of pseudo-affinity chromatography is expanded to chromatographic matrices based on sulphated carbohydrates, e.g., heparin.

Heparin and sulphated carbohydrates

Heparin is a heavily sulphated glycosaminoglycan consisting of hexuronic acid and D-glucosamine residues (Rabenstein 2002). The fact that influenza virus envelope proteins bind to heparin was earlier described (Anonym 2006). Column-based chromatographic material Cellufine[®] sulphate, which contains sulphated cellulose beads and imitates heparinized resins, was applied in vaccine production processes as pseudo-affinity chromatographic matrix by several groups (Oka et al. 1985; Palache et al. 1997; Peterka et al. 2007; Van Scharrenburg and Brands 1998). As cellulose beads contain a low concentration of sulphate esters, the charge density of Cellufine[®] sulphate is lower compared to commonly used ion-exchangers. Thus, adsorption of a wide range of viruses is caused by pseudo-affinity binding rather than electrostatic adsorption (O'Neil and Balkovic 1993). Furthermore, studies reported an influence of dextran-sulphate on virus attachment, and cell membrane fusion indicated the affinity of sulphated glucose to virus proteins (Herrmann et al. 1992; Lüscher-Mattli et al. 1993; Ramalho-Santos and Pedroso de Lima 2001). The structure similarity of heparin and sulphated cellulose is illustrated in Figure 6.

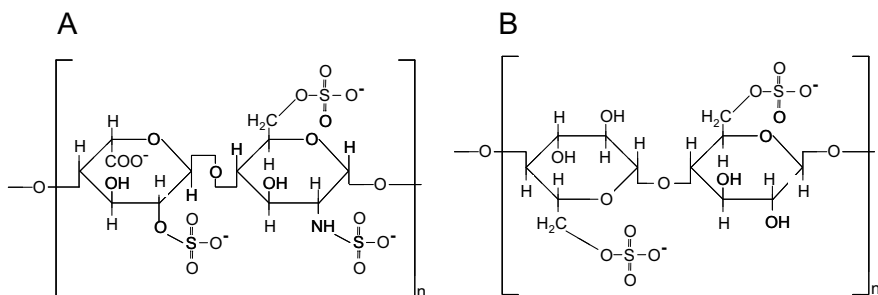


Figure 6: Example of a disaccharide unit of heparin (A, based on Rabenstein 2002) and sulphated cellulose (B, based on manufacturer's (Chisso Corporation, Japan) application notes of Cellufine[®] sulphate)

Both, heparin and Cellufine[®] sulphate chromatography were also used successfully for preparation of herpes simplex virus vaccines (O'Keeffe et al. 1999). In addition, retrovirus vectors were purified by adsorption to heparin resins (Segura et al. 2005).

Immobilized metal affinity chromatography

Immobilized metal affinity chromatography (IMAC) depends on the accessibility of the target component's histidine residues for attached metal ions and was first described by Porath and colleagues (Porath et al. 1975). It is used widely for purification of histidine-tagged recombinant proteins (Hochuli et al. 1988), but also for native proteins (Charlton and Zachariou 2007). There are only a few studies describing the application of IMAC for the purification of viral particles. For example, zinc chelate membrane adsorption was used to capture MDCK cell culture-derived influenza virus A/Puerto Rico/8/34 in the presence of 1 M NaCl leading to about 64% viral recovery based on hemagglutination activity (Opitz et al. 2009). This method could deplete the host cell DNA and total protein content to approximately 7% and 26%, respectively. However, this technique could not be used for various other influenza virus strains, which is crucial for vaccine production processes. Therefore, IMAC is not applicable for influenza virus vaccine production. A possible reason for that might be the inaccessibility of certain amino acids from the viral envelope proteins to the immobilized zinc ions (Opitz et al. 2009).

In addition, zinc chelate affinity chromatography was used for adsorption of adenoviruses and adeno-associated viruses (Lee et al. 2009; O'riordan et al. 2000) and viral vectors containing therapeutic genes (Shabram et al. 1998).

Following table summarizes different affinity as well as pseudo-affinity chromatography methods for the purification of influenza virus particles or viral proteins (Table 1).

Table 1: Examples of different approaches for capturing of whole influenza virus particles or viral proteins by affinity and pseudo-affinity chromatography

Ligands - targets	Properties	References
Lectin affinity chromatography		
lectins –	<ul style="list-style-type: none"> ● carbohydrate group specific 	Hayman et al. 1973
carbohydrate structures	<ul style="list-style-type: none"> ● adsorption and selectivity ● gentle competitive desorption using suitable carbohydrates ● lectins may be toxic and expensive 	Kristiansen et al. 1983
Immunoaffinity chromatography		
antibodies –	<ul style="list-style-type: none"> ● high selectivity 	Gerantes et al. 1996
antigens HA, NA	<ul style="list-style-type: none"> ● mostly very strong adsorption ● desorption at harsh conditions may lead to virus degradation ● antigenic drifts require frequent ligand adaptation 	Sweet et al. 1974a Sweet et al. 1974b
Receptor-ligand interaction chromatography		
sialic acid – HA;	<ul style="list-style-type: none"> ● high HA or NA receptor-specific selectivity 	Becht and Rott 1972 Bucher 1977
NA inhibitors – NA	<ul style="list-style-type: none"> ● ligands may be expensive ● desorption by e.g., salt or pH gradient 	Cuatrecasas and Illiano 1971 Hocart et al. 1995 Holmquist and Nilsson 1979 Kharitononkov et al. 1982 Sheffield et al. 1954
Aptamer affinity chromatography		
aptamers –	<ul style="list-style-type: none"> ● high selectivity 	not applied for influenza virus
envelope proteins	<ul style="list-style-type: none"> ● protection of aptamer by nucleotide backbone modifications necessary ● ligands may be expensive 	purification yet
Tagged recombinant protein affinity chromatography		
e.g.: metal ions –	<ul style="list-style-type: none"> ● high selectivity 	Daublebsky von Eichhain 1997
histidine residues	<ul style="list-style-type: none"> ● high variety of affinity tags available ● efficient capturing method ● antigenic drifts require frequent production of newly tagged proteins 	

Ligands - targets	Properties	References
Heparin and sulphated carbohydrates chromatography		
heparin or sulphated carbohydrates – envelope proteins	<ul style="list-style-type: none"> • lower selectivity than ligands listed above • high ligand stability • economic capturing method • gentle desorption using NaCl gradients 	Anonym 2006 O'Neil and Balkovic 1993 Oka et al. 1985 Palache et al. 1997 Peterka et al. 2007 Van Scharrenburg and Brands 1998
Immobilized metal affinity chromatography		
metal ions – native histidine residues	<ul style="list-style-type: none"> • economic capturing method • strong dependency on accessibility of native histidine residues • desorption using imidazole • metal ion leakage possible 	Opitz et al. 2009

2.3.3 Column versus membrane-based chromatography

Conventionally, bead-based column resins were used for chromatographic bioseparation processes. The majority of commercially available beads have porous structures leading to increased surface areas and therefore to higher protein-binding capacities compared to nonporous beads. But chromatography beads have several disadvantages, such as time-consuming pore diffusions (Charcosset 2006) or limited scalability in axial directions due to mechanical stability restrictions (Kang and Ryu 1991). Furthermore, bead-based column chromatography creates high back pressure leading to suboptimal flow rates. Monolithic columns (Alois Jungbauer 2004; Champagne et al. 2007; Kalashnikova et al. 2008) and membrane-based adsorption technologies (Charcosset 2006; Ghosh 2002) overcome these drawbacks. Due to much larger pores and channels in the micrometer range, both materials generate significant lower back pressures allowing higher velocities and lower residence times. Therefore, they became more important for biological separations.

Membrane adsorbers have several additional advantages, such as the avoidance of column packing and column validations or increased pressure tolerance (Charcosset 2006; Ghosh 2002). Furthermore, membrane adsorbers can be used as disposable units reducing the expenses for cleaning, sanitization and validation efforts. While pores from chromatographic beads increase the adsorption area and therefore the binding capacity for proteins, they are inappropriate for capturing large target particles, such as influenza viruses, due to steric hindrance. Hence, membrane adsorbers have

the potential to improve the productivity of influenza virus purification processes for vaccine production.

Schematic cross-sections of membrane adsorbers and porous beads, illustrating the advantages of membrane adsorption, are shown below (Figure 7).

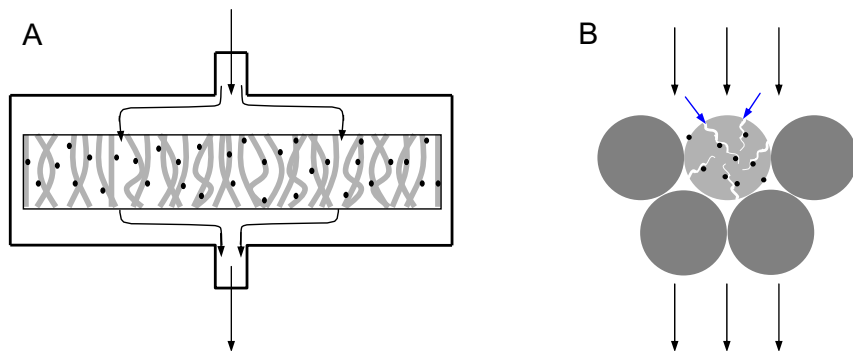


Figure 7: Schematic cross-section of a membrane layer (A) and chromatographic beads (B) (black dots: immobilized ligands; black arrows: flow direction of mobile phase; blue arrows: pore diffusion)

Membrane adsorbers have already been used for affinity separation of different target molecules, e.g., recombinant proteins (Cattoli et al. 2006; Mellado et al. 2007), antibodies (Boi et al. 2006b; Castilho et al. 2002; Platonova et al. 1999) or lectins (Boi et al. 2006a; Sorci et al. 2006). In addition, membrane-based ion-exchange chromatography was applied successfully for purification of several virus species, including, for example, insect baculoviruses (Wu et al. 2007), mosquito-specific parvoviruses (Czermak et al. 2008; Specht et al. 2004), alpha-herpesviruses (Karger et al. 1998), adenovirus vectors (Peixoto et al. 2008) or influenza viruses (Kalbfuß et al. 2007b). Furthermore, immobilized metal affinity membrane adsorption using zinc ions was applied for separation of adenoviral vectors (Lee et al. 2009) and influenza virus particles (Opitz et al. 2009).

2.4 Regulations and purity requirements for influenza vaccines

Concerning quality and safety issues human vaccines underlie strict criteria specified in the European Pharmacopoeia and edited by the European Directorate for the Quality of Medicines & HealthCare. According to these regulations all cell culture- and

egg-derived inactivated human influenza vaccines have to contain 15 µg HA per strain and trivalent dose unless clinical evidence requires a different amount (European Pharmacopoeia 6.0: 803, 808; European Pharmacopoeia 6.4: 4557, 4559). Independent of the virus origin the total protein content of whole human influenza virus vaccines has to be no higher than 6 times the total HA amount. However, there is a maximum limit of 100 µg total protein per strain and 300 µg per trivalent dose. The maximum protein content (other than HA) of subunit human influenza vaccines is 40 µg per virus strain and 120 µg per trivalent dose.

In addition, the nucleic acid contaminants of cell culture-derived whole and subunit influenza virus vaccines need to be depleted to at least 10 ng per dose.

To characterize the chromatographic separations and verify the product purities according to the European Pharmacopoeia several analytical methods are crucial. As described in Chapter 3, purification experiments were evaluated by balancing the viral content and impurity depletions of all chromatographic fractions using the hemagglutination activity assay as well as a total protein and DNA assay, respectively. In addition, an immunodiffusion assay served for viral quantification of the purified product fractions. Biological assays could have relatively high analytical errors. For example, the hemagglutination activity assay (Chapter 3.6.1), which is based on logarithmically scaled estimation of cell agglutination, has an analytical error of 15% (Kalbfuß et al. 2007a). Hence, balancing of virus particles or contaminants led to overall recoveries that differed from 100%.

In addition, qualitative analysis was done by separating the chromatographic fractions on an SDS-polyacrylamide gel to evaluate the protein depletion.

2.5 Binding studies by surface plasmon resonance technology

A useful tool to characterize the interaction of virus particles and ligands is the surface plasmon resonance (SPR) technology (Jönsson et al. 1991; Karlsson et al. 1991; Malmqvist 1993), which is a sensor-chip-based label-free method done with the Biacore system (GE Healthcare, Uppsala, Sweden).

The principle of SPR analysis using the Biacore system is illustrated schematically in Figure 8. Polarized light is reflected on one side of the glass sensor-chip. The intensity of the reflected light is measured by a photodetector. SPR appears at a certain light angle that is observable at the minimum of reflected light and depends on the

refractive index of the area, which is close to the chip surface. The other side of the sensor-chip can be modified with the ligand of interest. Immobilization is possible through biotin-streptavidine linkages or covalent bonds. Any binding or dissociation events to or from these ligands cause changes of the refractive index leading to variations of the angle where the reflected light has its minimum intensity. These resonance signals R are directly proportional to the adsorbed mass and are expressed as response units [RU]. Hence, real-time measurements can be used for kinetic analysis of association and dissociation events.

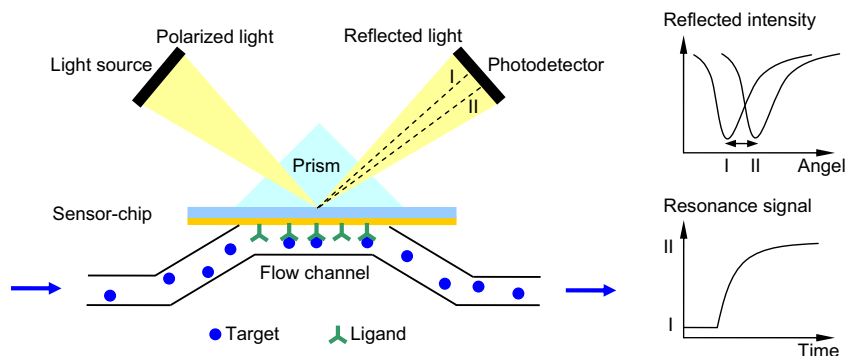


Figure 8: Schematic principle of interaction analysis by surface plasmon resonance technology (based on: Karlsson et al. 1991)

A typical binding experiment is designed in three parts. First, during the association phase target molecules are flushed over the ligand-modified surface. Second, the dissociation phase allows the targets to detach to some extent from the ligands, which depends on the binding strength between ligand and target, by using regular adsorption buffer. From this phase the dissociation rate can be obtained. Finally, the surface needs to be regenerated to detach all targets bound to the ligands. Therefore, regeneration conditions have to be chosen carefully to ensure reproducible analysis.

Karlsson et al. described the theoretical background for the evaluation of affinity and kinetic data obtained from the Biacore system studying antibody-antigen interactions that is summarized below (Karlsson et al. 1991). Assuming that the ligand is tightly bound to the sensor-chip surface and the buffer conditions stay constant during each single phase of the interaction experiments, all resonance signal changes rely on association or dissociation of the target molecules. The formation of target-ligand

complexes PL (1) is described in (3) and depends on the concentrations of the free targets [P] and ligands [L] as well as on the stability of the complex [PL].

$$\frac{d[PL]}{dt} = k_a[P][L] - k_d[PL] \quad (3)$$

Based on Karlsson et al. equation (3) can be rewritten in terms of the change of response signal R (Karlsson et al. 1991).

$$\frac{dR}{dt} = k_a C(R_{\max} - R) - k_d R \quad (4)$$

There, the complex concentration [PL] is proportional to the response signal R and the total ligand concentration is proportional to the maximum response signal R_{\max} . Hence, the free ligand concentration [L] is the difference of the response signals R_{\max} and R. The free target concentration [P] is given as symbol C [M].

From (4) follows:

$$\frac{dR}{dt} = k_a C R_{\max} - (k_a C + k_d) R \quad (5)$$

Subsequently, the slopes from a plot of dR/dt against R for several different target concentrations C can be used in another plot against C to estimate the association constant k_a [$M^{-1}s^{-1}$] and the dissociation rate constant k_d [s^{-1}]. In addition, k_d can also be obtained from the dissociation phase response signals. Since there is no target in the running buffer during the dissociation phase, equation 4 can be simplified to (6), which can be used for estimation of k_d .

$$\frac{dR}{dt} = -k_d R \quad (6)$$

From both kinetic constants the affinity constant K_a and dissociation constant K_d [M] can be calculated according to equation (2).

Virus particles have multiple potential ligand-binding sites on their surfaces leading to multivalent binding. In such cases a simple binding model established for monovalent interactions and described above cannot be used. However, this model serves to characterize the overall binding tendency of a multivalent interaction, which is also

called avidity constant (Lauffenburger and Linderman 1993). Multiple ligand-binding sites on virus particles may lead to increased binding to immobilized ligands on chromatographic resins.

3 Material and Methods

In this chapter the production of cell culture-derived influenza virus particles is presented followed by a description of the chromatography and analytical methods. These methods are structured in accordance with the classification into AC and PAC as well as to the subdivision of the LAC studies.

3.1 Influenza virus production, harvest, clarification, inactivation and concentration

The preparations of influenza virus particles differed regarding the cultivation systems, host cells, culture media, virus strains, harvests of cultivation broths and virus concentration methods depending on the particular dissertation part and aim. The descriptions of these virus preparations were classified regarding the corresponding project tasks.

LAC was first developed for the influenza virus A/Puerto Rico/8/34 (H1N1) produced in roller bottles, inactivated chemically, clarified by centrifugations and concentrated by a stirred ultrafiltration unit. Second, virus particles used for LAC matrix selection were from the same virus strain, but produced in bioreactors using microcarriers, clarified by filtration, inactivated chemically and concentrated by cross-flow ultrafiltration. Third, the transferability of the developed LAC method was evaluated using different host cells (MDCK and Vero cells) and two additional influenza virus strains (A/Wisconsin/67/2005 (H3N2), B/Malaysia/2506/2004) produced by the vaccine manufacturer Novartis Behring (Marburg, Germany).

All three influenza virus strains applied for PAC were produced in microcarrier bioreactor systems and treated again by filtration, inactivation and cross-flow ultrafiltration.

The virus production methods and the corresponding experimental applications are summarized below (Figure 9, Figure 10).

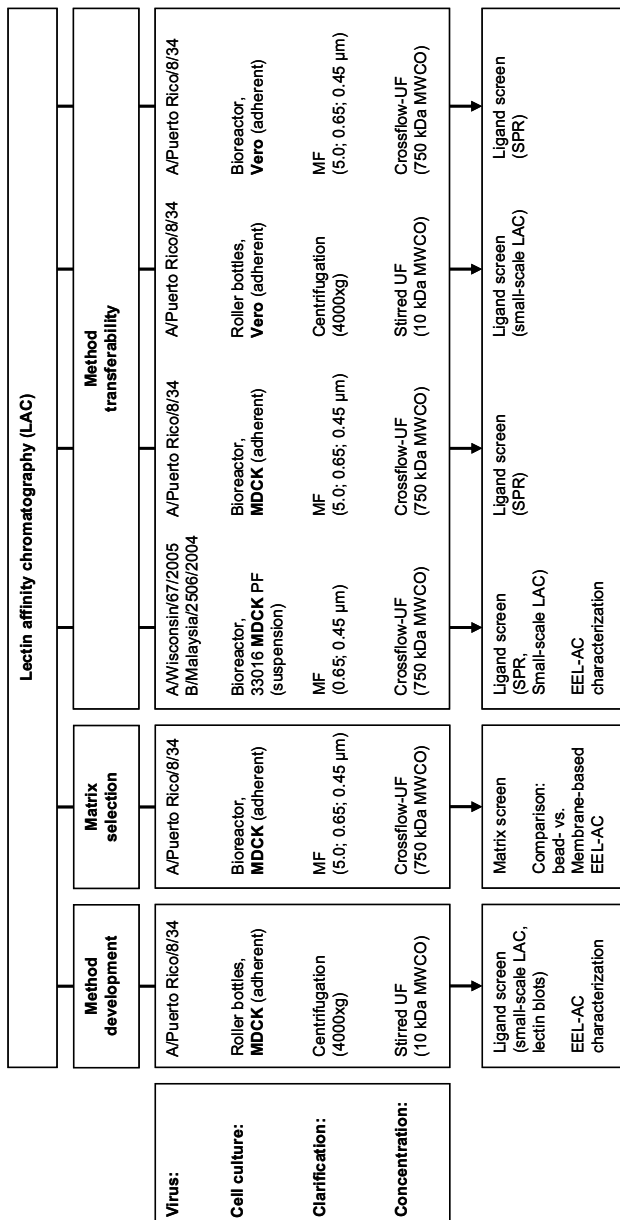


Figure 9: Overview of virus productions used for LAC experiments (MF: microfiltration, UF: ultrafiltration)

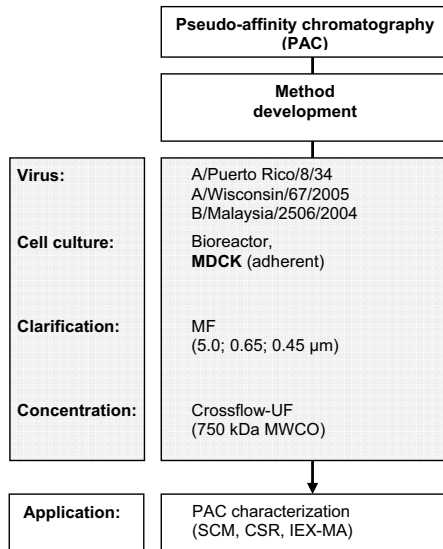


Figure 10: Overview about virus production used for PAC experiments (MF: microfiltration, UF: ultrafiltration)

3.1.1 Influenza virus A/Puerto Rico/8/34 production for LAC method development

Adherent MDCK cells (#841211903, ECACC, Salisbury, UK) were grown in roller bottles (Greiner, Germany, 850 cm²) containing 250 ml Glasgow minimum essential medium (GMEM) -based media (#22100-093, Invitrogen/Gibco, Karlsruhe, Germany). The cell growth medium was supplemented with 4 g/l NaHCO₃ (#1.06329.1000, Merck KGaA, Darmstadt, Germany), 10% (v/v) fetal calf serum (FCS, #10270-106, Invitrogen/Gibco, Karlsruhe, Germany), 2 g/l peptone (#MC33, International Diagnostic Group, London, UK) and with additional glucose to a final concentration of 5.5 g/l (#X997.2, Carl Roth GmbH & Co. KG, Karlsruhe, Germany). The cells were grown at 37 °C for 4 to 6 days until confluence. Afterwards the cells were washed with phosphate-buffered saline (PBS) and medium was changed to cell growth medium containing 10 mg/l porcine trypsin (#27250-018, Invitrogen/Gibco, Karlsruhe, Germany) without FCS and additional glucose. The confluent culture was infected with human influenza virus A/Puerto Rico/8/34 (H1N1; MOI=0.025) from NIBSC (#99-716, South Mimms, UK) at 37 °C. After 3 days the virus was harvested.

Prior to any of the downstream processes, all batches (a total of 6) of unclarified virus culture broth were inactivated by adding β -propiolactone (#33672.01, Serva Electrophoresis, Heidelberg, Germany) to a final concentration of 12 mM for 24 h at 37 °C. The inactivated broths were stored at 4°C until innocuity was confirmed. The cell debris was removed from the inactivated culture broth by centrifugation (4000 x g) at 4°C for 10 min. For all further investigations (lectin blot analysis, AffiSpin® column screening and lectin affinity chromatography) the preclarified cell culture broths containing inactivated human influenza A viruses were 15–20-fold concentrated using a stirred ultrafiltration unit (model 8200, #5123, Millipore Corporation, Schwalbach, Germany) with a 10 kDa MWCO polyethersulfone membrane under a pressure of 4 bar at 4 °C. The concentrate was aliquoted and stored at -80 °C until further usage.

3.1.2 Influenza virus A/Puerto Rico/8/34 production for LAC matrix selection

Human influenza virus A/Puerto Rico/8/34 (H1N1; #99-716, NIBSC, South Mimms, UK) was produced in adherent MDCK cells (#841211903, ECACC, Salisbury, UK) as described by Genzel et al., but with 2 g/l microcarrier (Cytodex 1, #17-0448, GE Healthcare, Freiburg, Germany) (Genzel et al. 2004).

After virus propagation the cultivation broths were harvested by sequential depth filtration (5 and 0.65 μ m, #CFAP0508YY, #CFAP9608YY, GE Water & Process Technologies, Trevose, USA) and inactivated chemically with β -propiolactone (final concentration: 3 mM, #33672.01, Serva Electrophoresis, Heidelberg, Germany) for 24 h at 37 °C. Innocuity of inactivated broths was confirmed by serial transfer in two 75 ml confluent MDCK cell cultures. Virus broths were clarified again by a 0.45 μ m membrane filter to remove remaining cell debris or precipitates (#CMMP9408YY, GE Water & Process Technologies, Trevose, USA). Subsequently, broths were concentrated by cross-flow ultrafiltration to a HA-activity titer of 3.3 to 3.7 (corresponding to about 20 to 50 kHAU/ml) using a polysulfone hollow-fibre membrane (750 kDa MWCO, 420 cm², UFP-750-E-4MA, GE Healthcare, Uppsala, Sweden) as described by Kalbfuß et al. (Kalbfuß et al. 2007a). Virus concentrates were aliquoted and stored at -80 °C until further usage.

3.1.3 Influenza virus production for LAC transferability studies

MDCK cell-derived influenza virus production

Human influenza virus A/Wisconsin/67/2005 (H3N2) and B/Malaysia/2506/2004 were produced in Novartis Behring proprietary suspension cell line 33016 MDCK PF (serum free medium), inactivated with β -propiolactone (end dilution 1:2000 v/v, Ferak Berlin) and filtered (0.65 μm and 0.45 μm , PN: 5232506D1-P, Sartorius Stedim Biotech GmbH, Göttingen, Germany) according to the Optaflu[®] process procedure by Novartis Behring, Marburg, Germany¹. The two virus broths supplied by Novartis Behring were clarified again at the Max Planck Institute with a 0.45 μm membrane filter and concentrated by cross-flow ultrafiltration as described before in Chapter 3.1.2.

Propagation of human influenza virus A/Puerto Rico/8/34 (H1N1, Robert Koch Institute, Berlin, Germany) in adherent MDCK (#841211903, ECACC, Salisbury, UK, cultivated in serum-containing medium) cells as well as cultivation broth harvest, virus inactivation, culture broth clarification, virus particle concentration and storage were performed as described in Chapter 3.1.2.

Vero cell-derived influenza virus production

MCDK-cell-derived human influenza virus A/Puerto Rico/8/34 (H1N1, #99-716, NIBSC, South Mimms, UK) was used to infect adherent Vero cells from ECACC (#88020401, Salisbury, UK) cultivated in roller bottles. Virus harvests were inactivated and concentrated as described previously under 3.1.1. The preparation procedure and the virus strain were chosen to ensure comparability to the lectin-binding study for LAC development using MDCK cell-derived influenza virus particles (see above).

In addition, Vero cell-adapted influenza virus A/Puerto Rico/8/34 (H1N1, Robert Koch Institute, Berlin, Germany) was produced in a microcarrier culture as described before for cultivation of adherent MDCK cells in bioreactors. Harvesting of cultivation bulk, inactivation and concentration were also carried out as reported before in 3.1.2. This virus batch was included in the comparative SPR analysis (see Chapter 3.4.1).

¹ personal communication: Lübben, H., Novartis Behring, Marburg, Germany

3.1.4 Influenza virus production for pseudo-affinity chromatography studies

The production of human influenza virus strains (A/Puerto Rico/8/34, H1N1, Robert Koch Institute, Berlin, Germany; A/Wisconsin/67/2005, H3N2, #06/112, NIBSC, South Mimms, UK; B/Malaysia/2506/2004, #06/104, NIBSC, South Mimms, UK) in adherent MDCK (#841211903, ECACC, Salisbury, UK) cells as well as harvesting, virus inactivation, clarification, concentration and storage were done as described in the previous section 3.1.2.

3.2 Material and methods for the LAC development

The following subchapters describe techniques used for the LAC development including lectin-virus adsorption screening for the influenza virus A/Puerto Rico/8/34. Furthermore, virus-capturing experiments using the two most promising lectins as ligands were described.

3.2.1 Ligand screening for LAC

The initial focus of this dissertation was the selection of a suitable lectin as affinity ligand for an influenza virus capture step. With respect to the potential HA glycostructures (see Chapter 2.1), some relevant lectins targeting terminal galactose in $\beta(1,4)$, $\alpha(1,3)$ and $\beta(1,3)$ -linkage, fucose and mannose were chosen for a lectin-binding screening via lectin blots and small-scale affinity chromatography studies. If viral neuraminidase activity is reduced, the N-glycan structure could be fully elaborated and contain terminal sialic acid (Debray et al. 2002). Therefore, sialic acid-binding lectins such as *Maackia amurensis* leucoagglutinin (MAL I) or *Sambucus nigra* lectin (SNA) were also screened for viral binding.

Lectin blot analysis

Biotinylated lectins were purchased from Vector Laboratories Inc., USA (Table 2). Human influenza virus A/PuertoRico/8/34 (H1N1) proteins were separated on 10% SDS-PAGE (Laemmli 1970) and transferred onto polyvinylidene difluoride (PVDF) membranes (#170-3958, BioRad, Munich, Germany). In addition, MDCK cell proteins from non-infected lysed cell cultures were loaded on the same protein gels. After protein transfer the membrane was blocked for 15 h (3% BSA or 5% dry milk in PBS with 0.1% Tween20) and treated with 0.01 mg/ml biotinylated lectins for 2 h (binding

buffer: 150 mM NaCl, 50 mM Tris, 0.1% Tween20, pH 7.4). The binding buffer for the negative control blots, which were treated separately, contained additionally an appropriate carbohydrate purchased from Sigma-Aldrich, Schnellendorf, Germany (AAL: 0.2 M fucose; Con A: 0.3 M mannose; ECL: 0.3 M lactose; EEL: 0.5 M lactose; jacalin: 0.2 M melibiose; MAL I: 0.5 M lactose; PNA: 0.2 M galactose; SNA: 0.5 M lactose). A biotinylated protein ladder from Cell Signaling Technology, Inc. (#7727, Danvers, USA) was used for protein size identification. Bound lectins were detected via chemiluminescence using a streptavidine-peroxidase polymer (#S-2438, Sigma-Aldrich, 1.1 µg/ml in binding buffer, 2 h) and the SuperSignal® West Pico chemiluminescent substrate from Pierce Biotechnology, Inc. (#34077, Rockford, USA). Membrane washing steps (3 times 10 min, PBS + 0.02% Tween20) were necessary between every incubation step.

Table 2: Biotinylated lectins from Vector Laboratories Inc. used for affinity screening towards human influenza virus A/Puerto Rico/8/34 glycoproteins via lectin blots

Lectin	Specificity	Cat. no.
<i>Aleuria Aurantia lectin (AAL)</i>	fuc(α 1,6)glcNAc; fuc(α 1,3)[gal(β 1,4)glcNAc]	B-1395
<i>Arachis hypogaea Agglutinin (PNA)</i>	β -gal, gal(β 1,3)galNAc	B-1075
<i>Artocarpus integrifolia (AIL, Jacalin)</i>	gal(β 1,3)galNAc; α -gal	B-1155
<i>Concanavalin A (Con A)</i>	α -man; α -glc; α -glcNAc	B-1005
<i>Erythrina Christagalli lectin (ECL)</i>	gal(β 1,4)glcNAc; galNAc, gal	B-1145
<i>Euonymus Europaeus lectin (EEL)</i>	gal(α 1,3)gal	B-1335
<i>Maackia Amurensis lectin I (MAL I)</i>	NeuAc(α 2,3)gal; gal	B-1315
<i>Sambucus Nigra Bark lectin (SNA)</i>	NeuAc(α 2,6)gal; NeuAc(α 2,6)galNAc	B-1305

Lectin screening using small-scale chromatographic columns

AffiSpin® kits, small centrifugal columns, were purchased from GALAB Technologies GmbH, Geesthacht, Germany (Table 3). These spin columns contained 100 µl affinity ligand matrix composed of a covalently bound lectin to polymer beads (particle mean diameter: 65 µm, pore size: 100 nm). The AffiSpin® columns were first equilibrated with 150 mM NaCl, 50 mM Tris, 1 mM MnCl₂, 1 mM CaCl₂ and 1 mM MgCl₂, pH 7.4 (adsorption buffer 1, AB1) and then loaded with 750 µl of the preclarified and

inactivated human influenza A virus concentrate (A/PuertoRico/8/34, H1N1). To ensure complete binding, the sample was circulated five times over the column. A washing step of 2 x 500 μ l AB1 removed all unbound sample material from the column. Elution was done in several steps using adsorption buffers containing the appropriate carbohydrates. In cases of slow release the elution buffer was incubated in the column without any flow for approximately 1 h until no further eluted HA-activity could be detected. All steps mentioned above were done by applying centrifugal forces of 10 x g until the buffer or sample, respectively, passed completely through the column. Finally, the lectin-virus affinity was analyzed by virus titration of all fractions. Therefore, HA activities of the individual elution fractions were summarized.

Table 3: AffiSpin[®] Kits (GALAB Technologies GmbH, Geesthacht, Germany) used for lectin-virus affinity screening

AffiSpin [®] Kit	Specificity	LD ^a [mg/ml]	Cat. No.
<i>Erythrina Christagalli lectin (ECL)</i>	gal(β 1,4)glcNAc; galNAc, gal	7,7	051161
<i>Euonymus Europaeus lectin (EEL)</i>	gal(α 1,3)gal	4,9	custom-made
<i>Maackia Amurensis lectin I (MAL I)</i>	NeuAc(α 2,3)gal; gal	4,5	051131
<i>Arachis Hypogaea Agglutinin (PNA)</i>	β -gal, gal(β 1,3)galNAc	8,0	051061
<i>Sambucus Nigra Bark lectin (SNA)</i>	NeuAc(α 2,6)gal; NeuAc(α 2,6)galNAc	4,6	051121

^a ligand density according to manufacturer

3.2.2 Characterization of LAC-FPLC using the model strain A/Puerto Rico/8/34 and the lectins ECL and EEL

After lectin screening, binding kinetics of two lectins, ECL and EEL, as affinity ligands were compared to each other. Finally, the lectin with the highest affinity towards the influenza hemagglutinin, the highest viral specificity versus host cell proteins and the best economic features was used as the ligand for the capture affinity chromatography.

All chromatographic runs were performed with an Äkta Explorer system (GE Healthcare, Uppsala, Sweden). The chromatographic material used for FPLC (ECL- and EEL-adsorbent matrix) was purchased from Galab Technology GmbH and was identical (except ligand density) to the one used for AffiSpin[®] column experiments.

One ml of each adsorbent (ligand density: ECL: 7.7 mg/ml, EEL: 3.1 mg/ml) was packed into a water-jacketed C 10/20 column (GE Healthcare-Uppsala Sweden). The temperated (4°C) columns were equilibrated and washed with AB1. For the scouting experiments 1 ml MDCK cell-derived 15 x concentrate of human influenza virus A/PuertoRico/8/34 was loaded.

Virus detection and monitoring were done by light scattering (90°, Dawn EOS, Wyatt Technology Europe GmbH, Dernbach, Germany) and by hemagglutination assays of pooled fractions. In addition, all pooled fractions were analyzed for protein and DNA content.

EEL – AC

The concentrate (44.1 kHAU/ml; ± 4.4) was loaded directly to the EEL-polymer column at 0.2 ml/min without sample recirculation. After washing with AB1 the bound viruses and viral membrane glycoproteins were eluted with 0.5 M lactose in AB1 until no further virus particles were detected by light scattering (elution 1, Figure 12). A second elution and column regeneration step was done by applying 0.5 M lactose in 2 M NaCl, 50 mM Tris, 1 mM MnCl₂, 1 mM CaCl₂ and 1 mM MgCl₂ at pH 7.4 until no further virus eluted, but for not longer than 20 min (elution 2, Figure 12). An intensive column cleaning with AB1 followed. Elution and regeneration were performed at a flow rate of 0.5 ml/min.

The dynamic binding capacity (0.2 ml/min) was estimated with 8 ml of 19 x concentrate (44.1 kHAU/ml; ± 4.4) and the mass balancing was done with 4 ml from same sample using a 3 ml EEL-polymer matrix (ligand density: 4,3 mg/ml).

ECL – AC

The immobilized lectin density was equal to the ECL AffiSpin® Kit with 7.7 mg/ml. Loading of the ECL-affinity column was performed as for the EEL column and by recirculation of the samples for 15 h (0.5 ml/min). After washing, virus release was achieved by applying 0.5 M lactose in AB1 until no further elution could be detected by light scattering. Subsequently, the flow was stopped and the affinity matrix was incubated in elution buffer (AB1 + 0.5 M lactose) for 2 hours. The elution was continued by rinsing the column with 5 column volumes of the same elution buffer. The second elution and regeneration of the column was done as before using 0.5 M

lactose in 2 M NaCl, 50 mM Tris, 1 mM MnCl₂, 1 mM CaCl₂ and 1 mM MgCl₂, pH 7.4, and a following washing step with AB1. Elution and regeneration were performed at a flow rate of 0.5 ml/min.

3.3 Material and methods for the LAC matrix selection

The following sections list the tested supports for the LAC-matrix screening and describe the chromatographic conditions used for screening. In addition, the detailed characterization experiments are explained.

3.3.1 Chromatographic materials

The polymer and agarose matrices were obtained from the supplier with immobilized EEL. All other materials were purchased without ligands. Here, lyophilized EEL from Vector Laboratories, Inc. (#L-1330, Burlingame, USA) was immobilized to the matrices. The ligand densities were estimated photometrically by measuring the absorption (280 nm) of the ligand solutions before and after ligand immobilization. Using the Lambert-Beer law (equation 7; A: absorption, ϵ : molar absorption coefficient, c_L : ligand concentration in solution, d: light path lengths) the remaining ligand concentration in the supernatant after immobilization can be estimated and, therefore, the immobilized ligand amount can be determined.

$$A = \epsilon * c_L * d \quad (7)$$

EEL-polymer resins were purchased from GALAB Technologies GmbH (custom-made, Geesthacht, Germany). Particles have a mean diameter of 65 μm and a mean pore diameter of 100 nm. The ligand densities of the two individual batches of covalently immobilized EEL were 4.3 mg/ml and 5.0 mg/ml (manufacturer information). *EEL agarose*– EEL immobilized on cross-linked Sepharose 4B was purchased from Vector Laboratories, Inc. (#AL-1333, Burliname, USA). The ligand density was 3 mg/ml of settled gel (manufacturer information). *EEL Actigel ALD* – Actigel ALD (#2701-13, Sterogene Bioseparation, Inc., Carlsbad, USA) has a bead size of 60 to 160 μm and consists of 4% agarose. Using the manufacturer's protocol and buffers 3.5 mg EEL was coupled to 1 ml matrix (6 h, room temperature).

EEL Trisopor[®] – Trisopor[®] 4000 Diol is a matrix consisting of activated porous glass particles (#5330, VitraBio GmbH, Steinach, Germany). It has a particle size from 125 to 200 μm and a pore size of 389 nm. Glass particles were activated by incubation over night with 1% sodium meta-periodate (#71859, Fluka, Germany) in water at room temperature. Afterwards, the beads were first washed with coupling buffer (1 M potassium phosphate, 0.1 M CaCl_2 , 0.1 M MnCl_2 , pH 8), then 5 times with deionised water and finally with coupling buffer containing an additional 0.02 mM sodium cyanoborohydrid. In the same buffer, 5 mg of lyophilized EEL (1 mg/ml) was dissolved and incubated with 1 ml activated glass beads. Finally, 1.4 mg EEL was coupled to 1 ml of glass beads.

EEL Cellufine[®] - Cellufine[®] Formyl was purchased from Chisso Corporation (#676 945 324, Tokyo, Japan). This aldehyde activated material is based on rigid spherical cellulose beads. It has a particle size of 125 to 210 μm . The pore size is comparable with 4% cross-linked agarose media. EEL was immobilized according to the manufacturer's protocol. Immobilization was carried out in coupling buffer (20 mM Na_2HPO_4 , 0.1 M NaCl and 0.06 M NaBH_3CN ; pH 7.0) by gently rotating the slurry for 6 h at room temperature. The remaining free sites were capped by an additional incubation for 1 h in 0.2 M tris blocking buffer (pH 8). Finally, 4.8 mg EEL were immobilized to 1 ml Cellufine[®] matrix.

EEL membranes – Two Sartobind[®] Epoxy membrane adsorbers were tested. One with a pore size of 0.45 μm (#93EPOX06DB-12-V, Sartorius Stedim Biotech GmbH, Göttingen, Germany) and a second custom-made membrane adsorber with a nominal pore size of 3 μm (Sartorius Stedim Biotech GmbH, Göttingen, Germany). Both membranes consisted of reinforced cellulose and have an area of 75 cm^2 . In both cases EEL immobilization was done according to the manufacturer's recommendations for the 0.45 μm membrane. However, to the recommended coupling buffer (prepared by addition of 1 M KH_2PO_4 to 1 M K_2HPO_4 until pH value was 8) was added CaCl_2 (0.1 mM), MnCl_2 (10 mM) and lactose (1.5 M). Finally, 5.1 mg EEL were immobilized onto the 0.45 μm membrane ($\sim 0.07 \text{ mg/cm}^2$) and 1.1 mg EEL to the 3 μm membrane ($\sim 0.02 \text{ mg/cm}^2$).

Cellufine[®] sulphate (#676 943 324, Chisso Corporation, Tokyo, Japan) is based on spherical cellulose beads containing 880 μg sulphur per g dry gel.

Heparin HP – Prepacked 1 ml HiTrap™ Heparin HP columns (#17-0406-01, GE Healthcare, Uppsala, Sweden) contained beads (Sepharose™ High Performance) with a heparin ligand density of about 10 mg/ml resin.

3.3.2 Matrix screen for LAC with influenza virus strain A/Puerto Rico/8/34

All chromatographic separations were performed on an Äkta Explorer system (GE Healthcare, Uppsala, Sweden). Monitoring was done by light scattering (90°, Dawn EOS, Wyatt Technology Europe GmbH, Dernbach, Germany).

EEL-affinity chromatography for matrix screening

One ml of all EEL-affinity bead-based matrices (Table 10) was packed in a water-jacketed C 10/20 column (4 °C, GE Healthcare, Uppsala, Sweden). The cellulose membranes were used at room temperature. For screening the polymer adsorbent with 4.3 mg/ml EEL ligand density and the 0.45 µm cellulose membrane adsorber were used.

Column-based adsorbents and membrane adsorber were equilibrated and washed with adsorption buffer 2 (AB 2), containing 150 mM NaCl, 50 mM Tris, 0.1 mM MnCl₂, 0.1 mM CaCl₂ at pH 7.4. After equilibration 1 ml of concentrated human influenza virus A/PuertoRico/8/34 from inactivated MDCK cell broth (20.5 kHAU/ml (±2.2)) were loaded onto the affinity media (0.2 ml/min). All affinity matrices were washed with AB2 (0.2 ml/min) until baseline of the light-scattering signal was achieved. Elution (0.5 ml/min) was done in two steps. First, AB2 with an additional 0.5 M lactose (#L2643, Sigma Aldrich, Schnelldorf, Germany,) was used until no virus elution was detected by light scattering (elution 1). Afterwards, remaining virions were eluted from the adsorbents by AB2 containing 0.5 M lactose and additional NaCl (final concentration: 2 M; elution 2) until no virus elution could be detected. Elution 2 was used to regenerate the affinity media and was terminated within 20 min. Subsequently, the media were re-equilibrated with AB2. Separated fractions were pooled into flow-through, wash, and elution 1 and 2. Pooled fractions were analyzed regarding virus content by HA-activity assay. All adsorbents were stored in AB2 containing 0.05% sodium azide.

Cellufine[®] sulphate and heparin chromatography

Cellufine[®] sulphate was packed into the same water-jacketed column and operated at 4 °C. The prepacked heparin resin was tested at room temperature. The separation procedures were identical to EEL-AC except for the chromatographic buffers. For equilibration and washing PBS and for elution PBS with increased NaCl content (final concentration: 1.5 M) was used. Analysis of pooled chromatographic fractions was done by HA-activity assay.

3.3.3 Comparison of EEL-membrane and EEL-polymer beads

Purification characteristics of membrane and polymer-based EEL-AC

The two most suitable matrices to capture influenza viruses were selected for a more detailed characterization. These studies were done with a virus concentrate from a different cultivation (A/Puerto Rico/8/34, 68.3 kHAU/ml (± 11.0)) compared to the previous screens. Prior to use, the variation between both virus batches regarding virus-ligand interaction was determined in sequential experiments (7 runs in total) with a 3 ml EEL-polymer column (ligand density 4.3 mg/ml). Pooled individual fractions were analysed via HA assay (Table 11).

Afterwards, the capturing efficiency of the EEL-modified polymer beads (ligand density: 4.3 mg/ml) was characterized in more detail. Therefore, 3 ml polymer adsorbent was packed into a water-jacketed C 10/20 column (4 °C, GE Healthcare, Uppsala, Sweden). Furthermore, the purification characteristics of the EEL-modified cellulose membrane adsorber (3 μ m, ligand density: 0.02 mg/cm²) was compared to the bead-based EEL-AC. Three times 4 ml of the concentrated virus broth (68.3 kHAU/ml (± 11.0)) were applied to both EEL-modified matrices.

Running conditions and buffers were equal to the screening experiments (Chapter 3.3.2). The separation specifications were characterized via HA-activity recovery and total protein as well as dsDNA reduction. In addition, the final HA content in the major product peak was quantified by an SRID assay.

EEL-membrane capacity

In separate experiments different volumes of virus concentrate were applied to the cellulose membrane (3 μ m). Four times 4 ml, 2 times 8 ml and finally 2 times 18 ml

concentrate (68.3 kHAU/ml (± 11.0)) were loaded to the membrane with a flow rate of 0.2 ml/min. The dynamic binding capacity was estimated by the recovered HA-activity in the eluted product fraction from the last two purification experiments where breakthrough was achieved.

Virus capturing and concentration by EEL-polymer beads

To 3 ml EEL-polymer adsorbent (Tricorn 5/150: GE Healthcare, Uppsala Sweden; EEL ligand density: 5 mg/ml) three times 100 ml inactivated, clarified (0.45 μm) but not concentrated virus culture broths (3.26 kHAU/ml (± 0.15)) were applied. In contrast to all other experiments, the binding flow rate was increased to 0.3 ml/min. Recovered HA activities from pooled chromatographic fractions were analyzed subsequently.

3.4 Material and methods for LAC transferability studies

Ligand screening experiments for LAC-transferability studies were performed initially with AffiSpin[®] columns, and afterwards for selected lectins by SPR technology as described below. Considering these screening results, capturing of both virus types, A/Wisconsin/67/2005 and B/Malaysia/2506/2004, by EEL-AC was evaluated.

3.4.1 Lectin binding to influenza virus strains used for vaccine production from 2006/07 and 2007/08 epidemic seasons

Lectin screening using small-scale chromatographic columns

Small centrifugal columns with a fixed-bed volume of 100 μl were purchased from GALAB Technologies GmbH, Geesthacht, Germany. These units contained polymer beads (mean particle diameter: 65 μm , mean pore size: 100 nm) that had been modified by covalently bound lectins (Table 4). Columns were equilibrated with 150 mM NaCl, 50 mM Tris, 0.1 mM MnCl_2 and 0.1 mM CaCl_2 at pH 7.4 (adsorption buffer 2, AB2). Afterwards, inactivated and concentrated virus harvests were applied to the columns (MDCK cell-derived A/Wisconsin/67/2005: 98.4 kHAU/ml (± 14.7) and B/Malaysia/2506/2004: 95.3 kHAU/ml (± 7.2), Vero cell-derived A/Puerto Rico/8/34 from roller bottle cultivations: 3.7 kHAU/ml (± 0.9)). The centrifuge was set between 10 and 200 \times g depending on the flow rate through the columns. The flow-through was

reloaded manually to make sure that the contact time between virus bulk and column media was at least 30 min. After resin washing with AB2, captured virions were displaced by AB2 containing appropriate carbohydrates (EEL, ECL, MAL I, PNA: 0.5 M lactose; SNA: 0.5 M lactose + 0.5 M galactose, jacalin: 0.2 M melibiose, PA-I: 0.5 M galactose). All carbohydrates were from Sigma-Aldrich (Germany). To ensure complete elution, columns were incubated for 1 h in carbohydrate-containing elution buffer. Finally, a high salt elution buffer containing the corresponding carbohydrate was passed through the units (2 M NaCl, 50 mM Tris, 0.1 mM MnCl₂ and 0.1 mM CaCl₂, pH 7.4) to regenerate the media. Experiments were conducted in duplicates at room temperature. The virus content of all chromatographic fractions was determined by HA-activity assay.

Table 4: AffiSpin® kits (GALAB Technologies GmbH, Geesthacht, Germany) used for ligand screening.

Lectin	Specificity	LD ^a [mg/ml]	Cat. no.
<i>Arachis Hypogaea</i> agglutinin (PNA)	β-gal, gal(β1,3)galNAc	8.0	051061
<i>Artocarpus Integrifolia</i> lectin (AIL, Jacalin)	gal(β1,3)galNAc; α-gal	9.3	051071
<i>Erythrina Christagalli</i> lectin (ECL)	gal(β1,4)glcNAc; galNAc, gal	6.4	051161
<i>Euonymus Europaeus</i> lectin (EEL)	gal(α1,3)gal	4.9	custom-made
<i>Maackia Amurensis</i> lectin I (MAL I)	NeuAc(α2,3)gal;	4.7	051131
<i>Pseudomonas Aeruginosa</i> lectin (PA-I)	Gal	0.68	custom-made
<i>Sambucus Nigra</i> Bark lectin (SNA)	NeuAc(α2,6)gal; NeuAc(α2,6)galNAc	4.18	051121

^a ligand density according to manufacturer

Comparative binding studies with SPR technology

For EEL and ECL detailed comparative binding studies were carried out by SPR technology using a Biacore 2000 system (GE Healthcare Biacore Life Sciences, Uppsala, Sweden). A streptavidin-coated sensor-chip SA (#BR-1000-32, GE Healthcare Biacore Life Sciences, Uppsala, Sweden) was first conditioned with 1 M NaCl in 50 mM NaOH (according to manufacturer's instruction) and then modified by biotinylated EEL (#B-1335, injection time: 1 min, flow rate: 10 µl/min, ligand

concentration: 20 µg/ml) and ECL (#B-1145, injection time: 10 min, flow rate: 10 µl/min, ligand concentration: 20 µg/ml) from Vector Laboratories Inc. (Burlingame, USA). Considering the molecular weight of both lectins (ECL: 54 kDa, EEL: 140 kDa) an approximately equal amount of EEL and ECL molecules was immobilized on different flow cells of the same chip (immobilization level in response units (RU): EEL: 1814 RU, ECL: 741 RU). An unmodified flow cell of the same chip was used as reference to correct for signal changes caused by differences in refractive index between sample matrix and adsorption buffer 2 (AB2, 150 mM NaCl, 50 mM Tris, 0.1 mM MnCl₂, 0.1 mM CaCl₂, pH 7.4). Virus concentrates produced in bioreactors were used for SPR experiments. Concentrated virus bulk from three strains (A/Wisconsin/67/2005, B/Malaysia/2506/2004, and model virus A/Puerto Rico/8/34) were set to 2000 HAU/100 µl by dilution in AB2 and applied to the chip at a flow rate of 25 µl/min for 2.5 min. Afterwards, AB2 was flushed over the chip surface for 2.5 min at the same flow rate. Sensor-chip surfaces of all flow cells were regenerated in two successive steps at 30 µl/min for 1 min (first: 0.5 M lactose in AB2, second: 2 M NaCl in AB). All SPR experiments were conducted at 25 °C.

A 1:1 binding model based on Karlsson et al. (1991) was used to estimate an avidity constant (Lauffenburger and Linderman 1993), which describes an overall tendency of multivalent virus ligand binding. Additionally, the apparent association and dissociation rates were estimated by the Biaevaluation software (Version 3.2, GE Healthcare Biacore Life Sciences, Uppsala, Sweden).

3.4.2 Purification of A/Wisconsin/67/2005 and B/Malaysia/2506/2004 by EEL-AC

Chromatography was performed using an Äkta Explorer system (GE Healthcare, Uppsala, Sweden) and a 3 ml Tricorn 5/150 column (GE Healthcare, Uppsala, Sweden) packed with EEL-modified polymer beads (GALAB Technologies GmbH, Geesthacht, Germany, ligand densities: batch 1: 5 mg/ml, batch 2: 4.56 mg/ml). Chromatographic runs were monitored by light scattering (90°, Dawn EOS, Wyatt Technology Europe GmbH, Dernbach, Germany).

After column equilibration with AB2, 4 ml of inactivated MDCK cell-derived influenza virus concentrates (A/Wisconsin/67/2005, 98.4 kHAU/ml (±14.7); B/Malaysia/2506/2004, 95.3 kHAU/ml (±7.2)) were loaded onto the column (resin batch 1) at a flow rate of 0.2 ml/min (61.1 cm/h). Subsequently, the column was washed (AB2) and elution was done in two steps at 0.5 ml/min (152.8 cm/h). Captured

virus particles were displaced from the chromatography media by 0.5 M lactose in AB2 until baseline was reached (Elution 1). During the initial elution process the flow was stopped for 5 min to incubate the column in elution buffer. Finally, the same buffer containing additional NaCl (final concentration 2 M) was applied until baseline was reached, but for not longer than 20 min (Elution 2). Purification was characterized by measuring viral recoveries (HA-activity), HA concentration (SRID), total protein and host cell dsDNA concentration. All experiments were performed in triplicates.

Dynamic virus particle-binding capacities for each virus type (including the model strain A/Puerto Rico/8/34) were determined by overloading the affinity column (resin batch 2) and measurement of the hemagglutination activity in the eluted product fraction. These experiments were performed in duplicates for each virus type.

3.5 Material and methods for the pseudo-affinity chromatography

This section contains the techniques for the preparation of sulphated membrane adsorbers. Furthermore, purification experiments conducted with these membranes were compared directly to experiments with cation-exchange membrane adsorbers and bead-based column chromatography.

3.5.1 Preparation of SCM

Unmodified reinforced cellulose sheets (pore size >3 μm , Sartorius Stedim Biotech GmbH, Göttingen, Germany) were cut into discs with a diameter of 25 mm. Membrane sulphatation was done according to Wolff et al. (Wolff et al. 2008). Briefly, chloresulfonic acid (1.2 ml) was dropwise added to pyridine (20 ml) on ice; afterwards the solution was heated to 65 °C and 10 ml additional pyridine was added. After completely dissolving the precipitated components, the solution was cooled to 37 °C and 20 cellulose membrane discs (diameter: 25 mm) were added. Membrane discs were incubated for 12 h at 37 °C. Subsequently, membranes were washed with PBS and stored in 20% ethanol in water until further usage. Membrane discs of 13 mm diameter were cut from modified 25 mm discs from the same sulphatation batch. Sulphate ion content of modified and blank membrane discs was estimated by the Schöniger decomposition method followed by ion-exchange chromatography (Currenta GmbH & Co. OHG, Leverkusen, Germany).

3.5.2 Experiments for comparison of influenza virus purification by SCM and Cellufine[®] sulphate

Experiments were conducted with an Äkta Explorer system (GE Healthcare, Uppsala, Sweden) at a flow rate of 0.5 ml/min, unless reported otherwise. Concentrated virus broths (A/Puerto Rico/8/34: 38 kHAU/ml (± 8) and 23 kHAU/ml (± 5), A/Wisconsin/67/2005: 22 kHAU/ml (± 9), B/Malaysia/2506/2004: 42 kHAU/ml (± 7) and 52 kHAU/ml (± 2)) were subjected to sulphated as well as unmodified cellulose membrane adsorbers, to cation-exchange membrane adsorbers (Sartobind C75, #C75X; Sartobind S75, #S75X, Sartorius Stedim Biotech GmbH, Göttingen, Germany) and to Cellufine[®] sulphate beads (#19845, Chisso Corporation, Tokyo, Japan) to determine virus capturing and removal of protein and host cell DNA contaminants. In addition, dynamic binding capacity was determined for several different cultivation batches (A/Puerto Rico/8/34). Chromatographic experiments were monitored by a 90° inline light-scattering signal (BI-MwA, Brookhaven Instruments Corporation, Holtsville, NY, USA). Purification efficiency was characterized regarding viral recoveries (HA-activity and SRID assay), total protein and host cell dsDNA depletion.

Influenza virus capturing by sulphated cellulose membrane adsorbers

Adsorption buffer selection – The effect of ionic strength of adsorption buffer on influenza virus capturing was studied using 10 sulphated cellulose membrane layers (d: 25 mm, A~50 cm²) packed into a stainless-steel housing (#1980 002, Whatman GmbH, Dassel, Germany). Two adsorption buffers ([1] 150 mM NaCl, 10 mM Tris, pH 8 and [2] 50 mM NaCl, 10 mM Tris, pH 8) were used for equilibration and 1 ml of inactivated and concentrated influenza virus culture broth (A/Puerto Rico/8/34) was applied to the packed SCM adsorbers. After loading of the adsorption membrane the unbound material was eluted by washing with adsorption buffer. Bound virus particles were displaced by flushing the membrane adsorber first with 1.2 M NaCl, 10 mM Tris, pH 8 and second with 2 M NaCl, 10 mM Tris, pH 8. Each elution step was carried out until baseline of light-scattering signal was reached. Performance was evaluated by results obtained from the HA assay.

All subsequent experiments using SCM, Cellufine[®] sulphate and cation-exchange membrane adsorbers were performed using a low-ionic-strength adsorption buffer (AB3, 50 mM NaCl, 10 mM Tris, pH 7.4).

Desorption buffer – Elution of influenza virus particles (A/Puerto Rico/8/34) from SCM adsorbers was optimized regarding viral recovery and contaminant reduction by adjusting the NaCl concentration in the elution buffer.

Dynamic adsorption capacity – For determination of dynamic virus-binding capacity 10 modified cellulose membrane layers (d: 13 mm, 13.3 cm²) were packed into a membrane housing (#301000, Advantec MFS, Inc., Dublin, CA, USA) and overloaded (by about 90%) by 3-fold-diluted (dilution buffer: 10 mM Tris, pH 7.4) virus broth concentrates (A/Puerto Rico/8/34). The final sample buffer contained approximately 50 mM NaCl. The captured material was displaced in two sequential steps: [1] 0.6 M NaCl, 10 mM Tris, pH 7.4 (elution buffer 1, EB1) and [2] 2 M NaCl, 10 mM Tris, pH 7.4 (elution buffer 2, EB2). Elution steps were conducted until baseline of light-scattering signal was reached. Capacity data were estimated based on displaced influenza virus amount determined by HA and SRID assay assuming full recovery of the adsorbed virus particles. Experiments for dynamic binding capacity estimation were done in duplicates. SCM adsorbers were regenerated with 20 ml of 1 M HCL, 1 M NaCl and afterwards with 20 ml of 1 M NaOH, 1 M NaCl.

Purification characteristics – 5 ml of concentrated virus culture broths (A/Puerto Rico/8/34, A/Wisconsin/67/2005, B/Malaysia/2506/2004) were 3-fold diluted in 10 mM Tris, pH 7.4 and applied to the SCM adsorbers (d: 25 mm, 10 layers, ~ 50 cm²). Desorption was done as described for the dynamic adsorption capacity study using EB1 and EB2. All experiments were carried out at about 10 to 25% of the dynamic virus-binding capacity.

In addition, a set of three experiments was done with an increased flow rate (15 ml/min) during adsorption of influenza virus A/Puerto Rico/8/34 onto the membranes. The elution flow was maintained at 0.5 ml/min.

To determine unspecific adsorption, 10 layers of unmodified cellulose membranes (d: 25 mm, A~50 cm²) were used for experiments with influenza virus strain A/Puerto Rico/8/34.

Influenza virus capturing by cation-exchange membrane adsorbers

Adsorption of virus particles (A/Puerto Rico/8/34) to commercially available cation-membrane adsorbers from Sartorius Stedim Biotech GmbH, Göttingen, Germany

(Sartobind C75, #C75X; Sartobind S75, #S75X) was determined. The chromatographic conditions for these experiments were selected as described above for determination of purification characteristics of SCM at 0.5 ml/min. These experiments were carried out at approximately 10 to 25% of the dynamic binding capacity.

Influenza virus capturing by column-based Cellufine[®] sulphate resin (CSR)

Cellufine[®] sulphate (3 ml) was packed into a Tricorn 5/150 column (GE Healthcare, Uppsala, Sweden). Concentrated virus culture broths (A/Puerto Rico/8/34, A/Wisconsin/67/2005, B/Malaysia/2506/2004) were 3-fold diluted in 10 mM Tris, pH 7.4 and 15 ml were applied to the column (20 to 70% of dynamic binding capacity). Elution was done as before using EB1 and EB2.

For dynamic binding capacity determination 1.2 ml CSR were packed into a Tricorn 5/50 column and overloaded (by about 40 to 60%) with 3-fold-diluted (dilution buffer: 10 mM Tris, pH 7.4) virus concentrates of two different cultivation batches (A/Puerto Rico/8/34). Capacity data were estimated based on HA-activity recovered in the product fraction.

3.6 Analysis

Several analytical assays have been applied for evaluation of chromatography experiments. Their names and standard operating procedures (SOP) are listed in Table 5.

Table 5: SOP's applied for characterization of chromatography experiments

Application	Name of SOP	Version / date
Total protein assay	Protein estimation in microtiter plates	V2.2 / 2008-03-07
dsDNA estimation	dsDNA estimation in microtiter plates	V2.3 / 2008-03-07
HA-activity assay	HA assay	V2.1 / 2006-12-04
SRID assay	Single radial immunodiffusion assay	V1.1 / 2009-03-24

3.6.1 Hemagglutination activity

Hemagglutination activity assay – The HA-activity measurement is related to the hemagglutination assay described by Mahy and Kangro, which is based on the influenza virus' ability to aggregate red blood cells (Mahy and Kangro 1996). Here, a modified procedure with a higher resolution first described by Kalbfuß et al. was used (Kalbfuß et al. 2007a). Serial $2^{0.5}$ -fold dilutions of the virus-containing samples in PBS (100 µl) were incubated with chicken erythrocytes (100 µl, $2 \cdot 10^7$ cells/ml) in 96-well plates. After over night incubation at room temperature the plates were scanned photometrically at 700 nm (Rainbow Spectra, Tecan Deutschland GmbH, Crailsheim, Germany). The evaluation of the point of inflection from red-blood-cell settlement to the agglutinated blood cells was done automatically by fitting a Boltzmann sigmoid to the scanned data, which were plotted against the negative logarithm of the dilution factor d (Kalbfuß et al. 2008). The specific dilution factor at this point was defined as the amount of hemagglutination activity units (HAU, HA-activity) per 100 µl. The automated evaluation was performed between the HA-activity titer of $-\log d = 1$ and 3, corresponding to 10 and 1000 HAU/100 µl. The estimated standard deviation of the HA-activity titer derived from a validation study was ± 0.027 for single determination corresponding to an analytical error of $\pm 15\%$ (Kalbfuß et al. 2008). The limit of detection is $-\log d = 0.15$. A more detailed and comprehensive description of the HA-activity assay development and validation can be found in Kalbfuß et al. (2008). All samples were analyzed in duplicates. The percentage HA-activity recovery from each single chromatographic fraction was calculated based on the initially applied HA-activity per experiment.

3.6.2 DNA concentration

Estimation of dsDNA content was performed in black flat-bottom 96-well microtiter plates using the Quant-iT™ PicoGreen® dsDNA reagent from Invitrogen GmbH, Karlsruhe, Germany (#P7581). The procedure based on the DNA assay described by Kalbfuß et al. and Wickramasinghe et al. (Kalbfuß et al. 2007a; Wickramasinghe et al. 2005).

The assay was calibrated with lambda DNA (#D1501, Promega GmbH, Mannheim Germany) in the linear and validated range between 4 and 1000 ng/ml (weighted regression, limit of detection: 0.66 ng/ml; limit of quantification: 2.36 ng/ml). High-salt-

containing samples were dialyzed (13-14 kDa MWCO, #0653.1, Carl Roth GmbH & CO KG, Karlsruhe, Germany) against 50 mM NaCl, 10 mM Tris, pH 7.4 prior to dsDNA concentration estimation. For standard and sample dilutions the chromatographic or dialysis buffers were applied. To 200 μ l standard or sample solution, respectively, 50 μ l of the 60-fold in TE-buffer (200 mM Tris, 20 mM EDTA, pH 7.5) diluted PicoGreen[®] working solution were added and incubated at room temperature on a thermomixer (Eppendorf, Hamburg, Germany) at 1000 rpm for 5 min. Afterwards the fluorescent signal was measured either at an emission wavelength of 535 nm (Mithras LB 940, Berthold Technologies GmbH & Co. KG, Bad Wildbad, Germany; excitation: 485 nm) or at an emission wavelength of 520 nm (Cary Eclipse Fluorescence Spectrophotometer, Varian, Inc., Palo Alto, USA; excitation: 480 nm). All measurements were done in duplicates.

3.6.3 Total protein concentration

Protein concentration measurements based on the method first described by Bradford were done in flat-bottom 96-well microtiter plates using the protein assay dye reagent concentrate from BioRad (#500-0006, Munich, Germany) (Bradford 1976). The assay was calibrated with 7 standard concentrations of BSA (#A3912, Sigma-Aldrich GmbH, Schnellendorf, Germany) in the range between 5 to 50 μ g/ml. All standard concentrations and samples (each 200 μ l) were incubated for 5 min with 50 μ l of dye reagent on a thermomixer (Eppendorf, Hamburg, Germany; room temperature, 1000 rpm). Afterwards, plates were scanned at 595 nm (Rainbow Spectra, Tecan Deutschland GmbH, Crailsheim, Germany). Calibration curve was set up by fitting a sigmoid curve to the standard concentrations. High-salt-containing samples (Elution 1 and 2) were dialyzed (13-14 kDa MWCO) against 50 mM NaCl, 10 mM Tris, pH 7.4 before measuring protein concentration. The matrices of calibration standards were adapted to the sample matrices by using chromatographic or dialysis buffers for standard dilutions. All measurements were done in triplicates.

3.6.4 Hemagglutinin content – single radial immunodiffusion assay

Single radial immunodiffusion assay (SRID) – HA antigen quantification of the major product peak after purification was done by an SRID assay (Wood et al. 1977) that is based on antigen-antibody precipitation circles in agarose gels. Anti-HA sera of each

virus type from NIBSC, South Mimms, UK, were resuspended in 1 ml distilled water and afterwards diluted in 1% agarose (Anti-A/Wisconsin/67/2005 (H3N2) HA serum, #05/236, 13 µl/ml agarose gel; Anti-A/Puerto Rico/8/34 (H1N1) HA serum, #03/242, 8 µl/ml agarose gel; Anti-B/Malaysia/2506/2004 HA serum, #07/184, 15 µl/ml agarose gel). For SRID quantification the relevant chromatographic samples were pre-purified by dialysis (14 kDa MWCO; 15 mM NaCl, 5 mM Tris, pH 7.4) and 20-fold concentrated by lyophilization. The assay was calibrated against the NIBSC, South Mimms, UK, standard for A/Wisconsin/67/2005 (#06/120) and B/Malaysia/2506/2004 (#06/126). For A/Puerto Rico/8/34 an in-house standard was applied, which was purified by a SCM virus capture step followed by EEL-affinity chromatography. Afterwards, the relative HA content was estimated by total protein assay in combination with gel densitometry quantifications.

The virus standard and chromatographic samples were treated with detergent, diluted to 4 different concentrations and added into wells from antibody-containing agarose gels. After incubation for 18 h the resulting precipitation circles were stained with Coomassie dye and their diameters, which are proportional to the viral HA concentrations, were measured. The HA concentrations were estimated and statistical analysis were done according to the slope-ratio model described in the European Pharmacopoeia (Version 5.03, Chapter 3.3 and 5.2.2). Chromatographic product fractions were analyzed in duplicates. The measurements for statistical analysis were done ten times for each virus strain standard used in this dissertation. Therefore, the mean values were 9.4 µg/ml (A/Puerto Rico/8/34, C.I. [95%]: 11.0, 8.0 µg/ml), 31.3 µg/ml (A/Wisconsin/67/2005, C.I.: 37.7, 23.4 µg/ml) and 44.8 µg/ml (B/Malaysia/2506/2004, C.I.: 50.4 µg/ml, 38.6 µg/ml).

3.6.5 SDS-PAGE

Protein separation by SDS-polyacrylamide gel electrophoresis (SDS-PAGE) was based on the procedure proposed by Laemmli (Laemmli 1970). Samples were run on 10% polyacrylamide gels under nonreducing conditions. For molecular weight identification, the protein marker Broad Range (#P7702, New England Biolabs, Inc., Ipswich, USA) was used. The gel was silver-stained based on the procedure described by Rabilloud (Rabilloud et al. 1988).

3.6.6 Size distribution analysis

Virus-size distribution from MDCK cell culture virus broths were determined by the Horiba dynamic light-scattering particle analyzer LB-500 (Horiba Europe GmbH, Oberursel, Germany) at room temperature (particle refraction index: 1.44, medium refraction index: 1.333).

This method relies on laser light, which is scattered by particles from the sample to be analyzed and finally registered by a photodetector. The scattered light depends on the Brownian movement of the particles. That means, if the particles can move independently from each other, then the Brownian movement provides information about the particle size. Smaller particles move faster than larger particles and, therefore, have a relatively high diffusion coefficient. Hence, smaller particles generate high-frequency light-scattering signals. On the other hand, larger particles lead to low-frequency signals. Analysis of the frequency component leads to particle-size distributions, which assume the particles as spheres. Therefore, dynamic laser light scattering determines the hydrodynamic radii of particles from few nanometers up to few micrometers (Alexander and Dalgleish 2006).

3.6.7 Quantification of sulphate content from membrane adsorbers

Sulphate ion content of modified and blank membrane discs was estimated by the Schöniger decomposition method followed by ion-exchange chromatography (Currenta GmbH & Co. OHG, Leverkusen, Germany).

4 Lectin affinity chromatography

The following chapter describes the establishment and characterization of LAC for purification of cell culture-derived influenza virus particles. Therefore, LAC was first developed based on the influenza virus strain A/Puerto Rico/8/34 (H1N1). Second, the impact of the adsorbent matrix on LAC efficiency was evaluated. Finally, robustness of the developed method regarding the general application of the LAC for different influenza virus strains was determined.

4.1 Development of an LAC step for DSP of MDCK cell culture-derived human influenza virus A/Puerto Rico/8/34

4.1.1 Results

Lectin Blot analysis

The lectin blot analysis (Table 6) displayed high affinity of EEL and ECL towards the human influenza A virus surface proteins and a relatively low affinity towards MDCK host cell proteins. PNA, SNA and MAL I had a moderate binding affinity to influenza virus envelope proteins as well as to MDCK host cell proteins. Con A and Jacalin showed either low binding towards the virus glycoproteins or too high affinity to the MDCK host cell proteins. Addition of the appropriate carbohydrates inhibited the lectin-viral protein binding sufficiently in lectin blot experiments, except for the negative control of SNA, since 0.5 M lactose was not the most suitable binding inhibitor. However, because SNA showed low virus binding this was not further investigated.

Lectin screening using small-scale AffiSpin® chromatographic columns

The three lectins EEL, ECL and MAL I showed the highest binding capability towards the human influenza virus surface glycoproteins based on AffiSpin® column experiments and subsequent HA-activity measurements. These results confirmed previous lectin blot data. EEL with the lowest HA-activity in the flow-through fraction and the highest eluted HA-activity was the best of all five tested ligands (Figure 11). In contrast, the influenza virus glycoproteins hardly bound to PNA and SNA reflected by the high HA-activity in the flow-through fraction. The total HA-activity recovery for all AffiSpin® runs amounted

to about 81 to 95%. Based on these screening results EEL and ECL were chosen for LAC.

Table 6: Lectin affinity towards human influenza A/PuertoRico/8/34 virus and MDCK cell proteins based on lectin blot analysis (number of “+” indicates the affinity level, most suitable lectins are highlighted)

Lectin	Specificity	Affinity to glycoproteins of	
		A/PuertoRico/8/34	MDCK cells
AAL	fuc(α 1,6)glcNaC	+++ +	+++ +
Con A	α -man; α -glc;	++	+++ +
ECL	gal(β 1,4)glcNAc; galNAc, gal	+++ +	++
EEL	gal(α 1,3)gal	+++ +	++
Jacalin	gal(β 1,3)galNAc; α -gal	+	++
MAL I	NeuAc(α 2,3)gal;	+++	+++
PNA	β -gal, gal(β 1,3)galNAc	++	++
SNA	NeuAc(α 2,6)gal; NeuAc(α 2,6)galNAc	++	+++

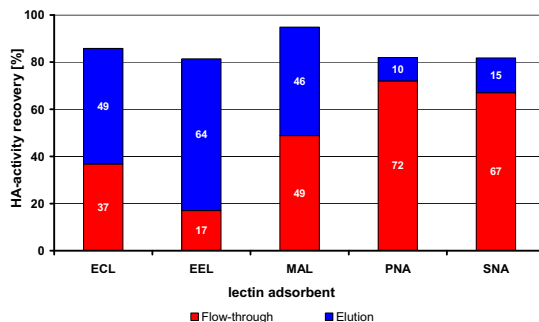


Figure 11: Total recovery of HA-activity after screening with Lectin-AffiSpin® columns

ECL and EEL – AC - FPLC

The HA activities of flow-through and elution of both matrices (EEL and ECL, each 1 ml lectin adsorbent) were compared. Therefore, the binding flow rate was set to 0.2 ml/min and the elution flow rate to 0.5 ml/min. Here, ECL showed only a very slow association

and dissociation compared to EEL (Table 7). More than half of the loaded HA-activity was found in the unbound flow-through fraction after applying the sample to the ECL column. For sufficient virus-ECL binding, a sample recirculation (0.5 ml/min for 15 h) during the column loading process was necessary. This reduced the unbound fraction to 1.3% (± 2.3) (Table 7). Moreover, the dissociation of virus from lectin in the presence of 0.5 M lactose was significantly slower compared to EEL. For maximum elution (79.8% ± 8.5) of bound viruses from the ECL matrix an adequate incubation (2 h) of the loaded column in elution buffer was required (Table 7). The viral glycoproteins bound faster to the EEL polymer even with a direct sample loading flow of 0.2 ml/min (no sample recirculation). A relatively low HA-activity of 7.6% (± 7.4) remained in the flow-through. Overall, 84.4% (± 5.1) of the HA-activity was recovered after release of EEL bound viruses by elution with lactose at 0.5 ml/min.

Table 7: Comparison of recovery [%] of HA-activity after EEL- and ECL-affinity purification concerning binding velocity using 1 ml lectin adsorbents

Lectin	EEL	ECL	ECL
run conditions			
loading flow:	0.2 ml/min	0.2 ml/min	0.5 ml/min; recirculation for 15 h
ligand density:	3.1 mg/ml resin	7.7 mg/ml resin	7.7 mg/ml resin
number of runs	5	3	3
HA-activity [%]^a			
Flow-through	7.6 (± 7.4)	56.3 (± 10.2)	1.3 (± 2.3) ^b
Elution	84.4 (± 5.1)	47.4 (± 13.2) ^c	79.8 (± 8.5) ^c
Total recovery	92.0 (± 8.0)	103.7 (± 7.9)	81.1 (± 6.4)

^a standard deviations are given in brackets; ^b high sample dilution due to sample recirculation; ^c maximum virus elution after column incubation in elution buffer for 2 h

The light-scattering signal during a typical EEL-AC of human influenza A concentrate without any sample recirculation and incubation is shown in Figure 12. The majority of virus was released during the addition of 0.5 M lactose in AB1 (elution 1). Further elution with an increased sodium chloride concentration of 2 M led to slightly increased virus recovery (elution 2).

The matrix stability of the EEL polymer was tested by repeating the runs for more than 50 times without any distinguishable loss of activity.

Capacity of EEL polymer column - The virus-binding capacity of the EEL-polymer adsorbent was estimated by determination of the HA-activity in the eluted sample considering the previous sample concentration factor. The capacity of the EEL-adsorbent (ligand density: 4.3 mg/ml) resulted in about 125 kHAU per ml resin (number of runs: 3). That corresponds to approximately 42 ml unconcentrated human influenza A virus cultivation broth per ml resin, which is not suitable for large-scale processes.

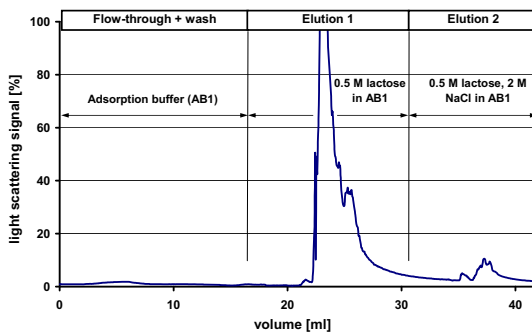


Figure 12: Light-scattering signal (90°) during purification of human influenza A virus concentrate with EEL-affinity chromatography (direct loading [0.2 ml/min] and elution [0.5 ml/min]; AB1: adsorption buffer 1)

EEL-AC mass balancing and eluate purity – Using a 3 ml EEL-polymer column with a ligand density of 4.3 mg/ml, only a small part of virus 12% (± 2) did not adsorb to the column (Table 8). The majority of virus bound to EEL and could be released by 0.5 M lactose (97% ± 7 eluted HA-activity). The EEL-AC step could reduce the total dsDNA content to 0.1% (± 0.02) and the total protein content (including viral and MDCK cell proteins) to 21% (± 2) of the loaded concentrate (Table 8). The protein and the dsDNA concentration in the second elution step (Figure 12) were below the quantification limit. Therefore, neither concentration was included in the protein or dsDNA balance, respectively. Analyzing only the major peak within elution 1 (Figure 12), the specific HA-activity amounted to 30.3 (± 3.4) kHAU per ml. In the same sample, protein concentration was 29.7 (± 1.7) $\mu\text{g/ml}$ and dsDNA concentration 0.054 (± 0.01) $\mu\text{g/ml}$ (Table 9). These experiments for mass balancing were done with sample volumes below column capacity.

Table 8: EEL-affinity chromatography mass balancing using 3 ml EEL-polymer adsorbent (number of runs: 4, standard deviations are given in parentheses)

Fraction name	HA-activity		Total protein		dsDNA	
	kHAU	%	µg	%	µg	%
Load	176 (±18)	100	775 (±32)	100	381.8 (±2.4)	100
FT^a	21 (±6)	12 (±2)	552 (±47)	71 (±3)	375.7 (±8.9)	98.4 (±2.0)
Elution 1	154 (±19)	87 (±7)	159 (±15)	21 (±2)	0.33 (±0.05)	0.1 (±0.02)
Elution 2	17 (±4)	10 (±2)	LOQ ^b	-	LOQ ^b	-
Elution 1+2	171 (±22)	97 (±7)	159 (±15)	21 (±2)	0.33 (±0.05)	0.1 (±0.02)
Total		109 (±8)		92 (±3)		98.5 (±1.9)

^a Flow-through, (wash-fraction was neglected); ^b LOQ: value below the limit of quantification (LOQ: protein: 5 µg/ml; dsDNA: 4 ng/ml)

Table 9: Concentration analysis of the major product peak of elution 1 after EEL-AC in comparison to the concentrated load and purification efficiency (number of runs: 4, standard deviations are given in parentheses)

	Measured concentrations			Calculated impurity,	
	HA-activity	Protein, c_{prot}	dsDNA, c_{DNA}	i_{prot}	i_{DNA}
	kHAU/ml	µg/ml	µg/ml	µg protein / kHAU	ng dsDNA / kHAU
Load	44.1 (±4.4)	193.8 (±8.1)	95.45 (±0.6)	4.4 (±0.37)	$2.2 \cdot 10^3$ (± $0.2 \cdot 10^3$)
Elution	30.3 (±3.4)	29.7 (±1.7)	0.054 (±0.01)	0.98 (±0.06)	1.8 (±0.54)

Visualization of purified virus proteins – As shown in the SDS-PAGE, the major product fraction of Elution 1 contained four major bands (Figure 13). Based on molecular weight the expected viral proteins were the matrix protein M1 (27 kDa), the viral NP (about 56 kDa) and the HA as a monomer (about 70 kDa). Peptide mass fingerprint of tryptic digested samples excised from an identical gel have confirmed the protein identity (Dr. E. Rapp, Max Planck Institute, Magdeburg, Germany). In addition, HA was identified at about 160 kDa, probably as a trimer. The major part of host cell proteins remained in the flow-through.

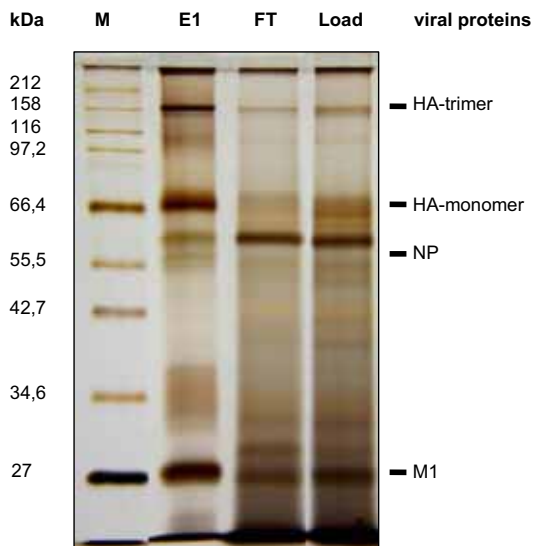


Figure 13: SDS-PAGE (nonreducing running conditions) with samples from EEL-AC (~2 μg protein per lane, M: protein ladder, E1: elution 1, FT: flow-through, viral proteins are indicated)

4.1.2 Discussion

The LAC-development studies focused on the identification of suitable lectins as affinity ligands for an affinity chromatography capture step of human influenza A virus. In a first step, potential lectins with different specificities have been screened.

AAL binds independently of the outer glycosylated chain structure to α -fucosyl residues (α 1,6)-linked to *N*-acetylglucosamine of the inner pentasaccharide core of *N*-linked glycoproteins (Yamashita et al. 1985). Since a lot of *N*-glycosylproteins, also the influenza hemagglutinin, possess α -1,6-fucosyl residues linked to *N*-acetylglucosamine (Mir-Shekari et al. 1997), the lectin AAL bound with a high affinity to viral as well as to host cell proteins (Table 6). Hence, AAL was not qualified as an affinity ligand for influenza virus purification, but it served as a positive control for the lectin blot screening method. Con A requires for binding to a glycoprotein at least two non-substituted α -mannosyl residues or extended residues with free hydroxyl groups at C-3,4 and 6 position like in biantennary glycosylated structures (Ogata et al. 1975). Host cell proteins and also the influenza HA possesses some of such structures (Mir-Shekari et al. 1997;

Roberts et al. 1993). Therefore, Con A bound to virus and host cell proteins. However, the Con A blot suggested that the influenza virus proteins did not contain a high degree of terminal or C-2 substituted mannose (Table 6). PNA and Jacalin revealed in lectin blot screening low binding ability to virus and host cell proteins. Both lectins have a high affinity toward the galactosyl-(β 1,3)*N*-acetylgalactosamine structure of O-linked oligosaccharide side chains. Hence, the original assumption that HA contains no or in low degree such glycan structures could be confirmed. The lectins ECL, EEL, PNA, MAL I and SNA showed in lectin blot analysis more or less affinity to the human influenza glycoproteins and also parallel low or medium affinity to the host glycoproteins (Table 6). Hence, these lectins were selected for a secondary screen with AffiSpin[®] columns, which was evaluated by HA-activity measurements (Figure 11). In accordance with the lectin blot, PNA showed after small-scale purification in an AffiSpin[®] column a low virus-binding rate to the ligand. SNA binds preferable to terminal sialic acids attached to galactose in (α 2,6) linkage and less in (α 2,3) linkage. MAL I has an affinity to sialic acids attached to galactose in (α 2,3) linkage. The relatively high HA-activity after MAL I- and the low activity after SNA-AffiSpin[®] column chromatography suggested a lack of sialic acid in (α 2,6) linkage and the existence of (α 2,3) linkages to galactose to some degree on human influenza viral glycoproteins propagated in MDCK cells. However, it seems that the degree of sialylation of viral glycoproteins propagated in MDCK cells is relatively low. Other research groups who worked on the glycosylation structure analysis of different influenza virus strains produced in different host cells made similar observations. For example, Basak et al. showed that influenza A/USSR/90/77 (H1N1) grown in MDCK cells contained glucosamine, mannose and galactose in their glycan structure but no sialic acid (Basak et al. 1981). Deom and Schulze observed galactose as the major terminal carbohydrate on HA from influenza A/WSN-F (H1N1) grown in MDBK cells and chicken embryo fibroblast cells (Deom and Schulze 1985). Keil et al. described the *N*-glycosylated structure of influenza A/FPV/Rostock/34 (H7N1) grown in CE cells. There, the illustrated structure comprised mainly of *N*-acetylglucosamine, mannose, galactose and fucose (Keil et al. 1985). The lack of terminal sialic acid traced probably back to the viral NA-activity (Mir-Shehari et al. 1997; Wilson et al. 1981). Due to that truncation of sialic acid from virus glycoproteins by NA, virus aggregation might be prevented (Palese et al. 1974).

Amongst all screened ligands EEL and ECL showed the highest binding potential toward human influenza A virus glycoproteins (Figure 11). ECL has relatively high

affinity to terminal galactose-(β 1,4)-*N*-acetylglucosamine. The existence of terminal sialic acid could prevent ECL binding to galactose. The high affinity of ECL to viral glycoproteins is another indication for low sialylation due to a high viral NA-activity. The frequency of galactosyl-(α 1,3)-galactose on influenza glycoproteins expressed in MDCK cells seemed to be at least equal to the structure of galactosyl-(β 1,4)-*N*-acetylglucosamine. EEL, a lectin from the spindle tree with high affinity to galactosyl-(α 1,3)-galactose (Petryniak and Goldstein 1987; Petryniak et al. 1977), presented an even higher binding affinity than ECL, based on HA-activity measurements after AffiSpin[®] column screening. Hence, viral protein glycosylation process in MDCK cells most likely ends partly with α -galactosyl residues, caused by a relatively high α (1,3)-galactosyl transferase activity. The overall recovery of HA-activity after AffiSpin[®] column screening experiments ranged between 81 and 95% (Figure 11). Considering the assay error range of 15% there was a slight loss in total HA-activity. On the basis of the screening results, ECL and EEL were selected for 1 and 3 ml LAC studies.

A sufficient virus-ECL binding during FPLC experiments could only be achieved by recirculation of the flow-through to the affinity column (Table 7). Otherwise, more than half of the total virus load would be lost, even though the ECL-ligand density was with 7.7 mg/ml significantly higher compared to the EEL material. Furthermore, complete ECL-virus dissociation required a relatively long incubation period with the competing carbohydrate. This is probably explained by the higher ligand density, which supports the strong binding. Due to the recirculation, loaded samples were highly diluted reducing the unbound virus concentration close to the detection limit of the assay. Therefore, the total recovery could have been reduced compared with the direct loading process (Table 7). Hence, purification of viruses using ECL would be very time-consuming and based on this economically uninteresting. Another ECL drawback is the dependence on terminal (β 1,4)-galactose of target glycoproteins and so on the viral NA-activity, which uncover the galactose by truncation of terminal sialic acid. As a consequence variations in culture harvesting times could result in variations of NA-activity and therefore batch-to-batch variations of ECL-based recovery.

The EEL-AC has quite different characteristics. Binding and release kinetics of EEL allowed an effective loading and elution of human influenza virus.

Among all tested lectins in the screening and FPLC runs, EEL was the most suitable ligand for the affinity purification capture step considering economical and reproducibility aspects. Hence, EEL was chosen for further detailed mass balancing studies.

A volume of 1 ml of EEL-polymer adsorbent binds the virus content of about 42 ml unconcentrated culture broth. The polymer material used for this study exhibit a mean pore diameter of 100 nm (manufacturer's information). This means most of the influenza viruses with a mean diameter of 100 nm (not to mention any virus aggregates) were not able to enter the pores and ligands immobilized inside these pores remained unused reducing the binding capacity of the matrix. Since pre-concentrated samples were applied to the affinity column a further concentration due to the affinity chromatography process was not achieved. The pre-concentrated samples enabled short column loading times.

Focusing on the major product peak of elution 1 the EEL capture step achieved a dsDNA reduction to 1.8 ng (± 0.54) dsDNA per kHAU and a total protein (including viral and MDCK cell proteins) reduction to 0.98 μg (± 0.06) per kHAU (Table 9). This is approximately a 1200-fold dsDNA and a 4.5-fold total protein reduction per kHAU, respectively. Those impurity reductions are sufficient for a capture step. Therefore, further purification is only necessary to remove small amounts of protein and DNA. It might even be possible to optimize the capture step in combination with a benzonase treatment to decrease further the DNA concentration. Even if the residual DNA was partly associated with the virus, this step might decrease the DNA to a satisfactory level. Hence, only a final polishing step would be required to use the eluate for blending vaccines.

The SDS-PAGE from an EEL-affinity chromatography with the fractions load, flow-through and elution indicated a low HA₀ monomer concentration in the flow-through and a high content in the final eluate (Figure 13). The same applied to the viral proteins M2 and NP. In contrast to that, the major host cell proteins remained in the flow-through. This represented high virus content in relation to the total protein mass.

Comprehensive purification studies showed long-term stability of the EEL-polymer resin (data not shown) indicating that ligand leakage is not significant. Therefore, the product fraction would contain only a very small amount of EEL. However, as most lectins are known to be toxic, eluates need to be tested for EEL impurities. The possibly leached EEL could be quantified by using anti-EEL antibodies for an ELISA or for immunoblotting analysis as done for the leached mistletoe lectin by Walzel et al. (Walzel et al. 1989). Alternatively, quantity of leached ligands may be estimated by a surface plasmon resonance assay (Thillaivinayagalingam et al. 2007). However, the toxicity of EEL still needs to be studied.

4.2 Impact of adsorbent selection on capture efficiency using LAC

In this chapter the matrix impact on virus purification efficiency is evaluated. The screening experiments included membrane and bead-based LAC and a comparison of LAC with PAC, using the chromatographic resin Cellufine[®] sulphate, which is used in commercial vaccine productions. Furthermore, two supports were investigated in detail regarding influenza virus purification.

4.2.1 Results

Matrix screening

Different chromatography media were screened for an affinity capture step of human influenza A virus. The pooled unbound flow-through (including wash) and the eluted fractions were characterized by the HA assay (Table 10). About 10% of the applied virus did not bind to the EEL-modified media Trisopor[®], the polymer and the cellulose membrane. In total, 93.7% (± 3.8) and 85.2% (± 7.3) product could be eluted from the membrane and the polymer, respectively. Other EEL adsorbents had a higher HA-activity in the flow-through and wash. Lowest influenza virus binding with 57.6% (± 12.1) HA-activity in the unbound fraction was determined for the Actigel ALD. A HA-activity of 67.6% (± 9.8) and 32.0% (± 5.3) could be obtained as product using Cellufine[®] sulphate and heparin HP. The ratios between eluted and unbound HA-activity were used to evaluate the performance of the adsorbents tested (Table 10). Thereby, the polymer and the cellulose membrane reached the highest ratios of 9.2 and 12.8, respectively.

Capture characteristics of the EEL-modified cellulose membrane and polymer beads

A comparison of both concentrated virus batches used for the matrix screen and the studies related to detailed purification characterization resulted in similar HA-activity binding and recovery (Table 11). In both cases about 5% of the HA-activity was found in the flow-through, whereas about 90% was eluted in the product fractions. The correlation between both batches was verified by a total of 7 LAC experiments.

The EEL-modified cellulose membrane (75 cm², ligand density: 0.02 mg/cm²) and the polymer (3 ml, 4.3 mg EEL/ml) were selected for detailed investigations. Virus concentrate (68.3 \pm 11.0 kHAU/ml) was loaded 3 times on both matrices. As an example, an EEL-polymer chromatographic experiment is shown in Figure 12.

Table 10: EEL-matrix screen: analysis of human influenza A virus binding by HA- activity tests in comparison to Cellufine[®] sulphate and heparin HP (standard deviations are given in parentheses)

Matrix	Ligand density [mg/ml or mg/cm ²]	Pore size [nm]	N ^a	HA-activity [%]			ratio: Elution / FT ^a
				FT ^b	Elution ^c	Total recovery	
EEL immobilized on 1ml adsorbent of:							
Actigel ALD (Sterogene Bioseparation Inc.)	3.5	-	3	57.6 (±12.1)	30.1 (±2.9)	87.7 (±13.1)	0.5
Agarose (Vector Laboratories. Inc.)	3	-	2	28.5 (±5.9)	41.1 (±8.2)	69.6 (±14.0)	1.4
Trisopor[®] (VitraBio GmbH)	1.4	390	3	10 (±3.6)	69.4 (±24.6)	79.4 (±27.1)	6.9
Cellufine[™] (Chisso Corp.)	4.8	-	4	23.2 (±6.8)	53.5 (±10.9)	76.7 (±16.1)	2.3
Polymer (Galab Technologies GmbH)	4.3	100	3	9.3 (±4.8)	85.2 (±7.3)	94.5 (±2.9)	9.2
EEL immobilized on :							
Membrane (0.45 µm, 75 cm ² , Sartorius Stedim Biotech GmbH)	0.07	450	2	7.3 (±10.3)	93.7 (±3.8)	101 (±6.6)	12.8
Comparison to:							
Cellufine[™] sulphate (Chisso Corp.)	≥ 0.7 mg/g dry gel	-	3	31.7 (±1.9)	67.6 (±9.8)	99.3 (±10.7)	2.1
Heparin HP (HiTrap [™] . GE Healthcare)	10	-	3	65.8 (±7.7)	32.0 (±5.3)	97.8 (±2.7)	0.5

^a number of experiments, ^bFlow-through incl. wash fraction, ^c elution 1 and elution 2 summarized

Table 11: Performance of EEL-polymer LAC (3 ml column, 4.3 mg/ml ligand density) using two different cultivation broths (standard deviations are given in parentheses)

Sample batch	N ^a	HA-activity [%]				
		No.	HA-activity [kHAU/ml]	Load	FT	Elution ^b
1	4	20.5 (±2.2)	100	5.5 (±3.3)	90.2 (±12.5)	95.7 (±14.4)
2	3	68.3 (±11.0)	100	4.6 (±0.9)	90.0 (±13.4)	94.6 (±14.2)

^a number of runs; ^b elution 1 and 2 summarized

Table 12: Comparison of purification characteristics from EEL polymer (3 ml column; 4.3 mg/ml ligand density) and EEL-cellulose membrane (3 µm pore size; 0.02 mg/cm² ligand density; 3 experiments per matrix; standard deviations are given in parentheses)

EEL-polymer	HA-activity		Total protein		dsDNA	
	kHAU	%	µg	%	µg	%
Load	284.3 (±3.8)	100	224.0 (±14.6)	100	41.3 (±0.8)	100
Flow-through^a	13.0 (±2.5)	4.6 (±0.9)	100.8 (±5.9)	45.1 (±3.9)	41.7 (±1.2)	101.1 (±1.5)
Elution 1	242.7 (±38.8)	85.5 (±14.2)	113.0 (±23.1)	50.4 (±8.9)	0.075 (±0.079)	0.2 (±0.2)
Elution 2	12.8 (±3.3)	4.5 (±1.1)				
Total recovery		94.6 (±14.2)		95.5 (±6.3)		101.3 (±1.3)
EEL-membrane	HA-activity		Total protein		dsDNA	
	kHAU	%	µg	%	µg	%
Load	227.6 (±4.5)	100	223.5 (±7.4)	100	40.0 (±0.9)	100
Flow-through^a	21.0 (±1.1)	9.3 (±0.6)	108.0 (±5.9)	48.4 (±3.4)	37.9 (±1.6)	94.6 (±1.8)
Elution 1	230.5 (±5.3)	101.3 (±0.9)	68.8 (±1.6)	31.3 (±1.6)	0.4 (±0.08)	1.0 (±0.2)
Elution 2	14.2 (±4.5)	6.2 (±1.9)				
Total recovery		116.8 (±1.7)		79.7 (±4.9)		95.6 (±1.5)

^a Wash: below limit of quantification

In both sets of experiments low HA-activity could be measured in the flow-through (EEL polymer: 4.6% (±0.9) HA-activity; EEL membrane: 9.3% (±0.6) HA-activity; Table 12). The majority of virus bound to the EEL-modified matrices and could be released in elution step 1 (EEL polymer: 85.5% (±14.2) HA-activity; EEL membrane: 101.3% (±0.9) HA-activity; Table 12). Based on the starting material both purification procedures reduced the total protein amount (viral and MDCK host cell proteins) to 50.4% (±8.9) and 31.3% (±1.6), respectively (Table 12). The level of contaminating dsDNA was reduced to 0.2% (±0.2) using the polymer-based adsorbent and to 1.0% (±0.2) with the

cellulose membrane. Considering only the major product peak within elution 1 (Figure 12) influenza virus activity was estimated to 50.8 kHAU/ml (± 9.5) for the polymer adsorbent and to 30.5 kHAU/ml (± 3.2) for the membrane adsorber (Table 13). The total protein and dsDNA concentration in the major product peak for the polymer experiments amounted to 24.6 $\mu\text{g/ml}$ (± 5.0) and 8.7 ng/ml (± 3.5), respectively. The corresponding concentrations for the membrane runs were 9.4 $\mu\text{g/ml}$ (± 1.1) and 4.5 ng/ml (± 1.3), respectively (Table 13). All experiments for product and contaminant mass balancing were carried out with sample volumes below the maximum binding capacity. The HA content estimated by SRID in the major product peak was 22 $\mu\text{g/ml}$ (± 5) for the polymer resin and 11 $\mu\text{g/ml}$ (± 0.3) for the membrane adsorber, which correlates well with the measured total protein concentration.

Table 13: Analysis of the major peak from elution 1 after EEL-membrane and EEL-polymer LAC based on concentrations of the loaded sample and the purification efficiency (each adsorbent 3 runs; standard deviations are given in parentheses)

		Measured concentrations			Calculated impurity	
		HA-activity kHAU/ml	Protein, C_{prot} $\mu\text{g/ml}$	dsDNA, C_{DNA} $\mu\text{g/ml}$	i_{prot} $\mu\text{g protein/kHAU}$	i_{DNA} $\mu\text{g dsDNA/kHAU}$
EEL- polymer beads	Load	71.1 (± 0.9)	56.0 (± 3.6)	10.3 (± 0.2)	0.8 (± 0.04)	0.145 (± 0.005)
	Elution	50.8 (± 9.5)	24.6 (± 5.0)	0.0087 (± 0.0035)	0.5 (± 0.22)	$1.8 \cdot 10^{-4}$ ($\pm 1.1 \cdot 10^{-4}$)
EEL- membrane adsorber	Load	56.9 (± 1.1)	55.9 (± 1.9)	10.0 (± 0.2)	1.0 (± 0.03)	0.176 (± 0.002)
	Elution	30.5 (± 3.2)	9.4 (± 1.1)	0.0045 (± 0.0013)	0.3 (± 0.02)	$14.7 \cdot 10^{-4}$ ($\pm 2.8 \cdot 10^{-4}$)

EEL-membrane capacity

With a load of 18 ml of concentrated fermentation broth (68.3 ± 11.0 kHAU/ml) to the membrane a breakthrough was achieved (Figure 14, about 40% overloading). Correspondingly, a HA-activity of 670.5 kHAU was estimated in the eluted product fraction as dynamic membrane capacity (Figure 15). This corresponds to approximately 9 kHAU/cm² membrane with an EEL ligand density of about 0.02 mg/cm².

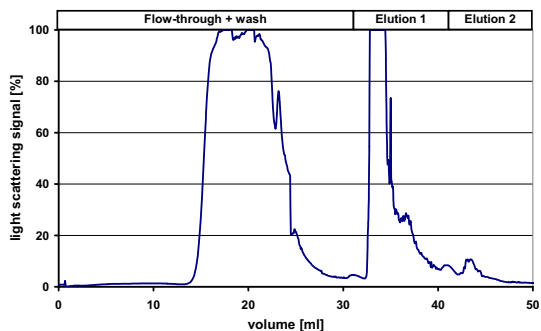


Figure 14: EEL-AC monitored by light scattering (90°): breakthrough of the EEL-membrane ($3 \mu\text{m}$ pore size, ligand density: 0.02 mg/cm^2) loading human influenza A virus A/Puerto Rico/8/34 concentrate

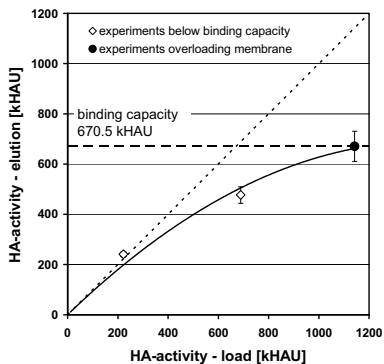


Figure 15: Binding capacity of the EEL membrane ($3 \mu\text{m}$ pore size, 75 cm^2 , 0.02 mg EEL/cm^2): eluted viral product fraction (vertical axis, HA-activity) against loaded virus amount (horizontal axis, HA-activity, \diamond : load below binding capacity, \bullet : load above binding capacity)

Virus capturing and concentration by EEL polymer

Capturing viruses from a clarified ($0.45 \mu\text{m}$) but unconcentrated broth ($3.3 \pm 0.2 \text{ kHAU/ml}$) by an EEL-polymer column (Figure 16) led to a recovery of 93% HA-activity in the product fraction based on the loaded sample (Table 14). The HA-activity of the flow-through was 19%. If only the first elution step is evaluated, an HA-activity of $25.9 \pm 1 \text{ kHAU/ml}$ was achieved, which corresponds to a concentration factor of $7.9 (\pm 0.5)$.

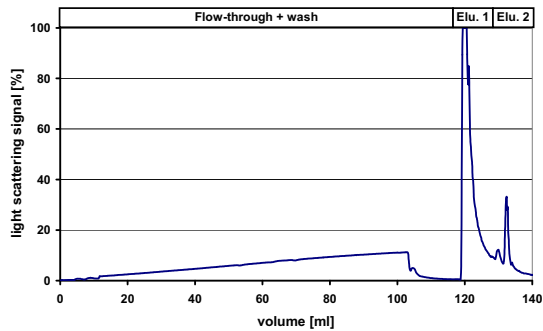


Figure 16: EEL-AC: human influenza virus A/Puerto Rico/8/34 capture from 100 ml unconcentrated cultivation broth by the EEL-polymer beads (3 ml column, 5.0 mg/ml ligand density; monitored by light scattering: 90°)

Table 14: HA-activity mass balance: influenza virus A/Puerto Rico/8/34 captured by EEL-polymer AC (3 ml column, 5.0 mg/ml ligand density) using unconcentrated culture broth (number of runs 3)

HA-activity [%]					
Load	Flow-through	Elution			Total recovery ^a
		1	2	total	
100	18.6 (± 8.0)	84.9 (± 5.5)	8.0 (± 0.8)	92.9 (± 5.7)	111.5 (± 5.9)

^a wash neglected

Virus size distributions

Dynamic light-scattering analysis resulted in a mean particle diameter of 122.8 nm for the unconcentrated virus and 115 nm for the concentrated virus sample. The particle sizes ranged in both cases from 60 to 600 nm (Figure 17) with a slight shift in size distribution towards larger particles for concentrated samples.

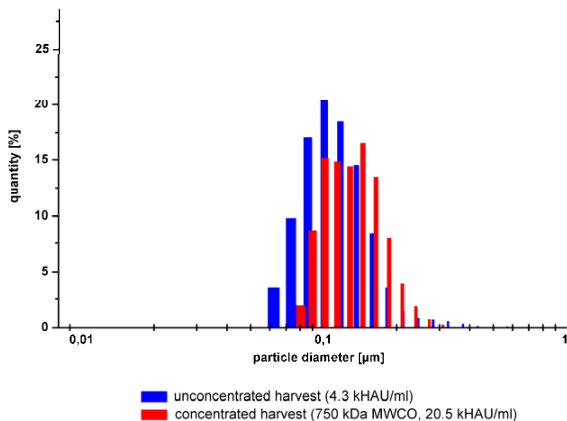


Figure 17: Particle-size-distribution analysis of concentrated (750 kDa MWCO) and unconcentrated cultivation broths containing influenza virus A/Puerto Rico/8/34

4.2.2 Discussion

This subproject focused on the evaluation of different matrices for a capture EEL-AC of influenza A viruses. Six chromatography media were screened. Two media were commercially available; four others were prepared by immobilization of EEL onto pre-activated matrices. Finally, the adsorbent characteristics were compared to 2 alternative affinity adsorbents currently used for influenza A virus purification (Anonym 2006; Oka et al. 1985; Palache et al. 1997; Peterka et al. 2007; Van Scharrenburg and Brands 1998; Vanlandschoot et al. 1996). The EEL ligand density ranged between 1.4 to 4.8 mg/ml depending on the immobilization efficiency. Cellulose membranes with a pore size of 0.45 µm and 3 µm allowed to bind 5.25 and 1.1 mg EEL, respectively, per 75 cm² membrane area. However, it seems that there is no direct correlation between ligand density and influenza virus-binding efficiency (Table 10). For instance, in the case of EEL-Actigel ALD (3.5 mg EEL/ml), approximately 58% of the loaded HA-activity did not bind. In contrast, only 10% of a comparable sample was not bound to EEL Trisopor[®] (1.4 mg EEL/ml).

The virus capturing efficiency of the adsorbents tested was determined by the ratio between the HA-activity in the product fractions and the flow-through and wash fractions. These ratios ranged between 0.5 and 12.8, with the cellulose membrane and the polymer as the most promising candidates with ratios of 12.8 and 9.2, respectively

(Table 10). The Trisopor[®] performance ranked below the polymer and cellulose membrane but was still superior to the remaining chromatography media. The efficiency of agarose-based media (EEL-Actigel ALD, EEL-Agarose, Heparin HP) for the capturing of MDCK cell-derived human influenza A virus was lower than that of any other screened medium. Here, only 30% to 40% of the loaded HA-activity could be eluted as product and the bound-to-unbound ratios were approximately one. Cellufine[®] sulphate, an alternative pseudo-affinity adsorbent for virus purification, was similar to EEL Cellufine[®]. Here, the HA-activity of unbound virus fractions ranged between 23 and 32% and the bound-to-unbound ratio between 2.1 and 2.3. No explanation was found for the low total recovery from the EEL-agarose and EEL-Cellufine[®] matrices. EEL agarose was included in the preliminary screen, because this matrix is commercially available. However, scalability of column-based chromatography using agarose media is limited and, therefore, economically uninteresting for large-scale processes. EEL Cellufine[®] had the same virus capturing efficiency than Cellufine[®] sulphate. Therefore, the process conditions for these media were not further evaluated.

Polymer-based matrices, e.g., Toyopearl AF-Tresyl-650 M, have already been applied successfully for specific glycoprotein purification using different lectins as ligand (Cartellieri et al. 2002; Cartellieri et al. 2001; Helmholtz et al. 2003). Cartellieri et al. compared the LAC purification of asialofetuin based on *Ricinus communis* agglutinin (RCA) immobilized on agarose and the polymeric matrix Toyopearl AF-Tresyl-650 M (Cartellieri et al. 2001). In these studies the RCA polymer had a significantly higher adsorption of the target glycoprotein than the RCA agarose. Cartellieri et al. suggested that the RCA-agarose binding sites were less accessible or less active than the RCA-Toyopearl-polymer binding sites. In our case, the internal binding sites of the polymer were most likely also not accessible to the virus. Virus aggregation could even boost steric hindrance. Agarose and sepharose are classified as gel matrices with weak mechanical stability. In contrast, cellulose and silica but also polymer-based matrices tolerate higher pressure (Kang and Ryu 1991). In our study, different adsorption behaviour has been observed between the soft gel adsorbents and the more rigid matrices. Due to the agarose particle size range (45 to 165 μm) a denser packing of the media could also reduce the accessible binding sites especially for larger particles such as virus particles. A diffusion of virions or small virus aggregates into the matrices is impossible except for Trisopor[®], which has an average pore size of 389 nm. Hence, only the outer surface of most matrices can adsorb virus particles.

The maximum pressure allowed often restricts the scale-up of an affinity chromatography process in axial directions using soft-gel matrices. Increasing the column height leads to an increase of the hydrostatic pressure that could damage the gel matrix irreversibly (Kang and Ryu 1991). Synthetic polymeric beads, e.g., Toyopearl resins, tolerate an operation pressure of up to 7 bar (manufacturer information) whereas Cellufine[®] sulphate or agarose beads have a lower pressure tolerance (≤ 2 bar, according to the manufacturer). Hence, the good mechanical properties of polymer beads allow an enhanced axial scalability of the column dimensions compared to, e.g., agarose-based gel matrices or conventionally applied Cellufine[®] sulphate beads. Consequently, the productivity of this unit operation can be significantly improved by this matrix. Furthermore, the ease of scalability of membrane adsorbers (maximum allowed pressure: 6 bar) with a pore size of $>1 \mu\text{m}$ suggests their application for large-scale downstream processes. Thus, the choice of which the superior matrices, compared to Cellufine[®] sulphate, will be applied in such a large-scale process is independent of the tested ligand, which can be readily immobilized on either matrix.

Size-distribution analysis indicated that the virus concentrate contained particles larger than the influenza virus (80-120 nm (Webster et al. 1992), Figure 17), suggesting the existence of virus aggregates. In particular, concentrated virus broths contained larger virus aggregates. Such aggregates probably caused fast blocking of the membrane pores ($0.45 \mu\text{m}$) and, therefore, resulted in a continuous pressure increase. Hence, the small porous membrane could be used only for a limited number of experiments. Therefore, a wide-porous EEL membrane ($3 \mu\text{m}$) was tested additionally. This membrane had a higher life time. For more than 18 experiments no significant increase in back pressure was noted. However, increasing of the pore size comes along with a reduction of surface leading to a lowered binding capacity.

All experiments were done with two cultivation batches. One batch was used for the matrix screen, the other to characterize the performance of the most favourable matrices, the EEL-cellulose membrane ($3 \mu\text{m}$) and the EEL polymer. A comparison by HA-activity mass balances indicated no significant variation between both batches (Table 11). For individual media, various other cultivation batches were tested in preliminary experiments, which also showed no significant variations.

The virus capturing efficiency of the EEL polymer was comparable to the EEL membrane (Table 12). The major HA-activity was detected in elution step 1. In the case of the polymer and the membrane about half of the total protein loaded did not bind

(Table 12). Approximately 50% (polymer) and 30% (membrane) of the total protein loaded were detected in elution 1, respectively. These are higher values than reported in the lectin screening section 4.1. For these experiments cultivation broths were concentrated by a 10 kDa MWCO membrane. Here, a 750 kDa MWCO membrane was used, leading to a lower protein concentration in the starting material. Hence, a larger portion of the total protein in the product fraction originated from the viruses. The overall protein recovery using EEL-membrane LAC was relatively low. This problem of a decreased protein recovery after membrane-based protein purification has already been observed by Sorci et al. (Sorci et al. 2006). On the other hand, dsDNA was almost completely removed from the product fraction (Table 12). Only 0.2% (polymer) and 1% (membrane) based on the sample loaded remained in elution 1. Due to the high NaCl content of the desorption buffer used for elution 2, the total protein and dsDNA concentration in elution 2 could not be analyzed. However, these elution fractions contained only small amounts of HA-activity (EEL polymer: 12.8% (± 3.3), EEL membrane: 14.2% (± 4.5)) and were therefore not of high economic interest. There is a small difference in final dsDNA content between the polymer and membrane adsorbent. Comparable EEL-polymer LAC experiments with the cultivation batch for media screening have led to 0.84% (± 0.18) dsDNA content in fraction elution 1 based on the loaded sample. These results indicated an equivalent dsDNA reduction performance for cellulose membrane and polymer LAC. Due to insufficient sample volumes for a complete comparison, these data are not shown. The measured concentrations of the major virus peak in elution 1 (Figure 12) are reported in Table 13. Based on these concentrations calculated impurities were 0.5 μg total protein and 0.18 ng dsDNA per kHAU for EEL-polymer LAC. The corresponding impurities for the EEL-membrane LAC were 0.3 μg total protein and 1.47 ng dsDNA per kHAU. Considering the SRID results and a HA input of 15 μg per dose (European Pharmacopoeia 6.4) about 8 to 10 ml of bioreactor harvest are required per dose of vaccine.

Compared to a column-based LAC the main advantages of the membrane adsorbents are the high capacity and the lack of diffusion limitations. In contrast to the EEL-polymer capacity (Chapter 4.1, approximately 125 kHAU/ml resin, ligand density 4.3 mg/ml), the EEL-membrane (3 μm) had a dynamic capacity of 670.5 kHAU per 75 cm^2 (1.1 mg EEL). This corresponded to approximately 610 kHAU/mg EEL for the cellulose membrane and 29 kHAU/mg EEL for the polymer, representing a 21-fold difference in binding capacity based on the ligand. Assuming an average hemagglutination titer (3.0)

from a clarified culture broth, the 75 cm² EEL-membrane module (3 μm) could bind the virus content from about 67 ml culture harvest. This corresponds to an area of 1119 cm² for 1 L of cultivation broth, a capacity that could be further increased by a higher ligand density.

Most of the screening and characterization experiments were done with concentrated samples to reduce the individual process time of the experiments. In addition, the applicability of EEL-AC for unconcentrated cultivation broths has been demonstrated, achieving a concentration factor of 8 under not-optimized process conditions. These experiments were conducted approximately 25% below the capacity of the adsorbents. Therefore, an increased load volume would result in a higher concentration factor. Additionally, the concentration factor can be even further increased by optimizing the column dimensions or increasing the number of membrane layers. Thus, EEL-AC seems to be a valuable capture step for unconcentrated influenza virus cell culture broth. Analysis of HA-activity (Table 14) assay and light-scattering signal (Figure 16) loading unconcentrated virus broths indicated a slightly higher HA-activity (about 10%) in the flow-through fractions compared to experiments using concentrated samples. This can be explained with the increased loading flow rate (0.3 ml/min). Capturing the virus from large-scale cultivations has to be conducted under more efficient conditions than those selected for the preliminary screen. Therefore, several flow rates were tested using the EEL-cellulose membrane as adsorbent. Here, it was found that a flow rate higher than 0.3 ml/min led to a high content of unbound virus in the flow-through fraction. Nevertheless, increased column lengths or membrane layers would reduce the unbound virus fraction again. With an increased number of membrane layers it would be possible to use even higher flow rates without significantly increasing the back pressure. However, as the wide-porous membrane was a custom-made adsorber, further tests could not be conducted.

Both matrices seemed to have good long-term stability. The EEL-polymer matrices were used for more than 50 runs and the EEL membrane (3 μm pore size) was used for 18 runs without any noticeable loss of binding activity or pressure increase. A similar stability of the polymer-based lectin column (8 months) was also observed by Cartellieri et al. (Cartellieri et al. 2002).

The cost for EEL, which is a ligand produced from natural sources, exceeds the production costs of alternative pseudo-affinity media for virus purification, such as heparinized (Anonym 2006) and sulphated matrices (Oka et al. 1985; Palache et al.

1997; Peterka et al. 2007; Van Scharrenburg and Brands 1998). For example, based on dynamic binding capacity data (A/Puerto Rico/8/34) the cost for the EEL-polymer matrix is about 20-fold higher compared to Cellufine[®] sulphate (small-scale experiments). However, sulphated matrices have a decreased target specificity compared to EEL. Furthermore, the cost effectiveness of the EEL-AC can be improved by using recombinant EEL versus the natural ligand. Recombinant EEL might be produced in *Escherichia coli* similar to the recombinant production process described for ECL that yielded in 870 mg ECL per liter cultivation broth (Stancombe et al. 2003). Robustness of the LAC, regarding transferability of the method to currently circulating influenza virus strains is shown in the following section.

4.3 Transferability of LAC: Different influenza virus strains and host cells

Previous chapters focused on a specific influenza subtype (H1N1) used as a model strain. However, production processes need to be virus-type independent. Hence, the general applicability of LAC for other MDCK cell-derived influenza viruses will be addressed in the following. For this purpose two virus types from the epidemical seasons 2006/07 and 2007/08 (A/Wisconsin/67/2005 (H3N2), B/Malaysia/2506/2004) were screened for virus binding by small-scale chromatographic experiments. The outcome was compared with results obtained previously for the influenza virus A/Puerto Rico/8/34 (H1N1). In addition, binding studies with all three influenza virus strains regarding to the two most promising candidates for LAC (EEL, ECL) were conducted by surface plasmon resonance technology (SPR). Furthermore, preparative LAC with the most suitable lectin (EEL) was characterized for A/Wisconsin/67/2005 and B/Malaysia/2506/2004. Finally, the influence of the host cell line and cultivation conditions on virus capturing by LAC is discussed. For this purpose, the lectin binding to viral strains, produced in industrial-relevant cell lines MDCK (adherent and suspension cells) and Vero, was studied. Virus harvests were obtained from roller bottles and bioreactors using several media.

4.3.1 Results

Small-scale affinity chromatography for ligand screening

Based on literature data on HA glycosylation and preliminary studies with the model virus A/Puerto Rico/8/34 various lectins were selected as ligands for small-scale affinity chromatography experiments. The amount of bound and displaced virus particles in product fractions was evaluated by HA-activity assay.

The major part of MDCK cell-derived influenza viruses (A/Wisconsin/67/2005, B/Malaysia/2506/2004) could be recovered from the EEL-modified matrix. Thus, results obtained by other lectin columns for both virus strains were normalized to EEL (Figure 18). ECL-modified polymer beads captured MDCK cell-derived virus strains in a similar way to EEL. However, due to the set-up of the experiment, these results cannot be used to characterize binding kinetics of the target virus to the ligand.

In contrast to MDCK cell-derived influenza virus particles, Vero cell-derived influenza virus A/Puerto Rico/8/34 bound less to EEL than to ECL. Hence, recovered product HA activities from Vero cell-derived virions obtained by all other lectin spin columns were normalized to ECL (Figure 18). Compared to ECL, only about 24% of the HA-activity (Vero cell-derived influenza virus A/Puerto Rico/8/34) was recovered from the EEL matrix.

Normalized to the optimal ligand (EEL or ECL), viral product recovery of all other tested lectins (AIL, MAL I, PA-I, PNA, SNA) was less than 30% (Figure 18).

For influenza virus A/Wisconsin/67/2005 about one fifth of the HA-activity value recovered from the EEL-modified spin column was obtained from the (β 1,3)-galactose-specific PNA (21%) and AIL (20%) matrices. Compared to EEL influenza virus B/Malaysia/2506/2004 was captured by MAL I, PNA, SNA, AIL and PA-I spin columns only to about less than 5%. Vero cell-derived virus particles showed some affinity to MAL I (29%), PNA (19%) and AIL (15%).

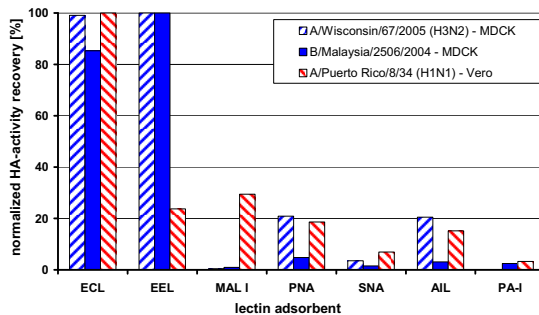


Figure 18: Recovery of HA-activity in product fraction after small-scale LAC (normalized to the value of the most suitable lectin per virus type) using MDCK cell-derived influenza virus types A/Wisconsin/67/2005 and B/Malaysia/2506/2004 (normalized to EEL) and the Vero cell-derived influenza virus A/Puerto Rico/8/34 (normalized to ECL). Due to the applied method, binding kinetics did not influence the HA-activity recovery.

Comparative binding analysis by SPR

A lectin-modified sensor-chip (type: SA) was used for comparative binding analysis between EEL and ECL for the three different MDCK cell-derived influenza virus strains. In addition, adsorption of Vero and MDCK cell-derived influenza viruses to both ligands was compared using the model virus A/Puerto Rico/8/34.

All sensorgrams (Figure 19, Figure 20) contain first an association phase, where virus bulk was flushed over ligand-modified surfaces. However, no steady states were reached. After 3 min of the association phase the sample injection was stopped. In a second phase, the dissociation phase, only adsorption buffer (AB2) was run through the flow cells. Virus-lectin complexes dissociated, but RU decreased only marginally with a very low dissociation rate ($\sim 10^{-5} \text{ s}^{-1}$) close to the detection limit.

SPR analysis: interaction between different MDCK cell-derived influenza virus types and lectins

All three MDCK cell-derived influenza virus types bound to both lectins. However, virus particles bound faster to EEL than to ECL (Figure 19). At the end of the association phase, EEL response signals of approximately 2000 RU were reached for both MDCK cell-derived influenza virus A subtypes. The influenza virus type B reached a final signal value of about 1100 RU. In contrast, the ECL-modified surface yielded for identical virus samples only about 20% of these values (Figure 19).

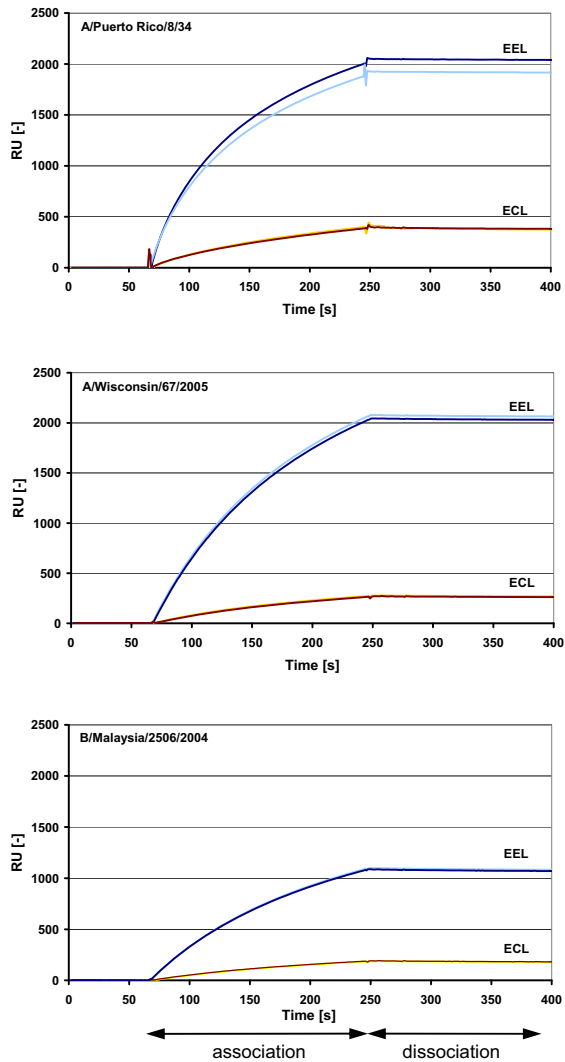


Figure 19: Comparative binding analysis of three MDCK cell-derived human influenza virus types to EEL and ECL by SPR technology (Biacore 2000, 2 cycles per virus type are shown, association and dissociation phases are marked, signal changes due to sample matrix were eliminated by subtraction of the reference flow cell signal)

SPR analysis: host cell line dependency of virus-lectin association

Vero cell-derived influenza virus (A/Puerto Rico/8/34) yielded significantly lower adsorption to EEL (final association signal ~400 RU) than virus propagated in MDCK cells (final association signal ~ 2000 RU; Figure 20). However, influenza virus particles (A/Puerto Rico/8/34) from both cell lines reached similar association response signals on the ECL-coated flow cell. Furthermore, association curves of the Vero cell-derived virus were similar for EEL and ECL.

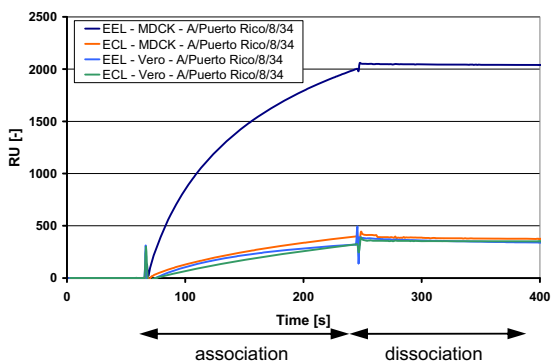


Figure 20: Comparative binding analysis of Vero- and MDCK cell-derived human influenza virus A/Puerto Rico/8/34 to EEL and ECL by SPR technology (Biacore 2000, association and dissociation phases are marked, signal changes due to sample matrix were eliminated by subtraction of the reference flow cell signal)

Dynamic virus-binding capacity of EEL-polymer beads

Overloading the affinity column with approximately 1000-1200 kHAU (61.1 cm/h) of each virus type (including the model strain A/Puerto Rico/8/34) dynamic virus-binding capacities were determined. Based on the HA-activity assay 156 kHAU/ml resin (A/Wisconsin/67/2005), 233 kHAU/ml resin (B/Malaysia/2506/2004) and 89 kHAU/ml resin (A/Puerto Rico/8/34) were eluted from the EEL-modified medium.

Capturing characteristics of MDCK cell-derived influenza virus by LAC

For experiments described in the following section the affinity column was loaded 14% (A/Wisconsin/67/2005) and 45% (B/Malaysia/2506/2004) below the dynamic binding capacity based on HA-activity analysis. HA-activity recovery of the eluted product fraction after EEL-AC was 86% (± 10) for A/Wisconsin/67/2005 and 77% (± 4) for

B/Malaysia/2506/2004 based on the total amount of the loaded virus (Table 15). The total protein content was reduced to 36% (± 2) and 16% (± 2) and host cell dsDNA content reduced to 2.6% (± 0.1) and 0.5% (± 0.04) for A/Wisconsin/67/2005 and B/Malaysia/2506/2004, respectively. The A/Wisconsin/67/2005 product fraction of the EEL-polymer column chromatography contained 37 kHAU/ml (± 5), a dsDNA concentration of 78 ng/ml (± 10), a total protein concentration of 50 μ g/ml (± 9), and a HA concentration of 27 μ g/ml (± 8), estimated by SRID (Table 16). Corresponding concentrations for B/Malaysia/2506/2004 were 48 (± 6) kHAU/ml, 78 ng/ml (± 8) dsDNA, 46 μ g/ml (± 5) total protein and 11 μ g/ml (± 2) HA concentration.

Table 15: Purification characteristics using EEL-AC to capture influenza virus types A/Wisconsin/67/2005 (H3N2) and B/Malaysia/2506/2004 (3 experiments per virus type, mean and standard deviations of three individual samples)

	HA-activity		Total protein		dsDNA	
	kHAU	%	μ g	%	μ g	%
A/Wisconsin/67/2005 (H3N2)						
Load	394 (± 59)	100	1262 (± 37)	100	27.1 (± 1.0)	100
FT^a	56 (± 6)	14 (± 1)	789 (± 19)	62 (± 3)	22.3 (± 1.1)	82.3 (± 2.2)
Elution 1	337 (± 22)	86 (± 10)	452 (± 34)	36 (± 2)	0.71 (± 0.009)	2.6 (± 0.1)
Elution 2^b	10 (± 3)	3 (± 1)				
Total		103 (± 10)		98 (± 2)		84.9 (± 2.2)
B/Malaysia/2506/2004						
Load	381 (± 29)	100	1810 (± 46)	100	96.9 (± 1.8)	100
FT^a	71 (± 9)	19 (± 1)	1420 (± 34)	78 (± 1)	94.9 (± 2.2)	97.9 (± 2.3)
Elution 1	294 (± 37)	77 (± 4)	282 (± 25)	16 (± 2)	0.48 (± 0.05)	0.5 (± 0.04)
Elution 2^b	20 (± 4)	5 (± 1)				
Total		101 (± 5)		94 (± 2)		98.4 (± 2.3)

^a Flow-through (incl. wash fraction, if not below limit of quantification)

^b due to high NaCl content, no total protein and dsDNA quantification

Table 16: Concentrations and impurities of product fraction (Elution 1) after EEL-AC (3 experiments per virus type, mean and standard deviations of three individual samples)

	A/Wisconsin/67/2005 (H3N2)	B/Malaysia/2506/2004
Measured concentrations		
HA-activity [kHAU/ml]	37.0 (± 4.8)	47.7 (± 5.8)
hemagglutinin c_{HA} [$\mu\text{g/ml}$]	27 (± 8)	11 (± 2)
total protein c_{prot} [$\mu\text{g/ml}$]	49.8 (± 9.0)	45.7 (± 4.5)
dsDNA c_{DNA} [ng/ml]	78 (± 10)	78 (± 8)
Calculated impurities		
i_{prot} [$\mu\text{g total protein} / \mu\text{g HA}$]	1.8 (± 0.3)	4.2 (± 0.7)
i_{DNA} [ng dsDNA / $\mu\text{g HA}$]	3 (± 0.6)	7.1 (± 1.3)
i_{prot} [$\mu\text{g protein} / \text{kHAU}$]	1.4 (± 0.08)	1.0 (± 0.2)
i_{DNA} [ng dsDNA / kHAU]	2 (± 0.1)	2 (± 0.3)

4.3.2 Discussion

The main scope of the third subproject was to confirm the general applicability of LAC for purification of cell culture-derived influenza virus particles. There are several studies about glycan analysis of influenza virus glycoproteins (Basak et al. 1981; Deom and Schulze 1985; Mir-Shekari et al. 1997). Based on the published glycan structures and previous results, using EEL and ECL to purify influenza virus A/Puerto Rico/8/34, various lectins were screened for binding to two MDCK cell-derived influenza virus types from season 2007/08 to evaluate strain independency of the capturing method. In addition, host cell line dependency of viral protein glycosylation and the influence on LAC was determined by the influenza virus model A/Puerto Rico/8/34 propagated in Vero cells and compared to previous results, where this model virus had been produced in MDCK cells. To compare both influenza virus production cell lines, these experiments were performed with the model strain A/Puerto Rico/8/34 produced in roller bottles and prepared under the same conditions as described earlier for the method development. No mannose (e.g., Concanavalin A) and fucose (e.g., *Aleuria aurantia* lectin) specific lectins were tested, as these carbohydrate residues are common in *N*-linked glycostructures, and both ligands showed a relatively high affinity to MDCK cell proteins in previous experiments. Hence, these lectins lack the required specificity for efficient separation of target protein from host cell protein.

Small-scale capturing experiments (Table 4, Figure 18) indicated that complex glycans of envelope glycoproteins from Vero and MDCK cell culture-derived influenza viruses contain low amounts of terminal (β 1,3)-galactose (PNA, Jacalin) and sialic acid (MAL I, SNA). The low degree of sialylation is most likely due to the viral NA-activity, which truncates terminal sialic acid residues (Mir-Shekari et al. 1997; Wilson et al. 1981).

For both MDCK cell-derived influenza virus types the capture efficiency in spin column experiments was high for ECL and EEL. This corresponds with previous findings from MDCK cell-derived influenza model virus A/Puerto Rico/8/34 and indicates the presence of terminal (α 1,3)-galactose (EEL) and (β 1,4)galactose (ECL) on glycans of viral envelope glycoproteins. In contrast, Vero cell-derived glycoproteins of influenza virus A/Puerto Rico/8/34 have most likely comparable amounts of terminal (β 1,4)-galactose (ECL) residues on complex glycans but a reduced number of (α 1,3)-galactose (EEL) residues (Table 4, Figure 18). Such differences in host cell dependent glycosylation of viral envelope glycoproteins have already been described (Geyer et al. 1990; Hsieh et al. 1983; Liedtke et al. 1994) and are known for therapeutic proteins produced in recombinant mammalian cell lines (Werner et al. 2007).

Due to repeated sample recirculation during loading, AffiSpin[®] column experiments did not allow an investigation of the dynamics of ligand-target molecule interaction. Therefore, differences in the binding kinetics for both lectins (EEL, ECL) were characterized by SPR analysis (Figure 19). Here, the value of the SPR response signal depended on the mass adsorbed to the sensor-chip surface. Binding rates of MDCK cell-derived influenza viruses to EEL were higher than to ECL. Assuming virus particles of similar size binding to comparatively small immobilized ligands, adsorption of both influenza A subtypes was similar. Adsorption of the influenza virus B type to both lectins was lower compared to influenza A. This is probably due to slight variations in the glycosylation of viral envelope proteins between different influenza virus types.

On the other hand Vero cell-derived influenza virus A/Puerto Rico/8/34 resulted in approximately 1/5 of the binding signal to EEL compared to MDCK cell-derived virus (Figure 20). This confirmed the findings from spin column experiments in which Vero cell-derived virus particles bound less to (α 1,3)-galactose-specific EEL. Hence, ECL but not EEL was considered as ligand for LAC of Vero cell-derived influenza viruses. However, ECL has two major drawbacks: (1) The binding kinetics is too slow for an economical process. Using the same chromatographic conditions as for EEL-AC, about half of the virions (Vero cell-derived A/Puerto Rico/8/34) were not captured by ECL-

modified polymer beads. Capturing the majority of virions from Vero cell culture bulk by ECL-affinity chromatography (ECL-AC) could only be achieved by sample recirculation as done during method development or by decreasing the flow rate (< 61.1 cm/h), which is economically unattractive. Hence, ECL is only of interest for analytical purposes, but not for the design of purification trains. (2) Lectin blot analysis has demonstrated that ECL lacks the required specificity to influenza viruses as compared to Vero cell proteins (data not shown). Thus, only a partial separation between host cell proteins and virions could be achieved. Consequently, capturing of Vero cell-derived influenza viruses by ECL-AC, was not investigated further. In contrast, EEL has shown only marginal affinity to MDCK host cell proteins in previous studies using western blot analysis. The galactose-specific lectin PA-I was tested as an alternative to ECL, but adsorbed even fewer viruses than EEL probably because of a low ligand density (Figure 18). Due to its general specificity to galactose and its derivatives, PA-I was also not investigated further as an affinity ligand.

SPR experiments determine the binding of virus particles to immobilized ligands on a sensor-chip surface by monitoring changes of the refractive index close to the sensor surface, which is proportional to the adsorbed mass (Malmqvist 1993). The sensorgrams obtained did not reach a steady state during association. Since influenza viruses tend to form aggregates, virus-virus binding after initial virus-lectin adsorption could result in formation of multiple layers and long-term signal changes in SPR. Even using highly concentrated virus samples and long association times, no steady state occurred in the association phases. However, Biacore analysis performed in duplicates showed high reproducibility.

Virus particles contain a high number of envelope glycoproteins with multiple glycosylation sites as target for the lectin interaction. The precise number of glycosylation sites is strain dependent and for the tested strains not known. Furthermore, the individual accessibility of these targets is not known. However, due to the size of the viral particles and number of potential glycosylation sites, the adsorption of virus particles to lectins on chromatographic media as well as on the sensor-chip surface can be assumed to be multivalent. Hence, an accurate calculation of binding rates and affinity constants is difficult. However, based on Lauffenburger and Linderman a 1:1 binding model can be used to estimate an avidity constant, which describes the overall tendency of multivalent binding (Lauffenburger and Linderman 1993). According to such a model (Karlsson et al. 1991), MDCK cell-derived influenza A/Puerto Rico/8/34

virions binding to EEL ligands would have an avidity constant of about 10^{12} M^{-1} (molar virus concentrations for this calculation were estimated from HA-activity measurements assuming that on average one virus particle is binding one red blood cell, molar virus mass $M_r=250 \times 10^6$, (Van Regenmortel et al. 2000)). The corresponding value for the ECL ligand would be about 10^{11} M^{-1} . The apparent high affinity reflects clearly the multivalent binding behavior.

The slow dissociation with dissociation rates close to the detection limit is probably also due to the multivalent binding (Figure 19, Figure 20). Based on a 1:1 binding model the dissociation rate constants k_d for MDCK cell-derived influenza virus particles and EEL were estimated to approximately 10^{-5} s^{-1} (Biaevaluation software, version 2.3). The k_d values for MDCK cell-derived viruses and ECL as well as Vero cell-derived virus particles and EEL or ECL were about 10^{-4} s^{-1} . The apparent association rate constants k_a using same 1:1 binding model (Biaevaluation software, version 2.3) were estimated for same binding partners to be in the range of 10^7 to $10^8 \text{ M}^{-1}\text{s}^{-1}$, with 20-60% lower values for association of virus particles and ECL than for virus particles and EEL. Hence, these results confirm that EEL is more suitable as an AC ligand than ECL.

With respect to downstream processing of influenza viruses, different chromatographic media for virus capturing using influenza A/Puerto Rico/8/34 as the model strain were characterized (Chapter 4.2). Two matrices, EEL-modified polymer beads and cellulose membranes, allowed an efficient purification of influenza virus particles. Thus, all further virus-capturing experiments were carried out using a commercially available EEL-polymer resin. In these studies the EEL-AC column was used successfully to capture the MDCK cell-derived influenza viruses A/Wisconsin/67/2005 and B/Malaysia/2506/2004 from concentrated cell culture supernatants. For both virus types, and for the model strain A/Puerto Rico/8/34, the dynamic virus-binding capacity was estimated. Capacities depended on the influenza virus type and ranged from 89 kHAU/ml resin (A/Puerto Rico/8/34) to 156 kHAU/ml resin (A/Wisconsin/67/2005) and 233 kHAU/ml (B/Malaysia/2506/2004). These variations in binding capacities could be due to the strain dependent virus particle size and differences in virus aggregation. Furthermore, it might also be related to a strain dependency of the hemagglutination assay (Wood et al. 1977). Binding capacity of A/Puerto Rico/8/34 (89 kHAU/ml resin) corresponds with previous findings (125 kHAU/ml resin), where different column dimensions and a different batch of EEL-polymer beads for the EEL-AC (column diameter 10 mm, 3ml EEL-polymer beads, 4.3 mg EEL/ml) had been used.

Considering feed virus concentrations and breakthrough data the column was loaded below the dynamic binding capacity for EEL-AC characterizations. EEL-AC could capture 89% (A/Wisconsin/67/2005) and 82% (B/Malaysia/2506/2004) of virus particles based on HA-activity measurements (Table 15, Elution 1 + 2), while only 14 to 19% HA-activity was found in the unbound flow-through fraction (Table 15). The total protein content was reduced to about 36% and 16% and the host cell dsDNA content to approximately 2.6% and 0.5% for both virus types. Hence, this affinity chromatography method results in a good separation for a single capture step. The captured product fraction (Elution 1) contained about 27 µg/ml (A/Wisconsin/67/2005) and 11 µg/ml (B/Malaysia/2506/2004) HA based on SRID (Table 16). This amounts to an input of about 3 to 10 ml cultivation bulk per strain for blending one dose of vaccine (15 µg HA/strain; European Pharmacopoeia 6.4). The level of contaminants could be reduced to 1.8 µg protein and 3 ng dsDNA per µg HA (A/Wisconsin/67/2005) and to 4.2 µg protein and 7 ng dsDNA per µg HA (B/Malaysia/2506/2004), respectively (Table 16). Based on an input of 15 µg HA antigen per strain and dose, a trivalent vaccine blend and a maximum dsDNA content of 10 ng per dose (European Pharmacopoeia 6.4), the dsDNA content after EEL-AC is, with 45 ng/ 15 µg HA (A/Wisconsin/67/2005) and 107 ng/ 15 µg HA (B/Malaysia/2506/2004), about 14 to 32-fold higher than required. Therefore, a further purification step for host cell dsDNA reduction is necessary, which could probably be achieved by subsequent benzonase treatment followed by ion-exchange and pseudo-affinity chromatography. Considering a maximum total protein content of 100 µg per virus strain and dose (European Pharmacopoeia 6.4), the AC-capturing step sufficiently reduced protein contamination. Considering purification efficiency LAC has, therefore, high potential as a downstream processing unit operation in vaccine production processes.

Previous studies for LAC method development focused on a MDCK (#841211903, ECACC, Salisbury, UK; roller bottle cultivation) cell-derived influenza virus model (A/Puerto Rico/8/34). There, the cultivation bulk was clarified by centrifugation and concentrated in a stirred ultrafiltration cell (10 kDa MWCO). Here, studies centered on two further influenza types propagated in MDCK cells relevant for vaccine production. Cells were maintained in bioreactors and virus harvests were not only clarified but also concentrated by different methods. Thus, upstream processing most likely does not affect the capturing step. Due to subtype independency shown here, the third influenza virus type from the epidemic season 2007/08 (A/Solomon Islands/3/2006, H1N1), which

is a similar subtype to the model virus from the initial study, was not investigated in EEL-AC. Besides strain independency the method indicated clearly batch-to-batch reproducibility, and suggested independency from the cultivation system.

In summary, this subproject demonstrated applicability of EEL-AC as a capturing process for different MDCK cell-derived influenza virus types from cell culture supernatants.

5 Pseudo-affinity chromatography using sulphated cellulose membrane adsorbers

The establishment of a robust and industrial-relevant influenza virus capture step based on regenerated and sulphated cellulose membranes is described below.

5.1 Results

5.1.1 Cellulose membrane sulphatation

The sulphate content of SCM adsorber discs was determined to 4.9 weight-percent (duplicated estimation). Blank cellulose membrane adsorbers discs were analyzed as well and showed no sulphate content (< 0.05 weight-percent).

5.1.2 Separation of influenza virus particles by sulphated cellulose membranes

The influence of the ionic strength in the adsorption buffer (50 and 150 mM NaCl) on influenza virus capture efficiency was evaluated for the model virus strain A/Puerto Rico/8/34. Based on the total amount of loaded virus about 28% of HA-activity was found in the unbound flow-through fraction at low ionic strength (50 mM NaCl) and about 66% could be desorbed from the matrix by 1.2 M NaCl (Table 17). In contrast, 150 mM NaCl-containing buffer resulted in a virus adsorption of about 47% HA-activity in the flow-through and reduced yield to about 60% in the product fraction (Table 17). Optimization of the elution profile achieved highest viral content and lowest contaminant coelution (dsDNA, host cell proteins) in the product fraction (Elution 1) by a two-step isocratic elution at 0.6 M NaCl and 2 M NaCl. Therefore, all further experiments were done using the 50 mM NaCl-containing adsorption buffer (AB3) and the optimized elution condition (buffers EB1 and EB2).

The dynamic adsorption capacity (breakthrough point) of the SCM stack was approximately 240 kHAU for influenza virus A/Puerto Rico/8/34. This corresponds to about 18 kHAU/cm² or 14 µg HA/cm² as determined by SRID assay.

Results obtained for non-specific binding experiments of the virus particles or contaminants to unmodified reinforced cellulose membranes, the backbone of the SCM, indicated low adsorption of virus particles (3%, HA-activity) and dsDNA (1%). The protein content in same fractions was below the limit of quantification (Elution 1+2,

Table 18). The majority of the virus particles did not adsorb to the membrane and could be detected in the flow-through fraction (about 85%, Table 18).

Table 17: Influenza virus (A/Puerto Rico/8/34, H1N1) capture using sulphated cellulose membrane adsorbers (10 layers, d: 25 mm, A~50 cm²) with two different ionic strength adsorption buffers, (flow rate: 0.5 ml/min, elution 1: 1.2 M NaCl, 10 mM Tris, pH 8, elution 2: 2 M NaCl, 10 mM Tris, pH 8, 3 experiments, mean and standard deviation of three individual samples, product fraction (elution 1) in bold)

Adsorption buffer	HA-activity [%]	
	50mM NaCl, 10 mM Tris, pH 8	150mM NaCl, 10 mM Tris, pH 8
Load	100	100
Flow-through^a	27.6 (±10.4)	46.8 (±4)
Elution 1	65.8 (±21.4)	59.8 (±8.8)
Elution 2	2.6 (±0.7)	1.6 (±0.4)
Total recovery	96.0 (±23.5)	108.2 (±8)

^a incl. wash fraction, if not below limit of quantification

Table 18: Unspecific adsorption (A/Puerto Rico/8/34) of unmodified cellulose membrane layers (10 layers, d: 25 mm, A~50 cm², flow rate: 0.5 ml/min, adsorption buffer: 50 mM NaCl, 10 mM Tris, pH 7.4, elution buffer 1: 0.6 M NaCl, 10 mM Tris, pH 7.4, elution buffer 2: 2 M NaCl, 10 mM Tris, pH 7.4, product fraction (elution 1) in bold)

	HA-activity [%]	Total protein [%]	dsDNA [%]
Unmodified cellulose membrane adsorber			
Load	100	100	100
Flow-through^a	85.3 (±2.6)	72.9 (±5)	89.6 (±2)
Elution 1	2.4 (±1.1)	LOQ^b	0.6 (±0.3)
Elution 2	0.2 (±0)	LOQ	0.3 (±0.4)
Total recovery	87.9 (±1.6)	72.9	90.5 (±1.9)

^a incl. wash fraction, if not below limit of quantification; ^b limit of quantification

The 10 SCM layers captured reproducibly all individual viral influenza strains, but with significant differences between the strains. About 82% (A/Puerto Rico/8/34, Figure 21), 94% (A/Wisconsin/67/2005, Figure 22) and 73% (B/Malaysia/2506/2004, Figure 22) HA-activity based on initial loaded amount could be recovered in the product fractions (Elution 1). Total protein content could be reduced to 16%, 43% and 42%,

respectively, and host cell dsDNA was reduced to 10%, 32% and 1%, respectively (Elution 1, Figure 21 and Figure 22).

5.1.3 Separation of influenza virus particles by column-based CSR

The dynamic binding capacity of a Cellufine[®] sulphate column (Tricorn 5/50, V=1.2 ml) was determined by loading a 3-fold-diluted virus concentrate until the (A/Puerto Rico/8/34) breakthrough point was reached. With approximately 121 kHAU/ml column medium, a capacity of about 67 µg HA/ml resin (based on the SRID assay) was obtained.

After capturing influenza virus particles by CSR about 57% (A/Puerto Rico/8/34), 99% (A/Wisconsin/67/2005) and 52% (B/Malaysia/2506/2004) HA-activity were recovered in the product fractions (elution 1, Figure 21 and Figure 22). Based on the loaded amount, the total protein content was reduced for all three strains to 18%, 63% and 23%, respectively. The corresponding dsDNA contamination in the product fraction was decreased to 24%, 9% and 18%, respectively (Figure 21 and Figure 22).

5.1.4 Influenza virus capturing by cation-exchange membrane adsorbers

Influenza virus capturing efficiency of SCM adsorbers was compared to commercially available cation-exchange membrane adsorbers Sartobind C75 and Sartobind S75. Here, the major part of virus particles (A/Puerto Rico/8/34) bound and were eluted from the adsorber with an HA-activity recovery of 63% (C75) and 76% (S75) in the product fractions (Elution 1, Figure 21). The total protein content was reduced to 16% and 19%, respectively. However, these product fractions still contained a high level of dsDNA contamination (40%, C75 and 39%, S75; Figure 21).

5.1.5 Enhanced process productivity of SCM compared to CSR

Capturing influenza virus A/Puerto Rico/8/34 by SCM adsorbers (10 layers, d=25 mm) at a velocity of 15 ml/min compared to 0.5 ml/min achieved viral product recoveries of about 62% HA-activity and reduction of total protein and dsDNA contents to about 15% and 5%, respectively (Elution 1, Figure 21).

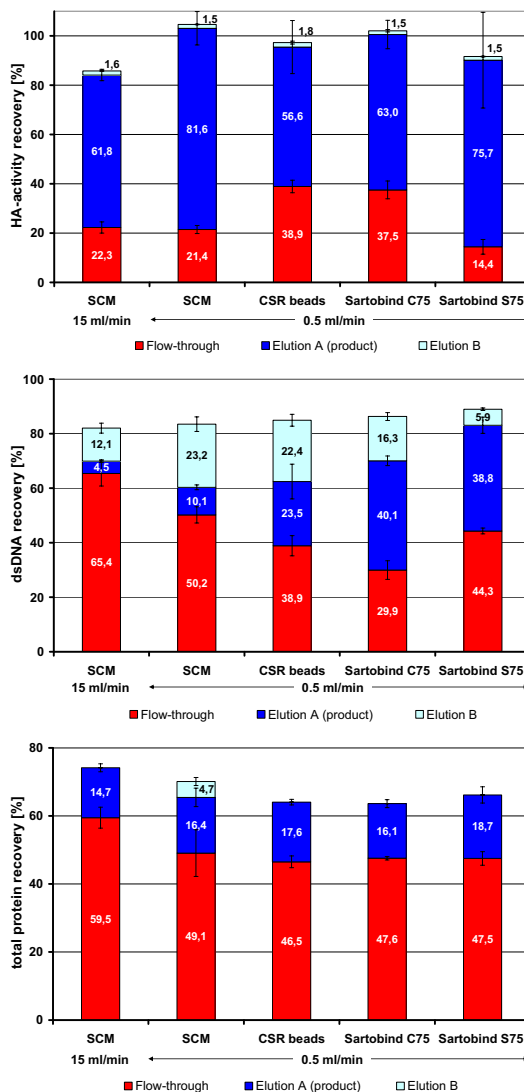


Figure 21: Recovery of HA-activity and depletion of dsDNA and total protein using SCM adsorbers (SCM, 10 layers, d: 25 mm, A~50 cm²), column-based Cellufine[®] sulphate beads (CSR beads, 3ml fixed-bed, Tricorn 5/150 column) and commercially available ion-exchange membrane adsorbers (Sartobind C75 and S75) for capturing influenza virus A/Puerto Rico/8/34 (H1N1, adsorption flow rates 0.5 and 15 ml/min, adsorption buffer 3: 50 mM NaCl, 10 mM Tris, pH 7.4, elution buffer 1: 0.6 M NaCl, 10 mM Tris, pH 7.4, elution buffer 2: 2 M NaCl, 10 mM Tris, pH 7.4). Mean and standard deviations of three experiments are shown.

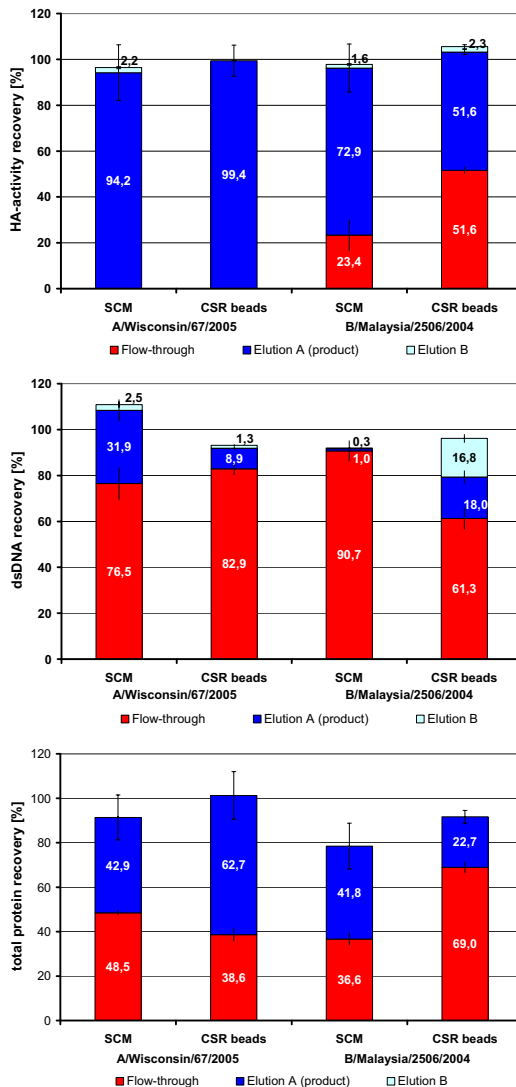


Figure 22: Recovery of HA-activity and depletion of dsDNA and total protein using SCM adsorbers (SCM, 10 layers, d: 25 mm, A~50 cm²) and column-based Cellufine[®] sulphate beads (CSR beads, 3ml fixed-bed, Tricorn 5/150) for capturing influenza virus strains A/Wisconsin/67/2005 (H3N2) and B/Malaysia/2506/2004 (adsorption flow rates 0.5 ml/min, adsorption buffer 3: 50 mM NaCl, 10 mM Tris, pH 7.4, elution buffer 1: 0.6 M NaCl, 10 mM Tris, pH 7.4, elution buffer 2: 2 M NaCl, 10 mM Tris, pH 7.4). Mean and standard deviations of three experiments per virus strain and adsorber media are shown.

5.2 Discussion

With respect to an increasing demand of human influenza vaccines (WHO 2007) efficient unit operations in downstream processing are crucial. The scope of this subproject was the development and characterization of SCM adsorbers for the capture of cell culture-derived influenza virus particles. In particular, productivity of such modified membrane adsorbers compared to commercially available cation-membrane adsorber units and column-based chromatography (Cellufine[®] sulphate) was characterized for influenza virus A/Puerto Rico/8/34. In addition, the study focused on the adsorption of three different influenza virus strains on reinforced cellulose membranes, which were sulphated in-house. Two of them were relevant vaccine strains from the 2006/07 and 2007/08 seasons. The chemical modification of the membrane layers used for this study led to a sulphur content of 4.9 weight-percent. This corresponds to about 16 µg sulphur/g dry membrane. Sulphate content estimation of unmodified cellulose membranes (<0.05 weight-percent sulphate) confirmed the successful chemical membrane modification. The sulphate content of Cellufine[®] cellulose beads is ≥ 700 µg sulphur/g dry media as stated by the manufacturer, which is significantly higher compared to the SCM adsorbers. However, it has to be considered that in contrast to the SCM adsorbers, due to the low exclusion limit of Cellufine[®] sulphate (3 kDa), most of the sulphate groups are not accessible for influenza virus particles.

Adsorption efficiency of influenza viruses to SCM depends on the ionic strength of the buffer or sample matrix. Virus particles (A/Puerto Rico/8/34) adsorbed significantly less to the SCM (47% HA-activity in flow-through) at salt concentrations of 150 mM NaCl compared to buffers at lower ionic strength (50 mM NaCl, 28% HA-activity in flow-through, Table 17). Optimization of the elution conditions concerning viral recovery as well as dsDNA and total protein reduction lead to a two-step isocratic elution profile with (1) 0.6 M NaCl and (2) 2M NaCl in 10 mM Tris, pH 7.4. Hence, all further purification experiments were done using a decreased ionic strength (50 mM NaCl) adsorption buffer and an isocratic elution profile. In addition, the concentrated virus broths were 3-fold diluted in 10 mM Tris, pH 7.4 prior purification in order to reduce the ionic strength of the sample matrix.

SCM adsorbers were applied successfully for purification of the three viral strains and compared to column-based CSR. The SCM adsorber captured about 82% (A/Puerto

Rico/8/34, Figure 21) and 73% (B/Malaysia/2506/2004, Figure 22) of the loaded influenza virus particles based on HA-activity, which was significantly more than for CSR-based chromatography (57% and 52%, respectively, Figure 21 and Figure 22). Repetition of capturing experiments using influenza virus strain B/Malaysia/2506/2004 from another cultivation batch resulted in similar low virus adsorption to CSR. Recovery of the influenza virus strain A/Wisconsin/67/2005 was similar for SCM and CSR-based separation. However, as adsorption and desorption conditions were optimized for the SCM adsorbers with the influenza virus strain A/Puerto Rico/8/34, an optimization using the two other strains may result in increased recoveries.

Summing up, at a velocity of 0.5 ml/min the SCM adsorbers recoveries were at least as good as the CSR recoveries depending on virus strain. In contrast, total protein as well as the dsDNA reduction differed between all three tested influenza virus strains. In addition, these values depend on the chromatographic matrix. The total recoveries of protein reached values in the range of 64% to 101%. Minor losses within the overall protein recoveries might be due to dialysis prior to protein measurements. However, the overall protein recoveries from unmodified cellulose membrane experiments showed comparable low values for the virus batch A/Puerto Rico/8/34 (73%, Table 18) indicating either unspecific protein adsorption to the cellulose matrix or protein loss during sample dialysis prior to the protein assay. Nevertheless, the total protein recoveries were reproducible within the different virus batches comparing all chromatographic matrices used. Capturing influenza virus particles (A/Puerto Rico/8/34) onto unmodified reinforced cellulose membrane sheets showed only minor unspecific adsorption. Only 2.6% (Elution 1 and 2, Table 18) of the virus particles could be displaced from the blank membrane layers, indicating the specificity of sulphate groups of the SCM-surface for virus adsorption. The binding of host cell dsDNA and proteins to the same unmodified membranes were also low (Table 18).

Compared to column-based processes membrane chromatography showed a reduced back pressure allowing increased flow rates and, therefore, improved productivities. Here, a maximum flow rate of 0.5 ml/min (153 cm/h, column: Tricorn 5/150, residence time: 6 min) was used for CSR-column chromatography. For comparability reasons all other chromatographic media including the SCM adsorbers were used at the same flow rate. Nevertheless, SCM adsorbers can be used at increased velocities. Therefore, the purification performance was characterized additionally at 15 ml/min using the influenza virus strain A/Puerto Rico/8/34, which corresponds to a 30-fold

increase of the volumetric velocity. The linear flow rate (SCM, 25 mm) is about 183 cm/h, which is comparable to the linear flow rate used for the CSR (Tricorn 5/150). Due to the increased flow rate and the lower volume of the membrane housing (2 ml) compared to the CSR column, the residence time was significantly decreased from 4 min (flow rate: 0.5 ml/min) to 8 s (flow rate: 15 ml/min). At 15 ml/min the majority of the viral HA-activity was found in the product fraction (about 62%, Elution 1, Figure 21) while only about 22% was lost in the unbound flow-through part. This is similar to the loss for the same virus strain using the SCM at 0.5 ml/min (21%, Figure 21). In addition, the increased flow rate reduced the dsDNA to about 5% (Elution 1, Figure 21). For the same virus strain this is about 20% of the dsDNA content compared to the CSR-product fractions (24%, Elution 1, Figure 21). The increase in dsDNA depletion of experiments with an adsorption flow rate of 15 ml/min could be due to a decrease in residence time or due to an increase in shear forces, which might reduce the adsorption of dsDNA. However, even at a lower residence time the SCM adsorber still allows efficient virus capture.

Based on SRID assay the SCM product fractions of all three virus strains tested contained between 2.1 to 5.9 µg total protein and between 23 to 59 ng dsDNA per µg HA (Table 19). The corresponding values after CSR-column chromatography were between 2.4 to 4.7 µg total protein and between 5 to 115 ng dsDNA per µg HA (Table 20). Hence, the purification performances of SCM adsorbers and CSR-column chromatography were comparable. One batch of influenza virus A/Wisconsin/67/2005 and two different batches of influenza virus A/Puerto Rico/8/34 and B/Malaysia/2506/2004, respectively, were used for this matrix comparison. Considering a maximal total protein content of 100 µg per virus strain and vaccine dose (European Pharmacopoeia 6.4) the SCM capture step reduced the total protein content sufficiently. However, based on the required amount of 15 µg HA per virus strain and vaccine dose, the maximum dsDNA content of 10 ng per trivalent dose (European Pharmacopoeia 6.4) is still exceeded up to 265-fold. Therefore, further purification steps are necessary. Additional nucleic acid depletion can be achieved by Benzonase[®] treatment of the product fraction after SCM-based virus purification. Due to the fact that the majority of dsDNA was already removed by the SCM adsorber, a relatively low amount of nuclease would be required. However, nuclease treatments should not be avoided entirely, because this step increases the safety margin of vaccines with respect to risks related to larger DNA fragments. The probability that

vaccines contain oncogenes or other functional sequences is lower when nucleic acids being digested to smaller fragments (Knezevic et al. 2008). Nucleotides and nucleic acid debris could be removed in a subsequent ion-exchange chromatographic step. Nevertheless, a final product concentration step would still be required.

Table 19: Impurities of product fraction (elution 1) after capturing three influenza virus strains by sulphated cellulose membranes (10 layers with A~50 cm², velocity: 0.5 ml/min, 3 experiments. mean and standard deviation of three individual samples)

	A/Puerto Rico/8/34	A/Wisconsin/67/2005	B/Malaysia/2506/2004
Measured concentrations			
HA-activity [kHAU/ml]	10.5 (±0.3)	8.5 (±0.5)	10.9 (±2.5)
hemagglutinin C_{HA} [µg/ml]	9.1 (±0.8)	4.5 (±0.6)	1.4 (±0.4)
protein c_{prot} [µg/ml]	19.2 (±3.2)	10.2 (±2.7)	8.2 (±2)
dsDNA C_{DNA} [ng/ml]	212 (±22)	267 (±43)	42 (±5)
Calculated impurities			
i_{prot} [µg protein / µg HA]	2.1 (±0.1)	2.3 (±0.8)	5.9 (±3)
i_{DNA} [ng dsDNA / µg HA]	23 (±1)	59 (±17)	30 (±3.)
i_{prot} [µg protein / kHAU]	1.8 (±0.3)	1.2 (±0.4)	0.8 (±0.1)
i_{DNA} [ng dsDNA / kHAU]	20 (±2)	31 (±7)	4 (±1)

Table 20: Impurities of product fraction (elution 1) after capturing three influenza virus strains by Cellufine® sulphate (Tricorn 5/150, velocity: 0.5 ml /min, 3 experiments. mean and standard deviation of three individual samples)

	A/Puerto Rico/8/34	A/Wisconsin/67/2005	B/Malaysia/2506/2004
Measured concentrations			
HA-activity [kHAU/ml]	5.7 (±0.1)	3.7 (±1.9)	6.7 (±0.3)
hemagglutinin c_{HA} [μg/ml]	3.1 (±0.3)	2.5 (±0.8)	2.6 (±0.1)
protein c_{prot} [μg/ml]	14.4 (±0.9)	10.6 (±1.8)	6.1 (±0.9)
dsDNA c_{DNA} [ng/ml]	356 (±111)	58 (±2)	12 (±3)
Calculated impurities			
i_{prot} [μg protein / μg HA]	4.7 (±0.8)	4.2 (±2.4)	2.4 (±0.3)
i_{DNA} [ng dsDNA / μg HA]	115 (±34)	23 (±8)	5 (±1)
i_{prot} [μg protein / kHAU]	2.5 (±0.2)	2.9 (±0.9)	0.9 (±0.1)
i_{DNA} [ng dsDNA / kHAU]	63 (±21)	16 (±8)	2 (±1)

A comparison of the SCM-based pseudo-affinity method with a lectin-based affinity capture method regarding the dsDNA depletion emphasizes clearly the high potential of a specific affinity ligand for purification efficiency. However, the costs for sulphated cellulose matrices are lower compared to specific affinity ligands purified from natural sources.

Due to the sulphatation, the cellulose backbone of SCM adsorbers is negatively charged. Thus, purification characteristics of these modified cellulose membranes were compared directly to commercially available cation-exchange membrane adsorbers Sartobind C75 (ligand: carboxylic acid) and S75 (ligand: sulfonic acid). The results from these experiments clearly indicated a higher dsDNA reduction by SCM adsorbers for same virus strain and chromatographic conditions (Figure 21). Here, the product fractions contained about 10% dsDNA, whereas the corresponding fractions from the cation-exchange membranes contained about 40% dsDNA, which is a 4-fold difference (Figure 21). Comparing the ligand surfaces, the SCM adsorbers contained covalently bound sulphate ions on the cellulose backbone and the Sartobind membrane adsorbers thin ligand films of about 0.5 -1 μ m thicknesses on the outer membrane area (manufacturer information). This particular type of membrane modification is a protected trade secret and could therefore not be reproduced on the

in-house-produced SCM adsorbers. Furthermore, it is likely that in contrast to ion-exchange membrane adsorbers the sulphated cellulose-based media (CSR, SCM) mimic the pseudo-affinity adsorption between virus particles and heparin, which consists of heavily sulphated glycosaminoglycan (Rabenstein 2002). The negatively charged glycosaminoglycan probably interact with positively charged amino acids of the viral envelope glycoproteins by electrostatic forces (Kalashnikova et al. 2008). However, several studies reported an influence of dextran sulphate on virus attachment and virus-membrane fusion. These studies suggested that dextran sulphate, which consists of sulphated glucose molecules like the SCM adsorbers, binds with high affinity to virus particles, such as influenza virus type A (Herrmann et al. 1992; Lüscher-Mattli et al. 1993; Ramalho-Santos and Pedroso de Lima 2001). Yamamoto and Miyagawa discussed the biological interaction between polysaccharide sulphate such as CSR beads and biomolecules (Yamamoto and Miyagawa 2000). Furthermore, another study discussed the influence of the conserved peptide sequence Phe-Leu-Gly from viral envelope transmembrane glycoproteins on virus-cell adsorption and fusion. This tripeptide may play a role in the adsorption of influenza virus type A to sulphated polysaccharides (Hosoya et al. 1991). Overall, it can be assumed that in contrast to the ion-exchange membrane adsorbers, the binding of viral particles to the SCM adsorbers is not only based on the charge of the adsorption matrix.

Kalbfuß et al. reported that the anion-exchange membrane adsorber Sartobind Q MA75 yielded in about 72% viral product recovery (A/Puerto Rico/8/34, flow rate: 22 ml/min) based on HA-activity (Kalbfuß et al. 2007b). However, due to the negative dsDNA charge, this adsorber was not able to separate influenza virus particles from host cell nucleic acid. Hence, the product fractions (desorption at 1.5 M NaCl) still contained the complete dsDNA. Peterka et al. compared CIM[®] monolithic columns containing quaternary amine (QA) with other anion-exchange and pseudo-affinity media including Cellufine[®] sulphate for purification of Vero cell culture-derived influenza virus (A/Puerto Rico/8/34 reassortment, serum free cultivation)(Peterka et al. 2007). According to these authors, viral product recovery from CIM QA (desorption at 0.5 M NaCl) was 77% based on an HA assay, while 95.5% of the host cell nucleic acid could be removed. Other tested anion-exchange media resulted in a recovery of 21% to 28% HA-activity (Peterka et al. 2007). Summing up, the SCM adsorbers are superior over anion- and cation-exchange membrane adsorbers and comparable to

CIM[®]-Q monolithic columns regarding nucleic acid reduction; however, the scalability of membrane-based unit operations in industrial processes seems easier compared to monolithic media.

The dynamic influenza virus binding capacity (flow rate: 0.5 ml/min, 22.6 cm/h, A/Puerto Rico/8/34) of the SCM adsorbers was estimated to be about 18 kHAU/cm², corresponding to about 1350 kHAU/75 cm², which represents the membrane area of commercially available Sartobind syringe adsorbers (Sartorius Stedim Biotech GmbH). Using an SRID assay about 13 µg HA/cm² membrane surface was determined. Comparing these values to the CSR, the volumetric-based binding capacity was 121 kHAU/ml and 69 µg/ml resin, as estimated with a 1 ml Tricorn column. Hence, a projected adsorption area of about 5.6 m² SCM or a volume of 8.3 L CSR would be required for purification of 100 L inactivated and clarified cell culture supernatant with an HA titer of 3. In contrast, from a membrane adsorber with the specific affinity ligand *Euonymus europaeus* lectin and a dynamic binding capacity of 671 kHA/75 cm² (Chapter 4.2), about 11 m² (unoptimized conditions) would be required for capturing 100 L of same cell culture supernatant. Kalbfuss et al. estimated the dynamic binding capacity of influenza virus A/Puerto Rico/8/34 (roller bottle cultivation in serum-containing medium, flow rate: 264 cm/h, capacity criterion: 10% breakthrough of feed activity) for a Sartobind Q anion-exchanger membrane adsorber to 5.2 kHAU/cm² (Kalbfuß et al. 2007b). This corresponds to about 389 kHAU/75 cm², which is approximately 3-fold lower than for SCM-adsorber membranes, which was estimated from the eluted product fraction after complete saturation of the adsorber.

Based on dynamic binding capacities, maximum applied flow rates, specific membrane area and specific column volume required for processing of culture broths (1000 kHAU), the productivity of the SCM adsorbers can be estimated to approximately 7 mg HA/h or 9072 kHAU/h. The corresponding estimates for the column-based CSR are about 0.2 mg HA/h or 301 kHAU/h, which is lower by a factor of 35 and 30, respectively. However, it has to be kept in mind that productivity was only estimated from small-scale experiments.

The SCM adsorbers are stable for multiple purification cycles and can be regenerated by successive application of 1 M NaOH and 1 M HCl in 1 M NaCl. However, due to the low production costs it is likely that these membranes will be considered as single-use products in order to ease process validation as well as cleaning and sanitation procedures. Summing up, SCM adsorbers allow reproducible influenza virus

purification with increased productivity compared to column-based CSR chromatography under similar conditions.

6 Summary

In this PhD thesis the development of affinity as well pseudo-affinity-based capturing of mammalian cell culture-derived influenza virus particles is addressed.

In the first part of the study, a lectin-based affinity adsorption unit operation was established. A ligand screening showed that the human influenza virus A/Puerto Rico/8/34 (H1N1) produced in MDCK cells exhibited a high degree of terminal galactose in (α 1,3) and (β 1,4) linkage and few (α 2,3)-linked terminal sialic acid. The lectin EEL, which has a high affinity to galactosyl(α 1,3)galactose, has been shown to be a reliable ligand for such a capture step. The following matrix screen, including EEL-modified porous polymer, glass, cellulose and agarose beads and a cellulose membrane, examined the influence of the support matrix on the influenza virus-capture efficiency. Among these tested EEL-affinity matrices human influenza virus particles A/Puerto Rico/8/34 were captured more efficiently from the culture broth by solid polymer beads and cellulose-based wide-porous membranes (3 μ m) than by soft-gel matrices such as agarose. The virus-binding capacity of the wide-porous cellulose membrane reached an estimated capacity of 670.5 kHAU per 75 cm² membrane area containing 1.1 mg EEL, which is about 20-fold higher than for the EEL-polymer beads based on the amount of immobilized ligand. In addition, EEL-AC offers a more efficient influenza virus capture step than conventional processes using heparin and Cellufine[®] sulphate resins. As demonstrated for two additional virus types from the epidemic seasons 2006/07 and 2007/08 (A/Wisconsin/67/2005 (H3N2) and B/Malaysia/2506/2004) the purification step is transferable to different influenza virus types propagated in MDCK cells. In contrast, the posttranslational modification, which depends on the host cell, has high impact on viral protein glycosylation and, therefore, on the lectin-binding properties. This was demonstrated for Vero cell-derived influenza virus A/Puerto Rico/8/34, where EEL was not suitable for purification. Here, the (β 1,4)-galactose-specific ECL would be a ligand candidate. However, as shown by SPR, the binding kinetics of this lectin is too slow for establishment of an efficient process compared to EEL. Hence, ECL is applicable only for analytical purposes. Depletion of dsDNA to about 0.4 to 7 ng/ μ g HA and total protein to 1 to 4 μ g/ μ g HA could be achieved. Finally, it can be stated that EEL-AC is an efficient, reproducible and influenza virus-strain-independent capture method, which is applicable for crude cultivation broths as well as for preconcentrated broths.

Table 21: Comparison of cell culture-derived influenza virus (A/Puerto Rico/8/34) capturing by different chromatographic techniques

Method	Virus yield [%]	Total protein [%]	DNA		Impurities (C _{prot} , C _{vNA})		Influenza virus		Reference
			[%]	[%]	[µg protein/ µg HA]	[ng DNA/ µg HA]	[µg protein/ kHAU]	[ng DNA/ kHAU]	
EEL-AC^a	86	50	0.2	1.1	0.4	0.5	0.2	A/Puerto Rico/8/34 ^b	current thesis
SCM^c	82	16	10	2.1	23	1.8	20	A/Puerto Rico/8/34 ^b	current thesis
CSR	57	18	24	4.7	115	2.5	63	A/Puerto Rico/8/34 ^b	current thesis
CSR	21	n/d ^d	8.4	n/d	n/d	n/d	n/d	A/PR/8/34 Mt. Sinai reassortment ^b	Peterka et al. 2007
AEX^e	72	23	105	n/d	n/d	13.4	8x10 ³	A/Puerto Rico/8/34	Kalbfuß et al. 2007a
AEX^f	77	n/d	4.5	n/d	n/d	n/d	n/d	A/PR/8/34 Mt. Sinai reassortment ^b	Peterka et al. 2007
AEX^g	28	n/d	5.5	n/d	n/d	n/d	n/d	A/PR/8/34 Mt. Sinai reassortment ^b	Peterka et al. 2007
SEC^h	85	35	34	n/d	n/d	2.1	390	A/Puerto Rico/8/34 ^b	Kalbfuß et al. 2007b
IMACⁱ	64	26	7	n/d	n/d	2.3	32	A/Puerto Rico/8/34 ^b	Opitz et al. 2009

^a EEL-polymer column, ^b influenza virus particles pre-concentrated by ultrafiltration, ^c adsorption flow rate 0.5 ml/min, ^d not determined, ^e Sartobind Q membrane adsorber (Sartorius Stedim Biotech GmbH, Göttingen, Germany), ^f CIM QA (BIA Separations, Ljubljana, Slovenia), ^g Q Sepharose XL (GE Healthcare, Uppsala, Sweden), ^h Sepharose 4 FF (GE Healthcare Uppsala, Sweden), ⁱ zinc modified Sartobind IDA 75 (Sartorius Stedim Biotech GmbH, Göttingen, Germany)

Comparing several chromatographic techniques for capturing of cell culture-derived influenza virus particles (Table 21) the EEL-AC indicated clearly superior purification behaviour, especially regarding nucleic acid depletion.

In the second part of the study, purification of influenza virus particles based on sulphated cellulose membranes (SCM) was established. SCM adsorbers, which exhibited high adsorption capacities of about 13 $\mu\text{g HA/cm}^2$, allowed the capture of MDCK cell culture-derived influenza viruses (A/Puerto Rico/8/34, H1N1; A/Wisconsin/67/2005, H3N2; B/Malaysia/2506/2004) at high loading velocity (15 ml/min). Hence, the process productivity was enhanced significantly compared to column-based Cellufine[®] sulphate chromatography. In addition, the higher loading flow rate enables further host cell dsDNA reduction in the viral product fraction to about 5% based on the initial loaded amount. These product fractions contained only 18 ng dsDNA and 2.3 μg total protein per $\mu\text{g HA}$. However, for vaccine formulation further dsDNA reduction is necessary. Finally, the SCM adsorbers improved dsDNA depletion compared to cation-exchange membrane adsorbers (Sartobind S75 and C75) as well as anion-exchange matrices (Table 21), which may be due to the adsorption properties of the pseudo-affinity matrix. In this context sulphated glucose molecules of the SCM may mimic the dextran sulphate, which is reported to play a role in virus attachment and virus-membrane fusion.

7 Outlook

The EEL-AC offered very high dsDNA and total protein depletion. However, due to the risk of ligand release into the product and the possible ligand instability during column-sanitisation procedures this unit operation might be used only for virus preparation under laboratory conditions. However, the potential of a specific affinity purification step right after culture-broth harvest and clarification is shown. Hence, application of similar specific ligands, e.g., synthetic or recombinant produced peptide ligands, could lead to analogous purification efficiencies. Thus, yield and productivity of vaccine downstream processes could be increased compared to today's vaccine productions based on centrifugation steps and adsorption processes applying sulphated cellulose beads.

The application of aptamers, which are specific for viral envelope proteins, and derivatives of neuraminidase inhibitors as affinity ligands for influenza viruses could be investigated. On the other hand, immunochromatography will most likely not be important for influenza vaccine production in the future.

Finally, to obtain pure virus bulks for vaccine formulations that comply with regulations from the Food and Drug Administration (FDA) or European Pharmacopoeia a combination of different purification steps would be necessary. This includes specific adsorption processes described in this dissertation and generic downstream processes, which are based on virus charge, size and hydrophobic interactions. In particular, the applicability of hydrophobic interaction chromatography should be investigated as polishing and alternative purification method for influenza virus particles.

8 References

- Alexander M, Dalglish DG. 2006. Dynamic light scattering techniques and their applications in food science. *Food Biophysics* 1(1):2-13.
- Alois Jungbauer RH. 2004. Monoliths for fast bioseparation and bioconversion and their applications in biotechnology. *Journal of Separation Science* 27(10-11):767-778.
- Alymova IV, Kodihalli S, Govorkova EA, Fanget B, Gerdil C, Webster RG. 1998. Immunogenicity and Protective Efficacy in Mice of Influenza B Virus Vaccines Grown in Mammalian Cells or Embryonated Chicken Eggs. *J. Virol.* 72(5):4472-4477.
- Anonym. 2006. Heparin as pseudo affinity chromatography ligand in influenza virus purification. *IP.com Journal* 6(10A):2.
- Banzhoff A, Pellegrini M, Del Giudice G, Fragapane E, Groth N, Podda A. 2008. MF59 (R)-adjuvanted vaccines for seasonal and pandemic influenza prophylaxis. *Influenza and Other Respiratory Viruses* 2(6):243-249.
- Bardiya N, Bae JH. 2005. Influenza vaccines: recent advances in production technologies. *Applied Microbiology & Biotechnology* 67(3):299-305.
- Barrett PN, Mundt W, Kistner O, Howard MK. 2009. Vero cell platform in vaccine production: moving towards cell culture-based viral vaccines. *Expert Review of Vaccines* 8(5):607-618.
- Basak S, Pritchard DG, Bhowan AS, Compans RW. 1981. Glycosylation sites of influenza viral glycoproteins: characterization of tryptic glycopeptides from the A/USSR(H1N1) hemagglutinin glycoprotein. *J. Virol.* 37(2):549-558.
- Becht H, Rott R. 1972. Purification of influenza virus hemagglutinin by affinity chromatography. *Medical Microbiology and Immunology* 158(2):67-8.
- Belongia Edward A, Kieke Burney A, Donahue James G, Greenlee Robert T, Balish A, Foust A, Lindstrom S, Shay David K. 2009. Effectiveness of Inactivated Vaccines Varied Substantially with Antigenic Match from the 2004-2005 Season to the 2006-2007 Season. *The Journal of Infectious Diseases* 199(2):159-167.
- Boi C, Cattoli F, Facchini R, Sorci M, Sarti GC. 2006a. Adsorption of lectins on affinity membranes. *Journal of Membrane Science* 273(1-2):12-19.
- Boi C, Facchini R, Sorci M, Sarti GC. 2006b. Characterisation of affinity membranes for IgG separation. *Desalination* 199(1-3):544-546.
- Bouvier NM, Palese P. 2008. The biology of influenza viruses. *Vaccine* 26(Supplement 4):D49-D53.
- Bradford MM. 1976. A rapid and sensitive method for the quantitation of microgram quantities of protein utilizing the principle of protein-dye binding. *Analytical Biochemistry* 72:248-254.
- Brady MI, Furminger IGS. 1976. A Surface Antigen Influenza Vaccine. 1. Purification of Haemagglutinin and Neuraminidase Proteins. *The Journal of Hygiene* 77(2):161-172.
- Brands R, Visser J, Medema, Palache AM, van Scharrenburg GJM. 1999. Infuvac: A safe Madin Darby canine kidney (MDCK) cell culture-based influenza vaccine. *Developments in biological standardization* 98:93-100.
- Brügmann M, Drommer W, Reichl U, Boge A. 1997. Iscom (Immuno Stimulating Complex)-vaccine of equine influenza virus--transmission electron microscopic investigation and literature review. *Dtsch. tierärztl. Wschr.* 104:196-202.

- Bucher DJ. 1977. Purification of neuraminidase from influenza viruses by affinity chromatography. *Biochimica Et Biophysica Acta* 482(2):393-399.
- Cartellieri S, Hamer O, Helmholz H, Niemeyer B. 2002. One-step affinity purification of fetuin from fetal bovine serum. *Biotechnology and Applied Biochemistry* 35(2):83-89.
- Cartellieri S, Helmholz H, Niemeyer B. 2001. Preparation and Evaluation of Ricinus communis Agglutinin Affinity Adsorbents Using Polymeric Supports. *Analytical Biochemistry* 295(1):66-75.
- Castilho LR, Anspach FB, Deckwer W-D. 2002. Comparison of affinity membranes for the purification of immunoglobulins. *Journal of Membrane Science* 207(2):253-264.
- Cattoli F, Boi C, Sorci M, Sarti G. 2006. Adsorption of pure recombinant MBP-fusion proteins on amylose affinity membranes. *Journal of Membrane Science* 273:2-11.
- Chalumeau HP. 1994. Vaccine manufacture at the time of a pandemic influenza. *European Journal of Epidemiology* 10(4):487-490.
- Champagne J, Delattre C, Shanthy C, Satheesh B, Duverneuil L, Vijayalakshmi MA. 2007. Pseudoaffinity chromatography using a Convective Interaction Media (R)-disk monolithic column. *Chromatographia* 65(11-12):639-648.
- Charcosset C. 2006. Membrane processes in biotechnology: An overview. *Biotechnology Advances* 24(5):482-492.
- Charlton A, Zachariou M. 2007. Immobilized Metal Ion Affinity Chromatography of Native Proteins. In: Zachariou M, editor. *Affinity Chromatography: methods and Protocols*. second ed. Totowa: Humana press. p 25-36.
- Chen M-W, Cheng T-JR, Huang Y, Jan J-T, Ma S-H, Yu AL, Wong C-H, Ho DD. 2008. A consensus-hemagglutinin-based DNA vaccine that protects mice against divergent H5N1 influenza viruses. *Proceedings of the National Academy of Sciences* 105(36):13538-13543.
- Cheung TKW, Poon LLM. 2007. Biology of Influenza A Virus. *Annals of the New York Academy of Sciences* 1102(Biology of Emerging Viruses: SARS, Avian and Human Influenza, Metapneumovirus, Nipah, West Nile, and Ross River Virus):1-25.
- Clark TW, Pareek M, Hoschler K, Dillon H, Nicholson KG, Groth N, Stephenson I. 2009. Trial of Influenza A (H1N1) 2009 Monovalent MF59-Adjuvanted Vaccine - Preliminary Report. *N Engl J Med*:NEJMoa0907650.
- Cox MMJ, Hollister JR. 2009. FluBlok, a next generation influenza vaccine manufactured in insect cells. *Biologicals In Press, Corrected Proof*.
- Cross KJ, Burleigh LM, Steinhauer DA. 2001. Mechanisms of cell entry by influenza virus. *Expert Reviews in Molecular Medicine* 3:1-18.
- Cuatrecasas P, Illiano G. 1971. Purification of neuraminidases from *Vibrio Cholerae*, *Clostridium Perfringens* and influenza virus by affinity chromatography. *Biochemical and Biophysical Research Communications* 44(1):178-&.
- Curling J, Gottschalk U. 2007. *Process Chromatography: Five Decades of Innovation*. BioPharm International 10.
- Czermak P, Grzenia DL, Wolf A, Carlson JO, Specht R, Han B, Wickramasinghe SR. 2008. Purification of the denonucleosis virus by tangential flow ultrafiltration and by ion exchange membranes. *Desalination* 224(1-3):23-27.
- Daublebsky von Eichhain M. 1997. Investigations on the enrichment of a histagged influenza hemagglutinin using affinity chromatography [dissertation]. Berlin: Freie Universität Berlin.

- Dawood FS, Jain S, Finelli L, Shaw MW, Lindstrom S, Garten RJ, Gubareva LV, Xu XY, Bridges CB, Uyeki TM. 2009. Emergence of a Novel Swine-Origin Influenza A (H1N1) Virus in Humans Novel Swine-Origin Influenza A (H1N1) Virus Investigation Team. *New England Journal of Medicine* 360(25):2605-2615.
- de Bruijn IA, Nauta J, Cramer WCM, Gerez L, Palache AM. 2005. Clinical experience with inactivated, virosomal influenza vaccine. *Vaccine* 23(Supplement 1):S39-S49.
- de Bruijn IA, Nauta J, Gerez L, Palache AM. 2006. The virosomal influenza vaccine Invivac®: Immunogenicity and tolerability compared to an adjuvanted influenza vaccine (Fluad®) in elderly subjects. *Vaccine* 24(44-46):6629-6631.
- Debray H, Strecker G, Montreuil J. 2002. Glycobiology and biochromatography. In: Vijayalakshmi M, editor. *Biochromatography: theory and practice*. London, New York:: Taylor and Francis. p 328-381.
- Deom CM, Schulze IT. 1985. Oligosaccharide composition of an influenza virus hemagglutinin with host-determined binding properties. *J. Biol. Chem.* 260(27):14771-14774.
- Doroshenko A, Halperin SA. 2009. Trivalent MDCK cell culture-derived influenza vaccine OptafluA® (Novartis Vaccines). *Expert Review of Vaccines* 8(6):679-688.
- Fouchier RAM, Munster V, Wallensten A, Bestebroer TM, Herfst S, Smith D, Rimmelzwaan GF, Olsen B, Osterhaus ADME. 2005. Characterization of a Novel Influenza A Virus Hemagglutinin Subtype (H16) Obtained from Black-Headed Gulls. *J. Virol.* 79(5):2814-2822.
- Furminger IGS. 1998. Vaccine Production. In: Nicholson KG, Webster RG, Hay AJ, editors. *Textbook of influenza*. Oxford, London, Edinburgh: Blackwell Science Ltd. p 324-332.
- Gambaryan AS, Karasin AI, Tuzikov AB, Chinarev AA, Pazynina GV, Bovin NV, Matrosovich MN, Olsen CW, Klimov AI. 2005. Receptor-binding properties of swine influenza viruses isolated and propagated in MDCK cells. *Virus Research* 114(1-2):15-22.
- Genzel Y, Behrendt I, Konig S, Sann H, Reichl U. 2004. Metabolism of MDCK cells during cell growth and influenza virus production in large-scale microcarrier culture. *Vaccine* 22(17-18):2202-2208.
- Genzel Y, Fischer M, Reichl U. 2006. Serum-free influenza virus production avoiding washing steps and medium exchange in large-scale microcarrier culture. *Vaccine* 24(16):3261-3272.
- Gerantes L, Kessler N, Thomas G, Aymard M. 1996. Simultaneous purification of influenza haemagglutinin and neuraminidase proteins by immunochromatography. *Journal of Virological Methods* 58(1-2):155-165.
- Gerdil C. 2003. The annual production cycle for influenza vaccine. *Vaccine* 21(16):1776-1779.
- Geyer H, Kempf R, Schott H-H, Geyer R. 1990. Glycosylation of the envelope glycoprotein from a polytropic murine retrovirus in two different host cells. *European Journal of Biochemistry* 193(3):855-862.
- Ghosh R. 2002. Protein separation using membrane chromatography: opportunities and challenges. *Journal of Chromatography A* 952(1-2):13-27.
- Gopinath SCB, Sakamaki Y, Kawasaki K, Kumar PKR. 2006. An Efficient RNA Aptamer against Human Influenza B Virus Hemagglutinin. *J Biochem* 139(5):837-846.

- Govorkova EA, Murti G, Meignier B, de Taisne C, Webster RG. 1996. African green monkey kidney (Vero) cells provide an alternative host cell system for influenza A and B viruses. *Journal of Virology* 70(8):5519-5524.
- Gröner A, Vorlop J; 1997. Animal cells and processes for the replication of influenza viruses patent WO 97/37000.
- Gupta MN, Kaul R, Guoqiang D, Dissing U, Mattiasson B. 1996. Affinity precipitation of proteins. *Journal of Molecular Recognition* 9(5-6):356-359.
- Hay AJ. 1998. The virus genome and its replication. In: Nicholson KG, Webster RG, Hay AJ, editors. *Textbook of influenza*. Oxford, London, Edinburgh, Malden, Carlton, Paris. p 43-53.
- Hayman MJ, Skehel JJ, Crumpton MJ. 1973. Purification of virus glycoproteins by affinity chromatography using *Lens-culinaris* Phytohemagglutinin. *FEBS Letters* 29(2):185-188.
- Hehme, Hehme N, Engelmann, Engelmann H, Künzel, Künzel W, Neumeier, Neumeier E, Sängner, Sängner R. 2002. Pandemic preparedness: lessons learnt from H2N2 and H9N2 candidate vaccines. *Medical Microbiology and Immunology* 191(3):203-208.
- Helmholz H, Cartellieri S, He L, Thiesen P, Niemyer B. 2003. Process development in affinity separation of glycoconjugates with lectins as ligands. *Journal of Chromatography A* 1006(1-2):127-135.
- Herrmann A, Korte T, Arnold K, Hillebrecht B. 1992. The influence of dextran sulfate on influenza A virus fusion with erythrocyte membranes. *Antiviral Research* 19(4):295-311.
- Hervé PC. 1994. Vaccine manufacture at the time of a pandemic influenza. *European Journal of Epidemiology* V10(4):487-490.
- Heyward JT, Klimas RA, Stapp MD, Obijeski JF. 1977. The rapid concentration and purification of influenza virus from allantoic fluid. *Archives of Virology* 55(1):107-119.
- Hilbrig F, Freitag R. 2003. Protein purification by affinity precipitation. *Journal of Chromatography B* 790(1-2):79-90.
- Hocart M, Grajower B, Donabedian A, Pokorny B, Whitaker C, Kilbourne ED. 1995. Preparation and characterization of a purified influenza virus neuraminidase vaccine. *Vaccine* 13(18):1793-1798.
- Hochuli E, Bannwarth W, Dobeli H, Gentz R, Stuber D. 1988. Genetic Approach to Facilitate Purification of Recombinant Proteins with a Novel Metal Chelate Adsorbent. *Nat Biotech* 6(11):1321-1325.
- Holmquist L, Nilsson G. 1979. Affinity chromatography of influenza virus on immobilized alpha- and beta-ketosides of neuraminic acid derivatives. *Acta pathologica et microbiologica Scandinavica* 87(section B):129-135.
- Hosoya M, Balzarini J, Shigeta S, De Clercq E. 1991. Differential inhibitory effects of sulfated polysaccharides and polymers on the replication of various myxoviruses and retroviruses, depending on the composition of the target amino acid sequences of the viral envelope glycoproteins. *Antimicrobial Agents and Chemotherapy* 35(12):2515-2520.
- Howard Allaker C. 1998. The use of affinity adsorbents in expanded bed adsorption. *Journal of Molecular Recognition* 11(1-6):217-221.
- Howard MK, Kistner O, Barrett PN. 2008. Pre-clinical development of cell culture (Vero)-derived H5N1 pandemic vaccines. *Biological Chemistry* 389(5):569-577.
- Hsieh P, Rosner MR, Robbins PW. 1983. Host-dependent variation of asparagine-linked oligosaccharides at individual glycosylation sites of Sindbis virus glycoproteins. *J. Biol. Chem.* 258(4):2548-2554.

- Hu AY-C, Weng T-C, Tseng Y-F, Chen Y-S, Wu C-H, Hsiao S, Chou A-H, Chao H-J, Gu A, Wu S-C and others. 2008. Microcarrier-based MDCK cell culture system for the production of influenza H5N1 vaccines. *Vaccine* 26(45):5736-5740.
- Hutanu D, Remcho VT. 2007. Aptamers as molecular recognition elements in chromatographic separations. *Advances in Chromatography* 45:173-196
- Ikizler MR, Wright PF. 2002. Thermostabilization of egg grown influenza viruses. *Vaccine* 20(9-10):1393-1399.
- Irwin JA, Tipton KF. 1995. Affinity precipitation: a novel approach to protein purification. *Essays in Biochemistry*, Vol 29, 1995. London: Portland Press. p 137-156.
- Jackson Lisa A. 2009. Using Surveillance to Evaluate Influenza Vaccine Effectiveness. *The Journal of Infectious Diseases* 199(2):155-158.
- Jones J, Krag SS, Betenbaugh MJ. 2005. Controlling N-linked glycan site occupancy. *Biochimica et Biophysica Acta (BBA) - General Subjects* 1726(2):121-137.
- Jönsson U, Fägerstam L, Ivarsson B, Johnsson B, Karlsson R, Lundh K, Löfas S, Persson B, Roos H, Ronnberg I and others. 1991. Real-time biospecific interaction analysis using surface plasmon resonance and a sensor chip technology. *Biotechniques* 11(5):620-627.
- Kalashnikova I, Ivanova N, Tennikova T. 2008. Development of a Strategy of Influenza Virus Separation Based on Pseudoaffinity Chromatography on Short Monolithic Columns. *Analytical Chemistry* 80(6):2188-2198.
- Kalbfuß B, Genzel Y, Wolff M, Zimmermann A, Morenweiser R, Reichl U. 2007a. Harvesting and concentration of human influenza A virus produced in serum-free mammalian cell culture for the production of vaccines. *Biotechnology and Bioengineering* 97(1):73-85.
- Kalbfuß B, Knochlein A, Krober T, Reichl U. 2008. Monitoring influenza virus content in vaccine production: Precise assays for the quantitation of hemagglutination and neuraminidase activity. *Biologicals* 36(3):145-161.
- Kalbfuß B, Wolff M, Geisler L, Tappe A, Wickramasinghe R, Thom V, Reichl U. 2007b. Direct capture of influenza A virus from cell culture supernatant with Sartobind anion-exchange membrane adsorbers. *Journal of Membrane Science* 299(1-2):251-260.
- Kalbfuß B, Wolff M, Morenweiser R, Reichl U. 2007c. Purification of cell culture-derived human influenza A virus by size-exclusion and anion-exchange chromatography. *Biotechnology and Bioengineering* 96(5):932-944.
- Kang K, Ryu D, Drohan WN, Orthner CL. 1992. Effect of matrices on affinity purification of protein C. *Biotechnology and Bioengineering* 39(11):1086 - 1096.
- Kang KA, Ryu DDY. 1991. Studies on scale-up parameters of an immunoglobulin separation system using protein A affinity chromatography. *Biotechnology Progress* 7(3):205-212.
- Karger A, Bettin B, Granzow H, Mettenleiter TC. 1998. Simple and rapid purification of alphaherpesviruses by chromatography on a cation exchange membrane. *Journal of Virological Methods* 70(2):219-224.
- Karlsson R, Michaelsson A, Mattsson L. 1991. Kinetic analysis of monoclonal antibody-antigen interactions with a new biosensor based analytical system. *Journal of Immunological Methods* 145(1-2):229-240.
- Keil W, Geyer R, Dabrowski J, Dabrowski U, Niemann H, Stirn S, Klenk HD. 1985. Carbohydrates of influenza virus. Structural elucidation of the individual glycans of the FPV hemagglutinin by two-dimensional ¹H n.m.r. and methylation analysis. *The EMBO Journal* 4(10):2711-2720.

- Kemble G, Greenberg H. 2003. Novel generations of influenza vaccines. *Vaccine* 21(16):1789-1795.
- Kharitononkov IG, Zakomyrdin YA, Elizarova GV. 1982. Isolation of preparative amounts of influenza virus neuraminidase by affinity chromatography. *Voprosy Virusologii*(2):184-189.
- Kistner O, Barrett P, Mundt W, Reiter M, Schober-Bendixen S, Eder G, Dorner F. 1999. A novel mammalian cell (Vero) derived influenza virus vaccine: development, characterization and industrial scale production. *Wiener klinische Wochenschrift* 111(5):207-214.
- Kistner O, Barrett PN, Mundt W, Reiter M, Schober-Bendixen S, Dorner F. 1998. Development of a mammalian cell (Vero) derived candidate influenza virus vaccine. *Vaccine* 16(9-10):960-968.
- Kistner O, Howard MK, Spruth M, Wodal W, Brühl P, Gerencer M, Crowe BA, Savidis-Dacho H, Livey I, Reiter M and others. 2007. Cell culture (Vero) derived whole virus (H5N1) vaccine based on wild-type virus strain induces cross-protective immune responses. *Vaccine* 25(32):6028-6036.
- Knezevic I, Stacey G, Petricciani J. 2008. WHO Study Group on cell substrates for production of biologicals, Geneva, Switzerland, 11-12 June 2007. *Biologicals* 36(3):203-211.
- Kristiansen T, Sparrman M, Heller L. 1983. Towards a subunit influenza vaccine prepared by affinity chromatography on immobilized lectin. *Journal of Biosciences* 5(1):149-155.
- Laddy DJ, Yan J, Khan AS, Anderson H, Cohn A, Greenhouse J, Lewis M, Manischewitz J, King LR, Golding H and others. 2009. Electroporation of Synthetic DNA Antigens Offers Protection in Non-Human Primates Challenged with Highly Pathogenic Avian Influenza. *J. Virol.*:JVI.02335-08.
- Laemmli UK. 1970. Cleavage of Structural Proteins during the Assembly of the Head of Bacteriophage T4. *Nature* 227:680-685.
- Lapidus M. 1969. Purification and concentration of influenza types A and B by chromatography on calcium phosphate. *Applied Microbiology* 17(4):504-8.
- Lauffenburger DA, Linderman JJ. 1993. *Receptors: Models for binding, trafficking and signaling*. New York, Oxford: Oxford University Press. 162 p.
- Lee D-S, Kim B-M, Seol D-W. 2009. Improved purification of recombinant adenoviral vector by metal affinity membrane chromatography. *Biochemical and Biophysical Research Communications* 378(3):640-644.
- Liedtke S, Adamski M, Geyer R, Pftzner A, Rubsamen-Waigmann H, Geyer H. 1994. Oligosaccharide profiles of HIV-2 external envelope glycoprotein: dependence on host cells and virus isolates. *Glycobiology* 4(4):477-484.
- Lis H, Sharon N. 1998. Lectins: Carbohydrate-specific proteins that mediate cellular recognition. *Chemical Reviews* 98(2):637-674.
- Lohr V, Rath A, Genzel Y, Jordan I, Sandig V, Reichl U. 2009. New avian suspension cell lines provide production of influenza virus and MVA in serum-free media: Studies on growth, metabolism and virus propagation. *Vaccine* 27(36):4975-4982.
- Lüscher-Mattli M, Glück R, Kempf C, Zanoni-Grassi M. 1993. A comparative study of the effect of dextran sulfate on the fusion and the in vitro replication of influenza A and B, Semliki Forest, vesicular stomatitis, rabies, Sendai, and mumps virus. *Archives of Virology* 130(3):317-326.
- Mahy B, Kangro H. 1996. *Virology method manual*. London: Academic press.
- Malmqvist M. 1993. Biospecific interaction analysis using biosensor technology. *Nature* 361(6408):186-187.

- Matheka HD, Armbruster O. 1958. Gradient elution of influenza viruses from anion exchange resin and demonstration of a biological difference between three components obtained from the PR8 strain. *Virology* 6(3):584-600.
- Matrosovich MN, Matrosovich TY, Gray T, Roberts NA, Klenk H-D. 2004. Human and avian influenza viruses target different cell types in cultures of human airway epithelium. *Proceedings of the National Academy of Sciences of the United States of America* 101(13):4620-4624.
- Matthews JT. 2006. Egg-based production of influenza vaccine: 30 Years of Commercial Experience. *The Bridge* 36(3):17-24.
- Mattiasson B, Ling TGI. 1986. Ultrafiltration affinity purification. In: McGregor WC, editor. *Membrane Separations in Biotechnology*. New York, Basel: Marcel Dekker, Inc. p 99-114.
- Mellado MCM, Curbelo D, Nobrega R, R. CL. 2007. Comparison of affinity membrane adsorbers for the purification of recombinant human erythropoietin (rhEPO). *Journal of Chemical Technology & Biotechnology* 82(7):636-645.
- Merkle RK, Cummings RD. 1987. Lectin affinity chromatography of glycopeptides. *Methods in Enzymology* 138:232-259.
- Miller GL, Lauffer MA, Stanley WM. 1944. ELECTROPHORETIC STUDIES ON PR8 INFLUENZA VIRUS. *J. Exp. Med.* 80(6):549-559.
- Miller HK, Schlesinger RW. 1955. Differentiation and Purification of Influenza Viruses by Adsorption on Aluminum Phosphate. *J Immunol* 75(2):155-160.
- Mir-Shekari SY, Ashford DA, Harvey DJ, Dwek RA, Schulze IT. 1997. The Glycosylation of the Influenza A Virus Hemagglutinin by Mammalian Cells. A site-specific study. *J. Biol. Chem.* 272(7):4027-4036.
- Mischler R, Metcalfe IC. 2002. Inflexal®V a trivalent virosome subunit influenza vaccine: production. *Vaccine* 20(Supplement 5):B17-B23.
- Misono TS, Kumar PKR. 2005. Selection of RNA aptamers against human influenza virus hemagglutinin using surface plasmon resonance. *Analytical Biochemistry* 342(2):312-317.
- Molinari N-AM, Ortega-Sanchez IR, Messonnier ML, Thompson WW, Wortley PM, Weintraub E, Bridges CB. 2007. The annual impact of seasonal influenza in the US: Measuring disease burden and costs. *Vaccine* 25(27):5086-5096.
- Morein B, Sundquist B, Höglund S, Dalsgaard K, Osterhaus. A. 1984. Iscom, a novel structure for antigenic presentation of membrane proteins from enveloped viruses. *Nature* 308:457 - 460.
- Nayak DP, Lehmann S, Reichl U. 2005. Downstream processing of MDCK cell-derived equine influenza virus. *Journal of Chromatography B* 823(2):75-81.
- Neurath AR, Rubin BA, Pierzchala WA. 1967. Importance of the ionic form of ion exchangers for chromatography of macromolecular substances: Purification of influenza viruses. *Archives of Biochemistry and Biophysics* 120(1):238-239.
- O'Keefe RS, Johnston MD, Slater NKH. 1999. The affinity adsorptive recovery of an infectious herpes simplex virus vaccine. *Biotechnology and Bioengineering* 62(5):537-545.
- O'Neil PF, Balkovic ES. 1993. Virus Harvesting and Affinity-Based Liquid Chromatography. *Nature Biotechnology* 11(2):173-178.
- O'riordan CE, Erickson AE, Smith AE; 2000. Chromatographic purification of adeno-associated virus (AAV). United States patent 6143548.
- Ogata S-i, Muramatsu T, Kobata A. 1975. Fractionation of Glycopeptides by Affinity Column Chromatography on Concanavalin A-Sepharose. *J Biochem* 78(4):687-696.

- Oka T, Ohkuma K, Kawahara T, Sakoh M; 1985. Method for purification of influenza virus. patent US4724210, EP0171086B1.
- Opitz L, Hohlweg J, Reichl U, Wolff MW. 2009. Purification of cell culture-derived influenza virus A/Puerto Rico/8/34 by membrane-based immobilized metal affinity chromatography. *Journal of Virological Methods* In Press, Accepted Manuscript(doi:10.1016/j.jviromet.2009.06.025).
- Oxford JS, Manuguerra C, Kistner O, Linde A, Kunze M, Lange W, Schweiger B, Spala G, Rebelo de Andrade H, Brena PRP and others. 2005. A new European perspective of influenza pandemic planning with a particular focus on the role of mammalian cell culture vaccines. *Vaccine* 23(46-47):5440-5449.
- Palache AM, Brands R, van Scharrenburg GJM. 1997. Immunogenicity and Reactogenicity of Influenza Subunit Vaccines Produced in MDCK Cells or Fertilized Chicken Eggs. *The Journal of Infectious Diseases* 176(s1):S20-S24.
- Palese P. 2006. Making better influenza virus vaccines? *Emerging Infectious Diseases* 12(1):61-65.
- Palese P, Tobita K, Ueda M, Compans RW. 1974. Characterization of temperature sensitive influenza virus mutants defective in neuraminidase. *Virology* 61(2):397-410.
- Patel DC, Luo RG, Dabrowski A. 1999. Protein adsorption dissociation constants in various types of biochromatography. *Studies in Surface Science and Catalysis: Elsevier*. p 829-845.
- Pau MG, Ophorst C, Koldijk MH, Schouten G, Mehtali M, Uytdehaag F. 2001. The human cell line PER.C6 provides a new manufacturing system for the production of influenza vaccines. *Vaccine* 19(17-19):2716-2721.
- Peixoto C, Ferreira TB, Sousa MFQ, J. T. Carondo M, Alves PM. 2008. Towards purification of adenoviral vectors based on membrane technology. *Biotechnology Progress* 24(6):1290-1296.
- Pepper DS. 1967. A Chromatographic Procedure for the Purification of Influenza Virus. *J Gen Virol* 1(1):49-55.
- Peterka M, Strancar A, Banjac M, Kramberger P, Maurer E, Muster T; 2007. Method for influenza virus purification. patent WO 2008/006780A1.
- Petryniak J, Goldstein I. 1987. Evonymus europaea lectin. *Methods in Enzymology* 138:552-561.
- Petryniak J, Pereira M, Kabat E. 1977. The lectin of Euonymus europeus: purification, characterization, and an immunochemical study of its combining site. *Archives of Biochemistry and Biophysics*. 178(1):118-134.
- Platonova GA, Pankova GA, Il'ina IY, Vlasov GP, Tennikova TB. 1999. Quantitative fast fractionation of a pool of polyclonal antibodies by immunoaffinity membrane chromatography. *Journal of Chromatography A* 852(1):129-140.
- Porath J, Carlsson JAN, Olsson I, Belfrage G. 1975. Metal chelate affinity chromatography, a new approach to protein fractionation. *Nature* 258(5536):598-599.
- Pyle SW, Chabot DJ, Miller TL, Serabyn SA, Bess JW, Arthur LO. 1991. Large-scale purification of gp70 from Moloney murine leukemia virus. *Journal of Virological Methods* 32(2-3):303-315.
- Rabenstein DL. 2002. Heparin and heparan sulfate: structure and function. *Natural Product Reports* 19:312-331.
- Rabilloud T, Carpentier G, Tarroux P. 1988. Improvement and simplification of low-background silver staining of proteins by using sodium dithionite. *Electrophoresis* 9(6):288-291.

- Ramalho-Santos J, Pedroso de Lima M. 2001. Fusion and Infection of Influenza and Sendai Viruses as Modulated by Dextran Sulfate: A Comparative Study. *Bioscience Reports* 21(3):293-304.
- Rangan Mallik DSH. 2006. Affinity monolith chromatography. *Journal of Separation Science* 29(12):1686-1704.
- Rao S, Kong W-P, Wei C-J, Yang Z-Y, Nason M, Styles D, DeTolla LJ, Sorrell EM, Song H, Wan H and others. 2008. Multivalent HA DNA Vaccination Protects against Highly Pathogenic H5N1 Avian Influenza Infection in Chickens and Mice. *PLoS ONE* 3(6):e2432.
- Rappuoli R. 2006. Cell-culture-based vaccine production: technological options. *The Bridge* 36(3):25-30.
- Reimer CB, Baker RS, vanFrank RM, Newlin TE, Cline GB, Anderson NG. 1967. Purification of Large Quantities of Influenza Virus by Density Gradient Centrifugation. *J. Virol.* 1(6):1207-1216.
- Rimmelzwaan GF, Baars M, van Beek R, van Amerongen G, Lovgren-Bengtsson K, Claas EC, Osterhaus AD. 1997. Induction of protective immunity against influenza virus in a macaque model: comparison of conventional and iscom vaccines. *J Gen Virol* 78(4):757-765.
- Rimmelzwaan GF, Osterhaus ADME. 1995. A novel generation of viral vaccines based on the ISCOM Matrix. *Pharmaceutical biotechnology* 6:543-558.
- Rimmelzwaan GF, Osterhaus ADME. 2001. Influenza vaccines: new developments. *Current Opinion in Pharmacology* 1(5):491-496.
- Roberts PC, Garten W, Klenk HD. 1993. Role of conserved glycosylation sites in maturation and transport of influenza A virus hemagglutinin. *Journal of Virology* 67():3048-3060.
- Romig TS, Bell C, Drolet DW. 1999. Aptamer affinity chromatography:: combinatorial chemistry applied to protein purification. *Journal of Chromatography B: Biomedical Sciences and Applications* 731(2):275-284.
- Sakudo A, Baba K, Tsukamoto M, Sugimoto A, Okada T, Kobayashi T, Kawashita N, Takagi T, Ikuta K. 2009. Anionic polymer, poly(methyl vinyl ether-maleic anhydride)-coated beads-based capture of human influenza A and B virus. *Bioorganic & Medicinal Chemistry* 17(2):752-757.
- Schoch-Spana M, Fitzgerald J, Kramer BR. 2005. Influenza Vaccine Scarcity 2004-05: Implications for Biosecurity and Public Health Preparedness. *Biosecurity and Bioterrorism* 3(3):224-234.
- Schulze IT. 1997. Effects of glycosylation on the properties and functions of influenza virus hemagglutinin. *The Journal of Infectious Diseases* 176(S1):s24-28.
- Schwarzer J, Rapp E, Hennig R, Genzel Y, Jordan I, Sandig V, Reichl U. 2009. Glycan analysis in cell culture-based influenza vaccine production: Influence of host cell line and virus strain on the glycosylation pattern of viral hemagglutinin. *Vaccine* 27(32):4325-4336.
- Schwarzer J, Rapp E, Reichl U. 2008. N-glycan analysis by CGE-LIF: Profiling influenza A virus hemagglutinin N-glycosylation during vaccine production. *Electrophoresis* 29(20):4203-4214.
- Scopes RK. 1994. Protein purification: Principles and Practice. Cantor CR, editor. New York: Springer Science+Business Media, LLC.
- Segura MD, Kamen A, Trudel P, Garnier A. 2005. A novel purification strategy for retrovirus gene therapy vectors using heparin affinity chromatography. *Biotechnology and Bioengineering* 90(4):391-404.

- Seo SH, Goloubeva O, Webby R, Webster RG. 2001. Characterization of a Porcine Lung Epithelial Cell Line Suitable for Influenza Virus Studies. *J. Virol.* 75(19):9517-9525.
- Shabram PW, Huyghe BG, Liu X, Shepard HM; 1998. Method of purification of viral vectors. United States patent 5837520.
- Sheffield F, Smith W, Belyavin G. 1954. Purification of influenza virus by red-cell adsorption and elution. *British journal of experimental pathology* 35(3):214-222.
- Shinya K, Ebina M, Yamada S, Ono M, Kasai N, Kawakoba Y. 2006. Avian flu: Influenza virus receptors in the human airway. *Nature* 440(7083):435-436.
- Skowronski DanutaÅ M, De Serres G, Dickinson J, Petric M, Mak A, Fonseca K, Kwindt TrijntjeÅ L, Chan T, Bastien N, Charest H and others. 2009. Component-Specific Effectiveness of Trivalent Influenza Vaccine as Monitored through a Sentinel Surveillance Network in Canada, 2006-2007. *The Journal of Infectious Diseases* 199(2):168-179.
- Smith DF, Torres BV. 1989. Lectin affinity chromatography of glycolipids and glycolipid-derived oligosaccharides. *Methods in Enzymology* 179:30-45.
- Sorci M, Boi C, Facchini R, Sarti GC. 2006. Purification of galacto-specific lectins by affinity membranes. *Desalination* 199:550-552.
- Specht R, Han B, Wickramasinghe SR, Carlson JO, Czermak P, Wolf A, Reif O-W. 2004. Densonucleosis virus purification by ion exchange membranes. *Biotechnology and Bioengineering* 88(4):465-473.
- Stancombe PR, Alexander FCG, Ling R, Matheson MA, Shone CC, Chaddock JA. 2003. Isolation of the gene and large-scale expression and purification of recombinant *Erythrina cristagalli* lectin. *Protein Expression and Purification* 30(2):283-292.
- Sweet C, Stephen J, Smith H. 1974a. The behaviour of antigenically related influenza viruses of differing virulence on disulphide-linked immunosorbents. *Immunochemistry* 11(12):823-826.
- Sweet C, Stephen J, Smith H. 1974b. Purification of influenza viruses using disulphide-linked immunosorbents derived from rabbit antibody. *Immunochemistry* 11(6):295-304.
- Szucs T, Behrens M, Volmer T. 2001. Costs of influenza in Germany 1996 - a cost-of-illness study. *Medizinische Klinik* 96(2):63-70.
- Terpe K. 2003. Overview of tag protein fusions: from molecular and biochemical fundamentals to commercial systems. *Applied Microbiology and Biotechnology* 60(5):523-533.
- Thillaivinayagalingam P, Newcombe AR, O'Donovan K, Francis R, Keshavarz-Moore E. 2007. Detection and quantification of affinity ligand leaching and specific antibody fragment concentration within chromatographic fractions using surface plasmon resonance. *Biotechnology and Applied Biochemistry* 48:179-188.
- Thompson WW, Shay DK, Weintraub E, Brammer L, Cox N, Anderson LJ, Fukuda K. 2003. Mortality Associated With Influenza and Respiratory Syncytial Virus in the United States. *JAMA* 289(2):179-186.
- Tree JA, Richardson C, Fooks AR, Clegg JC, Looby D. 2001. Comparison of large-scale mammalian cell culture systems with egg culture for the production of influenza virus A vaccine strains. *Vaccine* 19(25-26):3444-3450.
- Turkova J. 2002. Affinity chromatography. In: Vijayalakshmi M, editor. *Biochromatography: Theory and Practice* London New York. p 142-224.
- Valeri A, Gazzei G, Morandi M, Pende B, Neri P. 1977. Large-scale purification of inactivated influenza vaccine using membrane molecular filtration. *Cellular and Molecular Life Sciences* 33(10):1402-1403.

- Van Regenmortel MHV, Fauquet CM, Bishop DHL, Carstens EB, Estes MK, Lemon SM, Maniloff J, Mayo MA, McGeoch DJ, Pringle CR and others. 2000. *Virus Taxonomy: Seventh report of the International Committee on Taxonomy of Viruses* San Diego: Academic Press.
- van Riel D, Munster VJ, de Wit E, Rimmelzwaan GF, Fouchier RAM, Osterhaus ADME, Kuiken T. 2006. H5N1 Virus Attachment to Lower Respiratory Tract. *Science* 312(5772):399-.
- Van Scharrenburg GJM, Brands R; 1998. Influenza vaccine patent EP0870508B1.
- Vanlandschoot P, Beirnaert E, Neiryneck S, Saelens X, Jou WM, Fiers W. 1996. Molecular and immunological characterization of soluble aggregated A/Victoria/3/75 (H3N2) influenza haemagglutinin expressed in insect cells. *Archives of Virology* V141(9):1715-1726.
- Vijayalakshmi MA. 1989. Pseudobiospecific ligand affinity-chromatography. *Trends in Biotechnology* 7(3):71-76.
- Walzel H, Brock H, Franz H, Ziska P. 1989. Detection and quantification of ligand leakage from lectin affinity columns. *Biomedica Biochimica Acta* 48(4):221-226.
- Webster RG, Bean WJ, Gorman OT, Chambers TM, Kawaoka Y. 1992. Evolution and ecology of influenza A viruses. *Microbiological Reviews* 56(1):152-179.
- Werner RG, Kopp K, Schlueter M. 2007. Glycosylation of therapeutic proteins in different production systems. *Acta Paediatrica* 96(s455):17-22.
- WHO. 1995. Cell culture as a substrate for the production of influenza vaccines: memorandum from a WHO meeting. *Bulletin of the World Health Organization* 73(4):431-435.
- WHO. 2006. A review of production technologies for influenza virus vaccines, and their suitability for deployment in developing countries for influenza pandemic preparedness. http://www.who.int/vaccine_research/diseases/influenza/Flu_vacc_manuf_tech_report.pdf; 2009/04/01. Geneva.
- WHO. 2007. Projected supply of pandemic influenza vaccine sharply increases. <http://www.who.int/mediacentre/news/releases/2007/pr60/en/index.html>; 2008/07/31. Geneva.
- Wickramasinghe SR, Kalbfuß B, Zimmermann A, Thom V, Reichl U. 2005. Tangential flow microfiltration and ultrafiltration for human influenza A virus concentration and purification. *Biotechnology and Bioengineering* 92(2):199-208.
- Wilchek M, Miron T, Kohn J, William BJ. 1984. [1] Affinity chromatography. *Methods in Enzymology*: Academic Press. p 3-55.
- Wilschut J. 2009. Influenza vaccines: The virosome concept. *Immunology Letters* 122(2):118-121.
- Wilson IA, Skehel JJ, Wiley DC. 1981. Structure of the haemagglutinin membrane glycoprotein of influenza virus at 3 [angst] resolution. *Nature* 289(5796):366-373.
- Wolff M, Reichl U. 2008. Downstream Processing: From egg to cell culture derived influenza virus particles. *Chemical Engineering & Technology* 6:1-13.
- Wolff MW, Opitz L, Reichl U; 2008. Method for the preparation of sulfated cellulose membranes and sulfated cellulose membranes. patent WO2008/125361.
- Wood JM, Schild GC, Newman RW, Seagroatt V. 1977. An improved single-radial-immunodiffusion technique for the assay of influenza haemagglutinin antigen: Application for potency determinations of inactivated whole virus and subunit vaccines. *Journal of Biological Standardization* 5(3):237-247.

- Wu C, Soh KY, Wang S. 2007. Ion-Exchange Membrane Chromatography Method for Rapid and Efficient Purification of Recombinant Baculovirus and Baculovirus gp64 Protein. *Human Gene Therapy* 18(7):665-672.
- Yamamoto S, Miyagawa E. Dynamic binding performance of large biomolecules such as gamma-globulin, viruses and virus-like particles on various chromatographic supports. In: Endo I, Nagamune T, Katoh S, Yonemoto T, editors. *Bioseparation Engineering*, 16; 2000; Nikko, Japan. Elsevier.
- Yamashita K, Kochibe N, Ohkura T, Ueda I, Kobata A. 1985. Fractionation of L-fucose-containing oligosaccharides on immobilized *Aleuria aurantia* lectin. *J. Biol. Chem.* 260(8):4688-4693.
- Youil R, Su Q, Toner TJ, Szymkowiak C, Kwan WS, Rubin B, Petrukhin L, Kiseleva I, Shaw AR, DiStefano D. 2004. Comparative study of influenza virus replication in Vero and MDCK cell lines. *Journal of Virological Methods* 120(1):23-31.
- Zheng L, Wang F, Yang Z, Chen J, Chang H, Chen Z. 2009. A single immunization with HA DNA vaccine by electroporation induces early protection against H5N1 avian influenza virus challenge in mice. *BMC Infectious Diseases* 9(1):17.
- Zhilinsk. In, Sokolov NN, Golubev DB, Ivanova NA, Elsaed LH. 1972. Isolation of A2/Singapore/57 influenza-virus V and S antigens by isoelectric focusing *Acta Virologica* 16(5):436-&.

9 Index

9.1 Index of figures

Figure 1: Schema of influenza virus type A	5
Figure 2: Example for the production procedure of egg-derived influenza virus vaccines	9
Figure 3: Example for the production procedure of cell culture-derived influenza virus vaccines	11
Figure 4: Schematic illustration of covalent ligand immobilization to epoxy-activated matrices via amine (A) and hydroxyl (B) ligand residues (Rangan Mallik 2006; Scopes 1994)	15
Figure 5: Principle of bead-based affinity chromatography.....	16
Figure 6: Example of a disaccharide unit of heparin (A, based on Rabenstein 2002) and sulphated cellulose (B, based on manufacturer's (Chisso Corporation, Japan) application notes of Cellufine [®] sulphate)	20
Figure 7: Schematic cross-section of a membrane layer (A) and chromatographic beads (B) (black dots: immobilized ligands; black arrows: flow direction of mobile phase; blue arrows: pore diffusion)	24
Figure 8: Schematic principle of interaction analysis by surface plasmon resonance technology (based on: Karlsson et al. 1991)	26
Figure 9: Overview of virus productions used for LAC experiments (MF: microfiltration, UF: ultrafiltration)	30
Figure 10: Overview about virus production used for PAC experiments (MF: microfiltration, UF: ultrafiltration).....	31
Figure 11: Total recovery of HA-activity after screening with Lectin-AffiSpin [®] columns	54
Figure 12: Light-scattering signal (90°) during purification of human influenza A virus concentrate with EEL-affinity chromatography (direct loading [0.2 ml/min] and elution [0.5 ml/min]; AB1: adsorption buffer 1).....	56
Figure 13: SDS-PAGE (nonreducing running conditions) with samples from EEL-AC (~2 µg protein per lane, M: protein ladder, E1: elution 1, FT: flow-through, viral proteins are indicated).....	58

- Figure 14: EEL-AC monitored by light scattering (90°): breakthrough of the EEL-membrane (3 µm pore size, ligand density: 0.02 mg/cm²) loading human influenza A virus A/Puerto Rico/8/34 concentrate..... 66
- Figure 15: Binding capacity of the EEL membrane (3 µm pore size, 75 cm², 0.02 mg EEL/cm²): eluted viral product fraction (vertical axis, HA-activity) against loaded virus amount (horizontal axis, HA-activity, ◊: load below binding capacity, ●: load above binding capacity)..... 66
- Figure 16: EEL-AC: human influenza virus A/Puerto Rico/8/34 capture from 100 ml unconcentrated cultivation broth by the EEL-polymer beads (3 ml column, 5.0 mg/ml ligand density; monitored by light scattering: 90°) 67
- Figure 17: Particle-size-distribution analysis of concentrated (750 kDa MWCO) and unconcentrated cultivation broths containing influenza virus A/Puerto Rico/8/34 68
- Figure 18: Recovery of HA-activity in product fraction after small-scale LAC (normalized to the value of the most suitable lectin per virus type) using MDCK cell-derived influenza virus types A/Wisconsin/67/2005 and B/Malaysia/2506/2004 (normalized to EEL) and the Vero cell-derived influenza virus A/Puerto Rico/8/34 (normalized to ECL). Due to the applied method, binding kinetics did not influence the HA-activity recovery..... 75
- Figure 19: Comparative binding analysis of three MDCK cell-derived human influenza virus types to EEL and ECL by SPR technology (Biacore 2000, 2 cycles per virus type are shown, association and dissociation phases are marked, signal changes due to sample matrix were eliminated by subtraction of the reference flow cell signal)..... 77
- Figure 20: Comparative binding analysis of Vero- and MDCK cell-derived human influenza virus A/Puerto Rico/8/34 to EEL and ECL by SPR technology (Biacore 2000, association and dissociation phases are marked, signal changes due to sample matrix were eliminated by subtraction of the reference flow cell signal).. 78
- Figure 21: Recovery of HA-activity and depletion of dsDNA and total protein using SCM adsorbers (SCM, 10 layers, d: 25 mm, A~50 cm²), column-based Cellufine[®] sulphate beads (CSR beads, 3ml fixed-bed, Tricorn 5/150 column) and commercially available ion-exchange membrane adsorbers (Sartobind C75 and S75) for capturing influenza virus A/Puerto Rico/8/34 (H1N1, adsorption flow rates 0.5 and 15 ml/min, adsorption buffer 3: 50 mM NaCl, 10 mM Tris, pH 7.4, elution

- buffer 1: 0.6 M NaCl, 10 mM Tris, pH 7.4, elution buffer 2: 2 M NaCl, 10 mM Tris, pH 7.4). Mean and standard deviations of three experiments are shown..... 89
- Figure 22: Recovery of HA-activity and depletion of dsDNA and total protein using SCM adsorbers (SCM, 10 layers, d: 25 mm, A~50 cm²) and column-based Cellufine[®] sulphate beads (CSR beads, 3ml fixed-bed, Tricorn 5/150) for capturing influenza virus strains A/Wisconsin/67/2005 (H3N2) and B/Malaysia/2506/2004 (adsorption flow rates 0.5 ml/min, adsorption buffer 3: 50 mM NaCl, 10 mM Tris, pH 7.4, elution buffer 1: 0.6 M NaCl, 10 mM Tris, pH 7.4, elution buffer 2: 2 M NaCl, 10 mM Tris, pH 7.4). Mean and standard deviations of three experiments per virus strain and adsorber media are shown. 90

9.2 Index of tables

Table 1: Examples of different approaches for capturing of whole influenza virus particles or viral proteins by affinity and pseudo-affinity chromatography.....	22
Table 2: Biotinylated lectins from Vector Laboratories Inc. used for affinity screening towards human influenza virus A/Puerto Rico/8/34 glycoproteins via lectin blots	35
Table 3: AffiSpin® Kits (GALAB Technologies GmbH, Geesthacht, Germany) used for lectin-virus affinity screening	36
Table 4: AffiSpin® kits (GALAB Technologies GmbH, Geesthacht, Germany) used for ligand screening.	43
Table 5: SOP's applied for characterization of chromatography experiments	48
Table 6: Lectin affinity towards human influenza A/PuertoRico/8/34 virus and MDCK cell proteins based on lectin blot analysis (number of "+" indicates the affinity level, most suitable lectins are highlighted)	54
Table 7: Comparison of recovery [%] of HA-activity after EEL- and ECL-affinity purification concerning binding velocity using 1 ml lectin adsorbents	55
Table 8: EEL-affinity chromatography mass balancing using 3 ml EEL-polymer adsorbent (number of runs: 4, standard deviations are given in parentheses)....	57
Table 9: Concentration analysis of the major product peak of elution 1 after EEL-AC in comparison to the concentrated load and purification efficiency (number of runs: 4, standard deviations are given in parentheses)	57
Table 10: EEL-matrix screen: analysis of human influenza A virus binding by HA-activity tests in comparison to Cellufine® sulphate and heparin HP (standard deviations are given in parentheses).....	63
Table 11: Performance of EEL-polymer LAC (3 ml column, 4.3 mg/ml ligand density) using two different cultivation broths (standard deviations are given in parentheses)	64
Table 12: Comparison of purification characteristics from EEL polymer (3 ml column; 4.3 mg/ml ligand density) and EEL-cellulose membrane (3 µm pore size; 0.02 mg/cm ² ligand density; 3 experiments per matrix; standard deviations are given in parentheses)	64
Table 13: Analysis of the major peak from elution 1 after EEL-membrane and EEL-polymer LAC based on concentrations of the loaded sample and the purification	

efficiency (each adsorbent 3 runs; standard deviations are given in parentheses)	65
Table 14: HA-activity mass balance: influenza virus A/Puerto Rico/8/34 captured by EEL-polymer AC (3 ml column, 5.0 mg/ml ligand density) using unconcentrated culture broth (number of runs 3).....	67
Table 15: Purification characteristics using EEL-AC to capture influenza virus types A/Wisconsin/67/2005 (H3N2) and B/Malaysia/2506/2004 (3 experiments per virus type, mean and standard deviations of three individual samples).....	79
Table 16: Concentrations and impurities of product fraction (Elution 1) after EEL-AC (3 experiments per virus type, mean and standard deviations of three individual samples).....	80
Table 17: Influenza virus (A/Puerto Rico/8/34, H1N1) capture using sulphated cellulose membrane adsorbents (10 layers, d: 25 mm, A~50 cm ²) with two different ionic strength adsorption buffers, (flow rate: 0.5 ml/min, elution 1: 1.2 M NaCl, 10 mM Tris, pH 8, elution 2: 2 M NaCl, 10 mM Tris, pH 8, 3 experiments, mean and standard deviation of three individual samples, product fraction (elution 1) in bold)	87
Table 18: Unspecific adsorption (A/Puerto Rico/8/34) of unmodified cellulose membrane layers (10 layers, d: 25 mm, A~50 cm ² , flow rate: 0.5 ml/min, adsorption buffer: 50 mM NaCl, 10 mM Tris, pH 7.4, elution buffer 1: 0.6 M NaCl, 10 mM Tris, pH 7.4, elution buffer 2: 2 M NaCl, 10 mM Tris, pH 7.4, product fraction (elution 1) in bold).....	87
Table 19: Impurities of product fraction (elution 1) after capturing three influenza virus strains by sulphated cellulose membranes (10 layers with A~50 cm ² , velocity: 0.5 ml/min, 3 experiments. mean and standard deviation of three individual samples)	94
Table 20: Impurities of product fraction (elution 1) after capturing three influenza virus strains by Cellufine [®] sulphate (Tricorn 5/150, velocity: 0.5 ml /min, 3 experiments. mean and standard deviation of three individual samples).....	95
Table 21: Comparison of cell culture-derived influenza virus (A/Puerto Rico/8/34) capturing by different chromatographic techniques.....	100

Parts of this dissertation are already published and have been included in this book with kind permission from Elsevier Limited and John Wiley and sons:

Opitz L, Salaklang J, Büttner H, Reichl U, Wolff MW. 2007. Lectin-affinity chromatography for downstream processing of MDCK cell culture derived human influenza A viruses. *Vaccine* 25(5):939-947.

Opitz L, Lehmann S, Zimmermann A, Reichl U, Wolff MW. 2007. Impact of adsorbents selection on capture efficiency of cell culture derived human influenza viruses. *Journal of Biotechnology* 131(3):309-317.

Opitz L, Zimmermann A, Lehmann S, Genzel Y, Lübken H, Reichl U, Wolff MW. 2008. Capture of cell culture-derived influenza virus by lectins: Strain independent, but host cell dependent. *Journal of Virological Methods* 154(1-2):61-68.

Opitz L, Lehmann S, Reichl U, Wolff MW. 2009. Sulfated membrane adsorbents for economic pseudo-affinity capture of influenza virus particles *Biotechnology and Bioengineering* 103(6):1144-1154.

Lebenslauf

Name Lars Opitz
Geburtsdatum 10. Januar 1978
Geburtsort Elsterwerda

Ausbildung

09/1991 - 06/1997 Elsterschloß-Gymnasium Elsterwerda, Elsterwerda
Abschluss: Allgemeine Hochschulreife

07/1997 - 04/1998 Grundwehrdienst: 8./Sanitätsregiment 13, Halle

10/1998 - 03/2005 Studium der Bioverfahrenstechnik, Technische Universität Dresden
Abschluss: Diplom-Ingenieur

Wissenschaftlicher Werdegang

05/2005 - 12/2009 Wissenschaftlicher Mitarbeiter am Max-Planck-Institut für Dynamik komplexer technischer Systeme, Magdeburg
Arbeitsgruppe: Bioprozesstechnik

Praxis

06/1998–07/1998 MAN TAKRAF GmbH, Lauchhammer
Metalltechnisches Praktikum

09/2001 - 02/2002 Bayer AG, Wuppertal
Bioverfahrenstechnisches Praktikum: Virusinaktivierung durch UVC-Strahlung

05/2002 - 12/2002 New England Biolabs, Inc., Beverly, MA, USA
Biotechnologisches Praktikum: Entwicklung rekombinanter Enzyme

05/2004 - 12/2004 New England Biolabs Inc., Beverly, MA, USA,
Diplomarbeit: Klonierung und Expression der Restriktionsendonuklease HpyAV in *E.coli* und anschließende Optimierung der Hochzelllichtfermentation zur HpyAV-Produktion

Beruflicher Werdegang

01/2010 - dato GlaxoSmithKline Biologics, Branch of SmithKline Beecham Pharma GmbH & Co. KG, Dresden, Support Manager, Value Stream Secondary

Magdeburg, 02.03.2010

Dipl.-Ing. Lars Opitz

